UPPER LIMB EXOSKELETON USING EMG SIGNALS

UPPER LIMB EXOSKELETON USING EMG SIGNALS

By

SHAWN D'SOUZA

NIGEL FERNANDES

SHRIRAJ PRABHUDESAI

M.SC. PART-II ELECTRONICS

SCHOOL OF PHYSICAL AND APPLIED SCIENCE

GOA UNIVERSITY

2021-2022

CERTIFICATE

This is to certify that the project entitled

"UPPER LIMB EXOSKELETON USING EMG SIGNALS"

Is a record work done by

SHAWN D'SOUZA

NIGEL FERNANDES

SHRIRAJ PRABHUDESAI

M.Sc. Part II Electronics

For the year 2021-2022

The candidates themselves have worked on the project during the period of study under by guidance and to the best of my knowledge it has not previously formed the basis of award of any previous degree or diploma at Goa University or elsewhere.

____________________	______________	________________
Programme Director	Examiner	Project Guide

ACKNOWLEDGEMENT

We are extremely fortunate to be involved in an exciting and challenging project like this one. It has given us an opportunity to work in this field of research and development. This project increased our thinking and understanding capability in various aspects.

We would like to express our sincere gratitude to our Dr. Rajendra S. Gad (Vice Dean - Research) for giving us this opportunity to do this project and also thank Dr. Jivan S. Parab (Programme Director), Dr. Aniketh A. Gaonkar (Assistant professor), Dr. Narayan T. Vetrekar (Assistant professor), Dr. Marlon D. Sequeira (Assistant professor) for their guidance and support in our project.

We would like to thank Don Bosco College of Engineering for 3D printing the various parts of our exoskeleton and also the lab staff for co ordinating with a welcoming gesture. Also like to thank Mr. Vishant Malik (Lab Technician) for his help and support in providing us with the instruments and components for our project and Mr. William D'Souza (Clerk) and the support staff Pushpa Andrade, Ashwini Velip and Agnelo Lopez for their patience and assistance throughout our project.

A big thanks to our family members for their moral support during this time and everyone who encouraged us for this project to be successful along with our colleagues and friends who helped us along the way.

DECLARATION

We the students of Goa University's M.Sc. Electronics Batch hereby solemnly declare that this project report under the title "UPPER LIMB EXOSKELETON USING EMG SIGNALS" is a record of work that has been composed by us and this report has not been submitted anywhere else for the award of any diploma or degree to the best of our knowledge.

1. Shawn D'souza ____________________
2. Nigel Fernandes ____________________
3. Shriraj Prabhudesai ____________________

ABSTRACT

An exoskeleton is an external structural mechanism with joints and links corresponding to those of the human body. With applications in rehabilitation medicine and virtual reality simulation along with heavy duty and defence applications, exoskeletons offer benefits for both disabled and healthy populations. In other words designing kinematics of an exoskeleton generally consist of trying to replicate human limb kinematics.

We have designed an untethered, powered, upper body exoskeleton for use in the fields of rehabilitation and therapeutic application, as well as occupations requiring augmented strength. Though systems exist, past exoskeleton endeavours have led to bulky, expensive, invasive, and tethered solutions. The challenge is to build an exoskeleton system that is inexpensive, streamlined, and wireless and easy to use by anyone who needs it. Our solution will be a low-cost, ergonomic device actuated through sensors measuring the user's motion and feeding it to the exoskeleton. Sensing data can be collected for a wide range of motion for use in physical therapy. This data can be used by doctors and patients to more accurately track improvement over time and also help in rehabilitation.

With its low cost, hospitals could employ multiple devices and aid a larger audience of patients, the devices could even be used at home for physical therapy, which would dramatically increase quality of life for patients. Outside of physical therapy, augmented strength is applicable to physically intensive occupations, as well as search and rescue operations. Each year, thousands of workers must take leave due to injuries triggered by heavy lifting; with augmented strength, workers could avoid harmful situations.

TABLE OF CONTENTS

CHAPTER 1:

INTRODUCTION

1.1 INTRODUCTION

The earliest exoskeleton-like device was developed in 1890 by a Russian named Nicholas which does the operations like walk and help to move the arms as the aided equipment. The unit was passive in operation and required human power, that used compressed gas bags to store the energy and it would assist with movements [1].

The general categorization of exoskeleton suggests several feasible exoskeleton categories. Such categories have general classes, due to the wide quantity of exoskeletons in existence, and are the structure, the body part focused on, the action, the power technology, the purpose, and the application area varying from one to another.

Exoskeletons are not only designed for specific body parts, the exoskeletons may be designed more generally for only one hand, a leg, or even the complete body. There are classes for specific limbs and specific joints. These classes include exoskeletons designed for the knee, ankle, hand, arm, foot, etc [7].

Types of Exoskeleton:

By body part:

- Upper extremity exoskeletons: These provide support to the upper body, including the arms, shoulders, and torso.
- Lower extremity exoskeletons: These provide support to the legs, hips, and lower torso.
- Full body exoskeletons: These provide support to the whole body and are thus the most powerful exoskeletons.

By form:

- Hard/classic exoskeletons: These use rigid structures and actuators. They are tough and can provide a lot of power.
- Soft exoskeletons: These are made of fabrics and other soft materials. Power is applied to the body via compliant actuators, such as air muscles or cables. They are more comfortable than classic exoskeletons but don't provide as much power.

By actuation technology:

- Electric: These use electric servos or other electric actuators to provide support and extra power to the wearer's muscles. They usually use batteries, so can be very portable.
- Hydraulic: These use hydraulic actuators which are more powerful than electric ones. However, they require larger and more complex power sources, such as internal combustion engines or hydrogen fuel cells.
- Fully mechanical: These are also known as passive exoskeletons; these include no active actuators. Instead, they support the wearer using mechanical linkages.
- Others: Less common are exoskeletons with fuel cell actuators, shape memory alloys, and pneumatics.

There are also a range of different application areas, each of which has different requirements for what it would need from an exoskeleton. For example, rehabilitation applications are more suited to soft, low-power devices which support and develop the natural muscle use of the wearer. On the other hand, military and construction applications would want high-powered exoskeletons to augment the strength of the wearer.

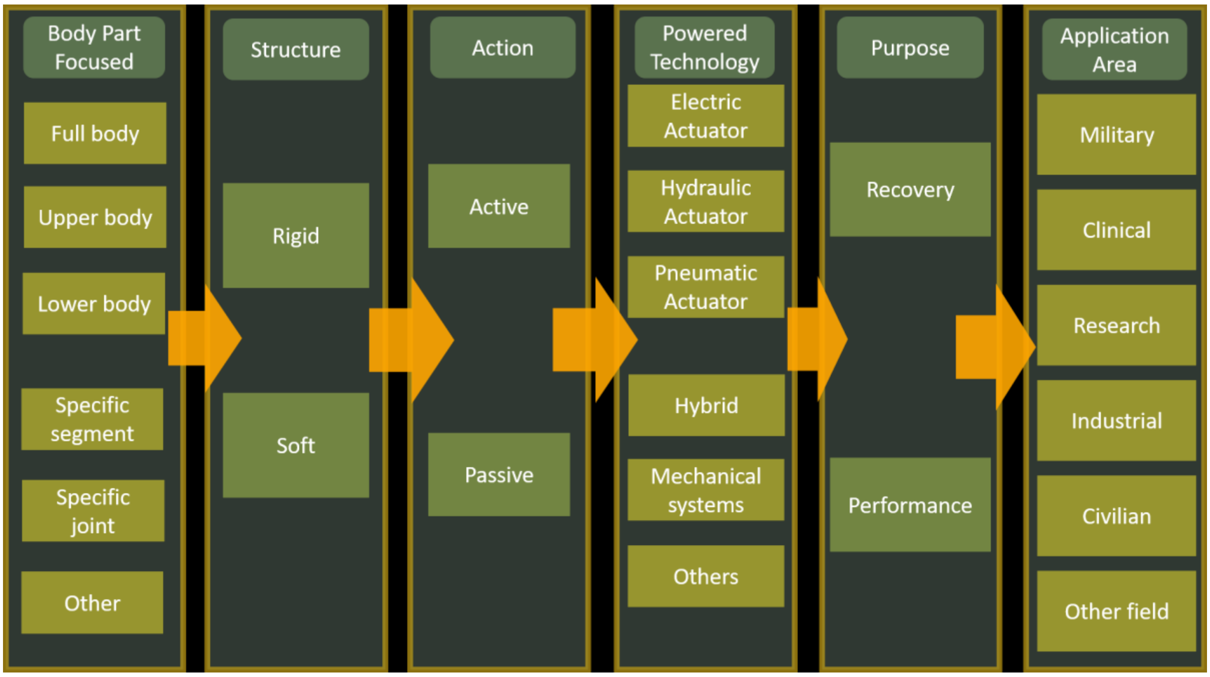

Figure 1.1.1: Types of Exoskeletons

Upper limb movement is very important for doing normal day to day activities; however, there are about 15 million people a year who suffer from stroke worldwide, with 5 million stroke survivors who experience permanent motor damage and require therapeutic and rehabilitation services overcome their injury and get some motor control back[8].

An exoskeleton is a wearable robotic device of the upper limb made to work comfortably with the human arm which will help in the rehabilitation of arm injuries and increase human muscle strength. The device is designed to apply a specific torque where the exoskeleton is attached [9].

The exoskeleton is a mechanical device that can increase the human arm strength and endurance. It detects the position of the exoskeleton and the movement intention of the human body in real-time through different sensing technologies. The brain sends relevant information to the muscles for movement and maintaining the human body. The exoskeleton can help the human arm movements by determining the trajectory by applying the necessary torque to the motors at the joints and can be predicted and incorporated into the control algorithm [10].

In recent years, there have been many myoelectric interfaces or devices using surface electromyogram signals that were developed for assisting people with physical injuries or disabilities. EMG has proven to be an essential tool in biomechanical investigations and is used to identify the exact muscle functions, injury location, pain, fatigue and other abnormalities [11].

The EMG signal is essentially a biomedical signal which measures electric currents generated within the muscular tissues. These currents are generated throughout the contraction of muscles representing neuromuscular activities. This neuromuscular activity is the result of a signal generated in the brain that is transmitted via the nervous system to the motor neuron connected to the muscle fibres within the muscle. A depolarization wave is generated throughout the muscle fibre when motor neuron fires which than creates an action potential within the muscle fibres resulting in the movement of electrical charges. This electric activity produces an electric signal in the muscle referred to as Electromyogram (EMG) signals [12]. Surface electromyographic (EMG) signals of patients with weak muscle in the arm have been found to have lower complexity and contain more rhythmic bursts compared to signals of healthy person’s arm. The muscle activation pattern differs from patients to patients with other motor diseases [13].

Physical sensors require some degree of volitional movement to trigger and those devices might not benefit patients who are unable to generate sufficient force to trigger robots. In contrast to physical sensors, bioelectrical sensors such as electromyography (EMG) sensors can detect patients voluntary muscle activation in real time and triggered the robot-assisted movement which could be beneficial for a broader range of patients [14].

Different types of exoskeleton prototypes:

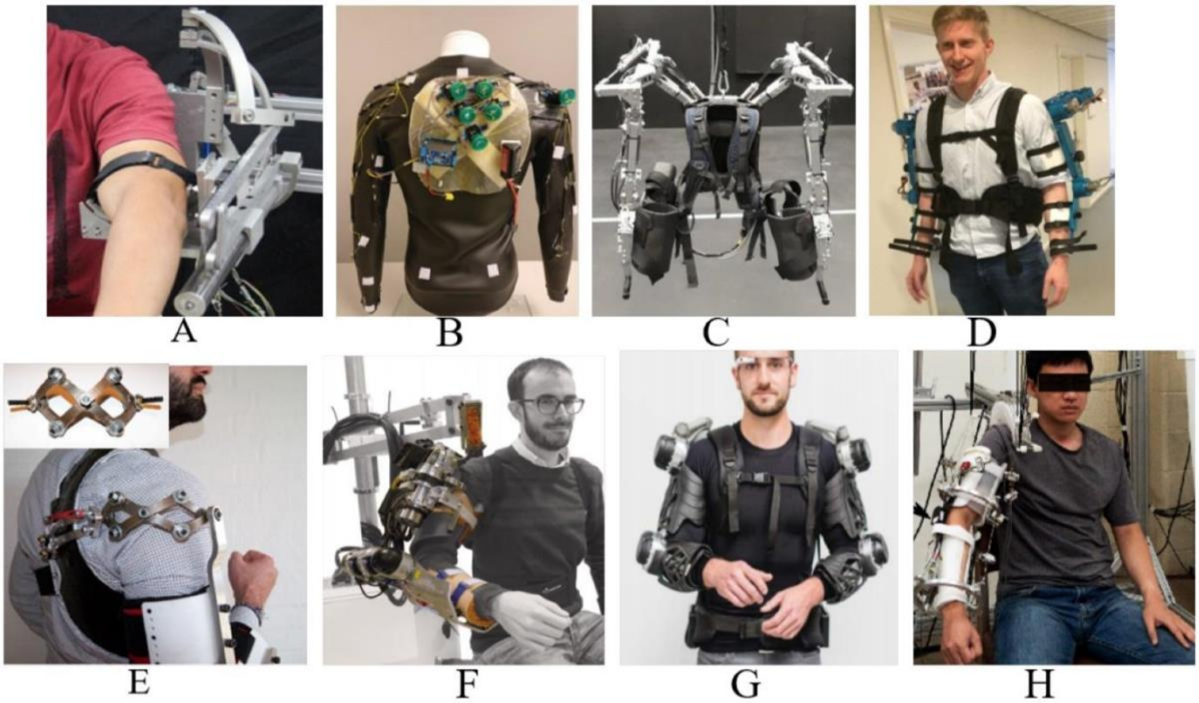

Figure 1.1.2

Figure 1.1.2 shows different types of exoskeleton prototypes

(A) parallel actuated shoulder exoskeleton [46].
(B) cmpliant robotic upper-extremity eXosuit (CRUX) [47].
(C) upper-limb exoskeleton for inferno [48].
(D) UB-EXO developed by Aalborg University [49].
(E) compact 3 degrees of freedom (DOF) scissors linkages for upper-limb exoskeleton [50].
(F) NESM [51].
(G) Stuttgart Exo-Jacket [52].
(H) CAREX 7 [53].

Even though there are different ways to help human beings to heal from their muscle injuries and motor disabilities, the resulting solutions for this issues are not always successful to help the patient with the injuries that they have sustained. Some of these solutions can be very expensive and not result in any improvement to the injuries. Only solutions to try and get your injuries healed is by going to the physiotherapy centres and getting the necessary help from the doctors. So basically, it means that physiotherapists get you involved in your own recovery and you have put in the efforts to do the exercises.

We propose a model that is fully automated and does not require any manual inputs. We develop and design an Upper Limb Exoskeleton to help the patients with a partially damaged arm. This model which was developed and designed using various technologies and components like the Myoware EMG sensor for acquisition of raw electromyogram signals from the arm. This signals are acquired in 7 channel mode. We used surface electrodes to extract the signals from the human arm which was then stored in the database for further execution. The database acquired is classified using various machine learning models. The database will help the model to learn about various predefined movements and position of the arm. This classified data is given to the ROS which can help the exoskeleton move accordingly with the help of various motors and joints in the structure. The exoskeleton was designed in Solidworks which is a software to design various 3-D models. The model is structured to have 7 DOF movements which will replicate the arm joint movements and have various flexibility of the human arm. This model is made to fit perfectly and comfortably on the human arm for easy use. The key element of our Upper Limb Exoskeleton is to support patients with weak arm during their recovery period and can also help elderly people for basic day to day life or be used in the industry for strength demanding tasks.

1.2 OBJECTIVE AND MOTIVATION

There is a growing population with limitations in day-to-day activities, the percentage of adults aged 18 years and above with limitations in this are increasing. People who are 75 years and above with limitations will require the help of another person when performing day to day activities. The limitations can range from physical or sensory impairments to cognitive and intellectual limitations.

Physical impairments are categorized into upper and lower limb, which can be caused due to trauma, muscular dystrophy, orthopaedic, stroke, and impairments in the central nervous system. Neuro-muscular impairments due to stroke affect a significant portion of the population around the world. 80% of all stroke survivors experience upper limb paresis, and only 18% of them gain full motor recovery within a year. Loss of upper limb motor functionality can significantly alter someone's quality of life and create emotional and physical burdens. However, some of these impairments could be recovered or improved by following proper therapy procedures. Traditional therapeutic techniques could be automated through robotic and exoskeleton systems to expedite the intervention and hence the recovery time.

The robotic assisted rehabilitation systems can be easily customized to adapt individual needs. The consistency and repeatability can be achieved when robotic systems are employed for rehabilitation. However, finding an exoskeleton design that fits and aligns properly with the human anatomical joints is very challenging. Misalignment can cause large stresses on attached systems and underlaying human anatomy. The misalignment and fitting challenges could result from the simplification of complex autonomy of human limb and joints into mechanically design exoskeleton joints.

Overall, understanding the correlation between parameters involved in joint movement mechanics as well as force interactions can provide insight in establishing an appropriate exoskeleton design. The main objective of this project is to design and develop a powered upper limb exoskeleton which is driven by EMG signals from the upper limb muscles to control and assist the movements of the joints. The proposed design is based on modelling and combining the robotic system with the human upper limb system bot electrically and mechanically. The materials should be cheap and readily available to provide a cost-effective powered system.

1.3: CONTRIBUTION

When we began working as a collective, none of us were very sure about how to proceed. We knew that for this to work everyone would have to take their roles within the group. As we were a small group everyone's full input indeed was necessary. Luckily everyone from our group was very committed to produce the best outcome we could and this involved not letting each other down. So we had divided our project into 3 parts were Shriraj was working on the database and the processing while Shawn was assigned the job of ROS and gazebo simulation and Nigel was given the job to design the exoskeleton arm in a 3D form.

At the beginning this work allowed us to have a lot of in dept discussions about the topic and all possible interpretations and meanings of our work. For a few days we all took a similar working roles where all were doing research on the same topic to collect information regarding our project. So as we went forward by deciding which EMG sensors and electrodes we would be using so we first ordered the sensor but simultaneously Shriraj was working on finding an appropriate database that could be used for our topic. Also, Shawn and Nigel were working on the hardware and software of how we could get proper EMG signals. So as days passed, the database was selected and the working was done by Shriraj and Shawn. All were helping each other since many things were new to learn. As we moved forward, we got signals and we tested the database, found the appropriate percentages.

The next task was learning about where the EMG signals can be detected on the arm. So for this we consulted with a physiotherapist and learnt where the main muscles were and where we could place the electrodes on the arm. There were 7 possible places so we took Shriraj as a subject and Shawn was dealing with the software and Nigel with the circuit connections. We took readings from 7 places on the arm and got a good signal. As this was done the next to move was on ROS and gazebo simulation. Here the task was given to Shawn and it was a challenging task since this topic was new and its working was quite different from other software's. All of us were involved to learn the installation and later Shawn learnt and created an arm in gazebo and using RVIZ. The final part was the 3d design which was given to Nigel where he and Shawn decided on which software we could use and which would be better supported for our needs of designing. Later the arm was designed under the guidance of our guides. It was designed and given for 3D printing.

For all of this to work it was very useful to have everyone's contribution as this created an open atmosphere where we could talk and give suggestions to each other which made a good bond among us and the ability to work and complete the task together.

CHAPTER 2:
LITERATURE REVIEW

LITERATURE REVIEW

Exoskeleton robotics has ushered in a new era of modern neuromuscular rehabilitation engineering and assistive technology research. The technology is to improve the upper-limb functionalities required for performing activities of daily living. Giving high utility and growing demand for upper-limb exoskeletons, the technology is still challenging in the area of mechanism designs, controls, and human–robot interaction. Mechanical design and kinematic analysis are the most crucial issues in developing an ergonomic exoskeleton system [15].

There are many talks about the hybrid exoskeletons, that combine electrically controlled actuation with functional electrical stimulation, potentially offer great benefits for muscular rehabilitation. The aim is always to provide an overview of the state of the art of current upper-limb hybrid exoskeletons with a focus on stroke rehabilitation. This field is still very new and further development of the current control methods used for hybrid exoskeletons is needed [16]. Ruben Fuentes-Alvarez et al, uses specific case of exoskeletons of the lower extremities, they generally depend only on control algorithms to develop the trajectories of the user's lower extremities. They also implement electromyography (EMG) interfaces as separate systems for measuring patient activity or improvements in the rehabilitation of the musculoskeletal system that carry their devices. The author uses a human in the loop scheme, a combination of a recurrent neural network (RNN) and an adaptive non-singular fast terminal sliding mode controller (ANFTSMC) strategy is employed to classify the user's movements and control the trajectories of an exoskeleton. This paper presents the construction of the electromyographic signals (EMGs) database, containing data acquired from brachii biceps and sternocleidomastoid muscles. This work is established, with the advantage of being an effective, precise, and intelligent system that can be used by people with high degrees of motor disability [18].

Christine Linnenberg et al, investigated the pressures occurring within the arm human-machine-interfaces (HMI) of four different exoskeletons that support static and dynamic work at or above head level, and the effects of the HMI on neurovascular supply of the upper extremity using an orthopaedic provocation manoeuvre with raised arms with and without the exoskeletons. Here, the decreased time in the provocation manoeuvre with exoskeletons indicated a negative effect of the HMIs on the vascular and neural supply of the arm. The pressures were higher than the pressure values that guarantee adequate tissue oxygenation. It remains unknown whether the way exoskeletons apply pressure affects vascular and neural supply to the arms, or whether the regular unloading during dynamic activity has a neutralizing effect [19].

Triwiyanto et al, found that the EMG signal has a random and stochastic characteristics, so it is difficult to predict the amplitude. The EMG signal also depends on the electrode's location. Therefore, a proper muscle selection determines the system's accuracy value. They studied and investigated the exact location of the electrodes to improve the accuracy of the wearable hand exoskeleton trainer based on electromyography (EMG) signal control. The discovery of the dominant muscle was carried out by investigating the dominant EMG signal in three muscles that plays a role in the open and close movements of the hand exoskeleton. Electrode was used to detect EMG signal activity and the EMG signal was then extracted using the root mean square (RMS) feature. After the evaluation, the results showed that the flexor digitorum superficialis muscle in the rest position produced higher accuracy value than the other muscles, which was 96.63±0.67% [20]. The same author also studied on another thesis using freedom of speech to control the exoskeleton. This is based on the number of exoskeletons that are controlled using the EMG signal where the EMG signal itself has the weakness of the complexity of the signal which is influenced by the position of the electrodes as well as muscle fatigue. The two feature extraction types namely mel-frequency cepstral coefficient (MFCC) and zero-crossing (ZC), and two machine learning algorithms, namely K-nearest Neighbour (K-NN) and Decision Tree (DT) was evaluated to get the relevant outcomes. A microphone was used to record voice commands and after model evaluation, it was found that the MFCC extraction combined with the K-NN algorithm and the best accuracy 96±7.0% and the accuracy is 79±14.46% and 90±14.14% for open and close commands [21].

To improve the classification framework by identification of the relevant feature that drive the pattern recognition algorithm. A. C. Turlapaty et al., [54] used a set of modified spectral moment-based features and another relevant inter-channel correlation feature that contribute to an improved classification performance and also conducted a sensitivity analysis of the classification algorithm to different EMG channels. Necmettin Sezgin et al.[55], analysed the EMG signal using bispectrum, which belongs to a family of higher-order spectra. The aggressive and normal EMG activities were analysed using bispectrum and the quadratic phase coupling of each EMG episode was determined. The best classification result was 99.75% for ELM which gave better accuracy than ANN, SVM, LR and LDA. Omer Alcin et al.[56], proposed method is composed of signal decomposition, feature extraction and feature classification. The signal decomposition is carried out using the wavelet packet transform (WPT). A one-dimensional local binary pattern (LBP) is used to code the approximation and detail coefficients of the decomposed EMG signals. The support vector machine (SVM), decision tree, linear discriminant, k-nearest neighbors (k-NN), boosted and bagged tree ensemble classifiers are used in the classification stage. N. Sukumar et al.[57], proposed an efficient method based on variational mode decomposition (VMD) is proposed for identification of physical activities of sEMG signals. VMD is an adaptive and non - recursive signal decomposition method which decomposes sEMG signals into several modes. Extracted features are fed into the multiclass least squares support vector machine (MC-LS-SVM) classifier with radial basis function (RBF) in order to classify normal physical actions of surface EMG signals. The performance of obtained results shows better classification accuracy of 98.17%.

Suman Samui et al, focused on data acquisition, pre-processing, feature extraction and classification along with their feasibility in practical scenarios regarding implementation and reliability. They have demonstrated Deep Neural Network (DNN) based classification system for the upper limb position invariant myoelectric signal. The classification of eight different hand movements is performed using a fully connected feed-forward DNN model and also compared with the existing machine learning tools. The time domain power spectral descriptors (TDPSD) are used as the feature set to train the DNN classifier. The experimental results in various analysis frameworks demonstrate that DNN based system can outperform the other existing classifiers such as k-Nearest Neighbour (kNN), Random Forest, and Decision Tree. The average accuracy obtained among the five subjects for DNN, SVM, kNN, Random Forest and Decision Tree is 98.88%, 98.66%, 90.64%, 91.78%, and 88.36% respectively [25]. Toledo-Pérez used SVM to classify the EMG signals. The paper includes the accuracy, the number of signals or channels used, the way the authors made the feature vector, and the type of kernels used and also includes a compilation about the bands used to filter signals, the number of signals recommended, the most commonly used sampling frequencies, and certain features that can create the characteristics of the vector [27].

Fahreddin Sadikoglu et al, talk about how EMG signals are usable in the applications of biomedical, clinical, modern human computer interaction and Evolvable Hardware Chip (EHW) improvement. Advanced methods are needed for perception, disassembly, classification and processing of EMG signals acquired from the muscles. Objective of this paper is to show various methods and algorithms in order to analyse an electromyogram signal to ensure effective and efficient ways of understanding signal and its nature. The latest diagnostic methods include evaluating the patient's story, blood tests, and muscle biopsies. System has been successfully implemented utilizing MATLAB software that can distinguish EMG signals from different patients [26].

Eric Weston et al, evaluated the three passive upper-extremity exoskeletons relative to a control condition. Independent measures of exoskeleton, exertion height (overhead, head height), time, and their interactions were assessed. Dependent measures included changes in tissue oxygenation (DTSI) in the anterior deltoid and middle trapezius, peak resultant lumbar spine loading, and subjective discomfort in various body regions. The experimental task was not highly fatiguing to the subjects, denoted by low DTSI values across conditions. Results may vary for tasks requiring constant arm elevation or higher force demands. This study quantified the benefits of upper-extremity exoskeletons using NIRS, complementary to prior studies using EMG. The exoskeletons offered little to no physiological benefit for the conditions tested. However, the results may vary for a task with greater demand on the shoulders [22].

Pawel Herbin et al, shows that the exoskeleton of the upper limb is an external parallel kinematic chain to the human arm. The device is designed to apply a specific torque of interaction to the human body resulting from bilateral teleoperation or rehabilitation. The author presents the structure of the developed device and the control system of its joints. The construction of the joints drive system was performed based on the Bowden cable transmission. Based on the Bowden cable flexibility, it is possible to control the generated drive torque following the serial elastic actuator concept. They also showed the methods of estimating the torque of interaction with the operator based on the ExoArm 7-

DOF exoskeleton dynamics model [17]. Chuang Liu et al, reviews the research on upper limb exoskeleton for hemiplegia rehabilitation. Under the condition of rehabilitation training for mild patients in the workspace of 7-DOF exoskeleton with uncertain trajectory, a control algorithm used for motion detection is carried. This paper shows the algorithm where the patient's operation can be detected by real-time data collected by Force/Torque sensors and encoders, so that quantitative assistance will be supplied by exoskeleton according to the patient's motion intention. The joint simulation of ADAMS and MATLAB proves the accuracy of trajectory tracking and the feasibility of the control strategy is verified by the experiment on 3-DOF translational manipulator platform [23].

Feilong Jiang et al, shows how the biceps and triceps alternatively act as agonists and antagonists to realize upper limb movement. Pneumatic artificial muscle (PAM), which is inflated and deflated with compressed air instead of water, has similar characteristics to those of human muscle. They wanted to find precise signal collection and control process and adopt the synergy control of PAM and upper limb. In this system, the biceps and triceps provide the main signals in synergy control, electrodes are pasted outside of biceps and triceps to sample their electromyogram signal (EMGs), and the mechanical structure and control system of the pneumatic exoskeleton are proposed. The envelope is taken to extract muscle contraction information through upper limb muscles in a static contraction experiment. Then, the processes of biceps and triceps EMGs feature changes including rapid swing, slow swing, and discontinuous swing under various loads are analysed during upper limb muscle dynamic contraction. The duty-ratio-controlled variables can be divided into five levels, which correspond to exertion rating from powerless to very strong in two EMG characters. These can be reflected in a scatter diagram of duty-ratio-controlled variables and average EMG characters. A nonlinear relationship can be transferred into the continuous system by the polynomial interpolation method, solving the problem of saturation. The net duty-ratio-controlled variables are adopted to control the on-off state and pulse-width modulation (PWM) duty ratio of the high-speed on-off valve. The forearm lifting up movement is unpowered and powered with various load EMGs, and elbow discontinuous swing angle overshoot is performed to analyse the coordination effect in a synergy control experiment [24].

The majority of the studies made were performed on a single user, focusing solely on the gesture classification. These studies are restrictive in practical sense because it is either focusing on just gestures, multi-user compatibility, or rotation independence. The variations in EMG signals due to these conditions present a challenge to the practical application of EMG devices, often requiring repetitious training per application. Fu zinvi et al, presented a review of works related to the practical issues of EMG with a focus on the EMG placement, and recent acquisition and computing techniques to reduce training. They also provided an overview of existing electrode placement schemes and compared the techniques and results of single-subject against multi-subject, multi-position settings [30]. Akira Furui et al, has utilized EMG signal to interface signals for prosthetic hands and information devices owing to its ability to reflect human motion intentions. An EMG pattern classification method incorporating a scale mixture-based generative model was used. A scale mixture model is a stochastic EMG model in which the EMG variance is considered as a random variable, enabling the representation of uncertainty in the variance. The proposed method is trained by variational Bayesian learning, thereby allowing the automatic determination of the model complexity. The comparison using public EMG datasets revealed that the proposed method outperformed the various conventional classifiers [29].

Glowinski uses the kinematic modelling of an arm exoskeleton for human rehabilitation. The biomechanics of the arm was studied and the 9 Degrees of Freedom model was obtained. The model of upper arm was obtained by using

Denavit – Hartenberg notation. The exoskeleton human arm was modelled in MathWorks package. The optimal solutions were found applying a genetic algorithm. Two variants of motion with and the visualization of the change of joints angles were shown. By the use of genetic algorithms, movement trajectory with the Pareto-optimum solutions has been presented as well. Creating a utopia point, it was possible to select only one solution from Pareto-optimum results. The obtained results demonstrate the efficiency of the proposed approach that can be utilized to analyse the kinematics and dynamics of exoskeletons using the dedicated design process [28]. Redundancy resolution techniques have been widely used for the control of kinematically redundant robots. Maaroof et al, uses one of the redundancy resolution techniques that is employed in the mechanical design optimization of a robot arm. Although the robot arm is non-redundant, the proposed method modifies robot arm kinematics by adding virtual joints to make the robot arm kinematically redundant. The robot arm's end-effector is fixed at critical positions while the redundancy resolution algorithm moves its joints including the virtual joints because of the self-motion of a redundant robot. Hence, the optimum values of the virtual joints are determined, and the design of the robot arm is modified accordingly [36].

Simulators are being used more and more during the development of robotic systems due to the efficiency of the development and testing processes of such applications. These simulators save time, resources and costs, as well as enable ease of demonstrations of the system. Specifically, tools like the open-source Robotic Operating System (ROS) and Gazebo have gained popularity in building models of robotic systems. ROS is extensively used in robotics due to the pros of hardware abstraction and code reuse. The Gazebo platform is used for visualisation because of its high compatibility with ROS. Al-Rashid Agha et al, have integrated ROS and Gazebo to build an interface for the visualisation of the Katana Arm manipulator. Simulators for robots are used to build embedded applications for any robot without having the need to depend on the actual device and the applications can even be transmitted onto the actual robot directly due to the functionality of the simulators [31].

Similarly, the autonomous robots are playing an important role to solve the Simultaneous Localization and Mapping (SLAM) problem in different domains. To generate flexible, intelligent, and interoperable solutions for SLAM, it is a must to model the complex knowledge managed in these scenarios (i.e., robots characteristics and capabilities, maps information, locations of robots and landmarks, etc.) with a standard and formal representation. Some studies have proposed ontologies as the standard representation of such knowledge; however, most of them only cover partial aspects of the information managed by SLAM solutions. M. A. Cornejjo-Lupa made a model called OntoSLAM, which models all aspects related to autonomous robots and the SLAM problem, towards the standardization needed in robotics, which is not reached until now with the existing SLAM ontologies. Additionally, OntoSLAM was integrated into the Robot Operating System (ROS) and Gazebo simulator to test it with Pepper robots and demonstrate its suitability, applicability, and flexibility. Experiments show how OntoSLAM provides semantic benefits to autonomous robots, such as the capability of inferring data from organized knowledge representation, without compromising the information for the application and becoming closer to the standardization needed in robotics [32].

An autonomous mobile robot must be able to generate a collision-free trajectory while avoiding static and dynamic obstacles from the specified start location to the target location. Machine learning, a subfield of artificial intelligence, is applied to create a Long Short-Term Memory (LSTM) neural network that is implemented and executed to allow a mobile robot to find the trajectory between two points and navigate while avoiding a dynamic obstacle. The input of the network is the distance between the mobile robot and the obstacles thrown by the LiDAR sensor, the desired target location, and the mobile robot's location with respect to the odometry reference frame. Using the model to learn the mapping between input and output in the sample data, the linear and angular velocity of the mobile robot are obtained. The mobile robot and its dynamic environment are simulated in Gazebo, which is an open-source 3D robotics simulator which is synchronized with ROS (Robot Operating System). The computational experiments show that the network model can plan a safe navigation path in a dynamic environment [35].

The fusion of different technologies is the base of the fourth industrial revolution. Companies are encouraged to integrate new tools in their production processes in order to improve working conditions and increase productivity and production quality. The integration between information, communication technologies and industrial automation can create highly flexible production models for products and services that can be customized through real-time interactions between consumer, production and machinery throughout the production process. The future of production, therefore, depends on increasingly intelligent machinery through the use of digital systems. The key elements for future integrated devices are intelligent systems and machines, based on human–machine interaction and information sharing. The implementation of shared languages that allow different systems to dialogue in a simple way is necessary. In this perspective, the use of advanced prototyping tools like Open-Source programming systems, the development of more detailed multibody models through the use of CAD software and the use of self-learning techniques will allow for developing a new class of machines capable of revolutionizing our companies. Rivera et al, presents a waypoint navigation activity of a custom Wheeled Mobile Robot (WMR) in an available simulated 3D indoor environment by using the Gazebo simulator. They tested the high-performance physics Open Dynamics Engine

(ODE) and the sensor feature present in Gazebo for prototype development activities. The integration tools available with Solidworks and MATLAB-Simulink, well known commercial platforms of modelling and robotics control were explored [33].

Guowei Cui et al, aims to test and evaluate task planning algorithms. After building the environment and the service robot model, a 2D map is built. To make use of semantic navigation, they construct a topological map from the 2D map. Several functions are written to realize the robot's necessary actions, including navigation, grasping, placing, handing over, and searching person/object. They test the task planning system within the uncertain Gazebo environment [34].

Effective control of trunk muscles is fundamental to perform most daily activities. Stroke affects this ability also when sitting, and the Modified Functional Reach Test is a simple clinical method to evaluate sitting balance. Marchesi et al, characterizes the upper body kinematics and muscular activity during this test. They mainly focused on the analysis of muscles of the trunk and of the contralesional, not moving, arm. The bilateral activations of latissimus dorsi, trapezii transversalis and oblique externus abdominis were left/right asymmetric, for both test directions, except for the obliquus externus abdominis in the frontal reaching. Stroke survivors had difficulty deactivating the contralesional muscles at the end of each trial, especially the trapezii transversalis in the lateral direction. Core stability and proper trunk muscle control are fundamental in most daily living activities, such as standing up, sitting down, walking and stabilizing distal limbs. Both are necessary for sitting balance, to maintain stable posture and to shift the body weight inside the base of support while performing a variety of self-initiated actions, such as eating or taking a glass from the table. Following a stroke, the upper motor neuron syndrome induces abnormal muscular activations and motor patterns, with phenomena categorized as “positive” or “negative” in relation, respectively [37].

Most humanoid robots are equipped with seven-degree-of-freedom (DoF) arms that allow them to be flexible in different scenarios. To date, no suitable approach has been developed for identifying appropriate human-like postures for a robotic arm with an offset wrist configuration. Y. Deng et al, proposed a novel algorithm that considers the movement of the human arm to consistently find a suitable human-like posture. A one-class support vector machine model is employed to classify human-like postures. Then, the algorithm uses the redundancy characteristic of a 7-DoF robotic arm with a linear regression model to enhance the search of human-like postures [38].

Modelling errors and robust stabilization/tracking problems under parameter and model uncertainties complicate the control of the flexible underactuated systems. A lightweight robot arm subject to external and internal dynamic effects was taken into consideration. The precise control of this kind of system demands an accurate system model and knowledge of all sources that excite unmodeled dynamics. The equations of motion for a flexible robot arm were derived and formulated for the large motion via Lagrange’s method. The goals were determined to achieve high-speed, precise position control, and satisfied accuracy by compensating the unwanted torque ripple and friction that degrades performance through an adaptive robust control approach. A 2-DOF flexible robot arm considering actuator dynamics was modelled, and the theoretical implication of the chattering-free sliding mode-adaptive linearizing algorithm, which ensures robust stabilization and precise tracking control, was designed based on the full system model including actuator dynamics with computer simulations. Stability analysis of the zero dynamics originated from the Lyapunov theorem was performed. The conceptual design necessity of nonlinear observers for the estimation of immeasurable variables and parameters required for the control algorithms was emphasized [39]. In recent years, dual-arm robots have attracted more and more attention due to their advantages such as strong cooperation ability and high flexibility. With the improvement of real-time requirement of dual-arm cooperation, the inverse kinematics solution of robot becomes a key problem to be solved urgently. To solve the time-consuming problem of inverse kinematics of robot arm, a closed inverse kinematics solution algorithm for humanoid dual-arm robot was proposed by wang et al. The inverse kinematics of manipulator mainly includes geometric method, analytical method and numerical method. The geometric method is a special case of analytic method in some cases, and its applicability is weak. Analytical inverse kinematics of the manipulator can efficiently obtain all the inverse solutions of the manipulator in the desired position, but the manipulator must satisfy the Piper criterion. The numerical method has no special requirements for the joint number and structure of the manipulator [40].

The body articulation units, commonly referred to as body joints, play significant roles in the musculoskeletal system, enabling body flexibility. These articulation units suffer from several pathological conditions, such as osteoarthritis (OA), rheumatoid arthritis (RA), ankylosing spondylitis, gout, and psoriatic arthritis. There exist several treatment modalities based on the utilization of anti-inflammatory and analgesic drugs, which can reduce or control the pathophysiological symptoms. Despite the success, these treatment modalities suffer from major shortcomings of enormous cost and poor recovery, limiting their applicability and requiring promising strategies. To address these limitations, several engineering strategies have been emerged as promising solutions in fabricating the body articulation as unit models towards local articulation repair for tissue regeneration and high-throughput screening for drug development. They have presented challenges related to the selection of biomaterials (natural and synthetic sources), construction of 3D articulation models, architectural designs and the type of culture conditions [43].

Voluntary hand movements are usually impaired after a cerebral stroke, affecting millions of people per year worldwide. The use of hand exoskeletons for assistance and motor rehabilitation has become increasingly widespread. So D. Esposito et al, designed a model to be low cost, wearable, easily adaptable and suitable for home use. Most of the components of the exoskeleton are 3D printed, allowing for easy replication, customization and maintenance at a low cost. A strongly underactuated mechanical system allows one to synergically move the four fingers by means of a single actuator through a rigid transmission, while the thumb is kept in an adduction or abduction position. Force-myography was used instead of the standard electromyography to voluntarily control the exoskeleton with more simplicity. The user can activate the flexion/extension of the exoskeleton by a weak contraction of two antagonist muscles. The entire exoskeleton including batteries can be worn on the patient's arm. The trajectories described by the phalanges of the natural and the exoskeleton finger were compared by means of cross-correlation coefficients; a similarity of about 80% was found. A rigid cylindric handlebar containing a load cell measured an average power grasp force of 94.61 N, enough to assist the user in performing most of the activities of daily living [41]. Optimal ergonomic design for consumer goods (such as garments and furniture) cannot be perfectly realised because of imprecise interactions between products and human models. Cheng Chi proposed a new body classification method that integrates human skeleton features, expert experience, manual measurement methods, and statistical analysis (principal component analysis and K-means clustering). The method enables the classification of upper bodies into a number of levels at three key body segments. From several experiments, they found that the proposed method can lead to more accurate results than the classical classification methods based on three-dimensional (3 D) human model and can provide semantic knowledge of human body shapes [42].

CY Lee talked about how the natural human motion was modelled using a three-dimensional simulation involving a biped robot. Exoskeleton assistance was examined through the extraction and analysis of kinematic and dynamic parameters. The present findings can serve as a reference for a study on exoskeleton design in which user effort is considered. A biped robot simulator of human gait was constructed. A participant's movement was recorded using a Vicon motion capture system. The effect of exoskeleton assistance on gait performance was evaluated under admittance control for user interaction [44]. Wearable pressure sensors are highly desirable for monitoring human health and realizing a nice human–machine interaction. CS/MXene/PU sponge/PVA - based 3D pressure sensor is developed to simultaneously achieve wearability, washability, and high sensitivity in a wide region. In the force-sensitive layer of the sensor, MXene and CS are fully attached to the PU sponge to ensure that the composite sponge has remarkable conductivity and washability. Benefiting from the highly resistive PVA-nanowire spacer, the initial current of the sensor is reduced significantly so that the sensor exhibits extremely high sensitivity (84.9 kPa^{-1} for the less than 5 kPa region and 140.6 kPa^{-1} for the 5–22 kPa region). The sensor has an excellent fast response time of 200 ms and a short recovery time of 30 ms, as well as non-attenuating durability over 5000 cycles. With the high sensitivity in a wide range, the sensor is capable of detecting multiple human and animal activities in real time, ranging from the large pressure of joint activities to a subtle pressure of pulse. Overall, such a multifunctional pressure sensor can supply a new platform for the design and development of wearable health-monitoring equipment and an efficient human–machine interface [45].

CHAPTER 3: METHODOLOGY

3.1: SYSTEM BLOCK DIAGRAM

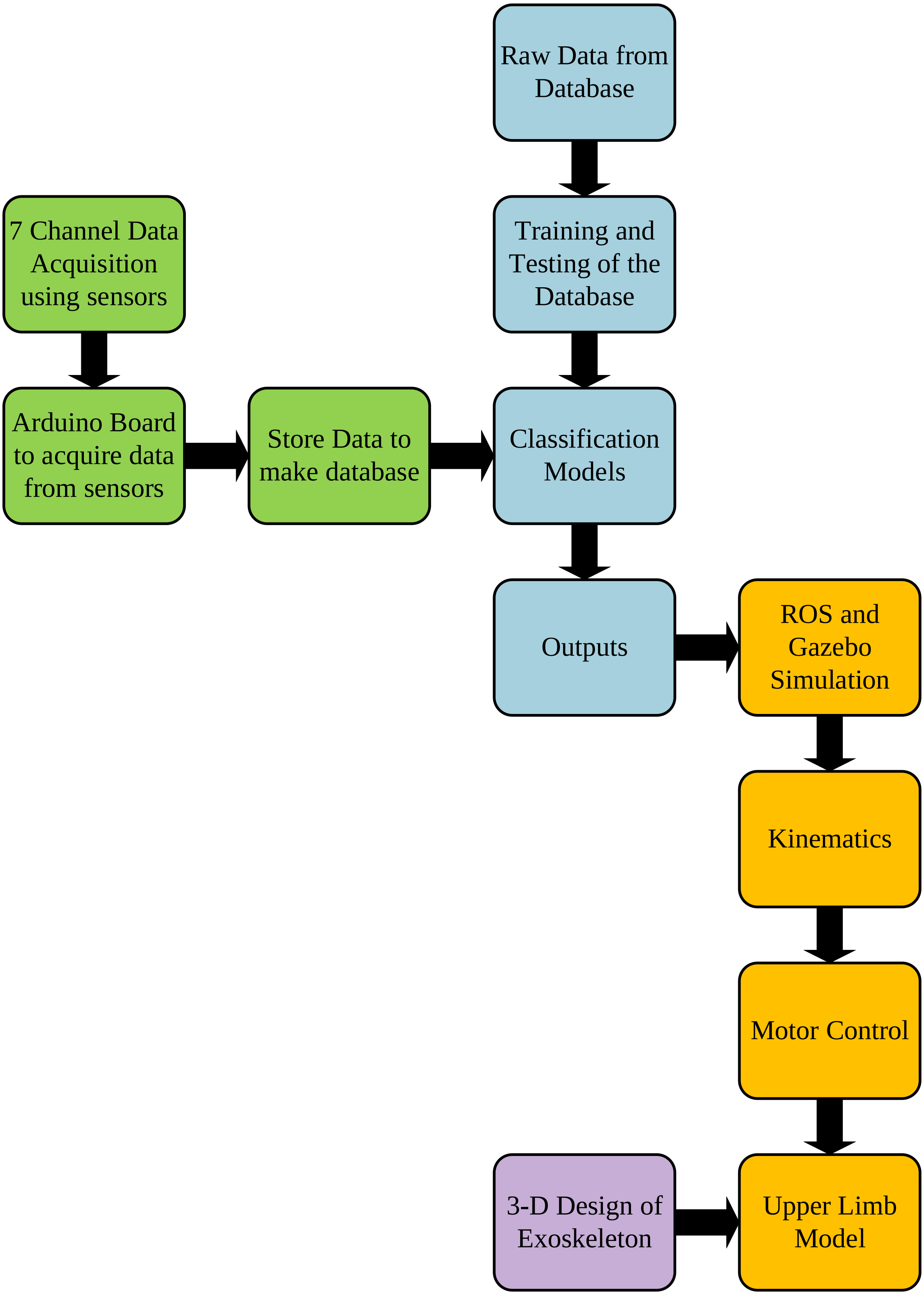

Figure 3.1.1: Block Diagram

3.2: WORKING PRINCIPLE:

The system block diagram in Figure 3.1.1 shows the overview of the whole process. This is the working of the upper limb exoskeleton. The model is fully automated and does not require any manual inputs. This model uses the Myoware EMG sensor placed at the 7 areas of the arm for the acquisition of raw electromyogram signals. These signals are acquired in 7 channel mode using the Arduino board and Arduino IDE to view the waveforms. Medical grade surface electrodes were used to extract the signals from the human arm which was then stored in our own database for further execution. The database acquired is classified using various machine learning models. The classification model is trained using other databases to get better accuracy for training and testing. The outputs from the models are than given to the ROS – Gazebo system for running of the motors and other various joints according to the pre-defined movements and positions of the arm from the classification model. The upper limb exoskeleton 3D model is designed in Solidworks and is structured to have 7 DOF movements which will replicate the arm and shoulder joint movements and have more flexibility of the human arm. The 3D file is given for 3D printing to get the final base of our model. This model is made with proper dimensions to fit perfectly and comfortably on the human arm for easy use and should be cost effective.

Block Diagram Description:

The first part of the system is to collect the signals from the human arm. The signals are collected using a sensor called Myoware Muscle Sensor. It's an advance sensor which has a lots of features like the inbuilt 3 electrode connectors which are the Mid-muscle Electrode, End of Muscle electrode and the Reference Electrode as seen in Figure 3.2.1 so that everything is in for easy use.

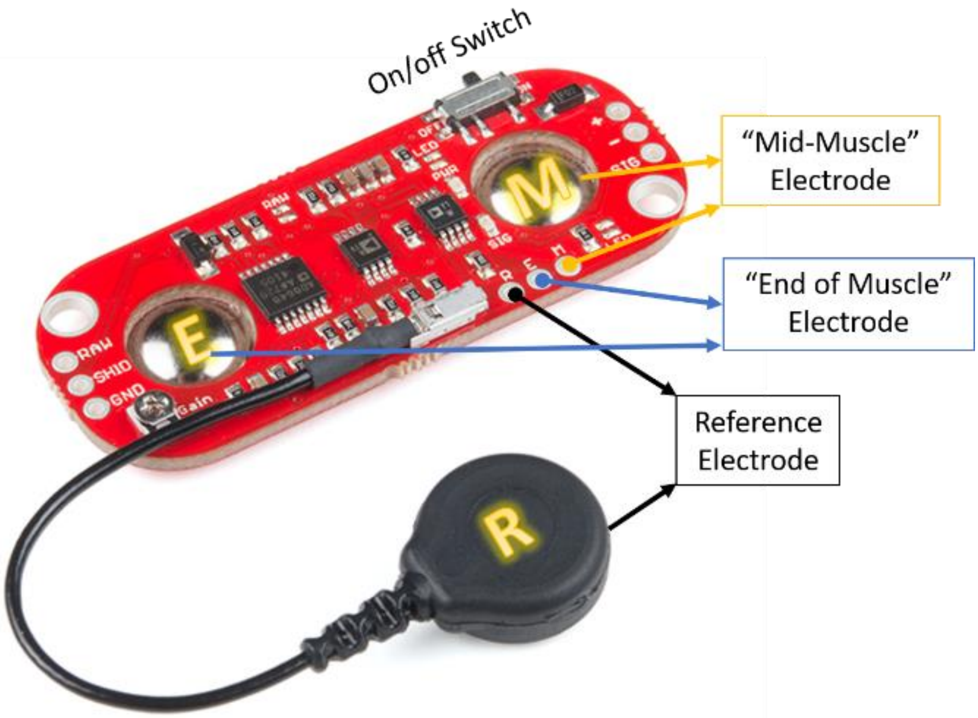

Figure 3.2.1: Electrode Connectors

The electrodes are placed on the arm in specify places to extract the signals. Out of the 3 surface electrodes connected, 2 of them are placed on the muscle area to record the signals and the other one is the ground connection to be placed on bone area. For 7 channel data collection we placed the electrodes and sensors on 7 main muscle places of the arm are Bicep Brachii, Brachialis (Above Elbow), Tricep Brachii, Brachioradialis (Below Elbow), Extensor Carpi Radialis Longus (Exterior Forearm), Flexor Carpi Radialis (Inner Forearm), Flexor Carpi Ulnaris (Wrist). The proper placement of sensor is shown in Figure 3.2.2 to get accuracy and better signal values.

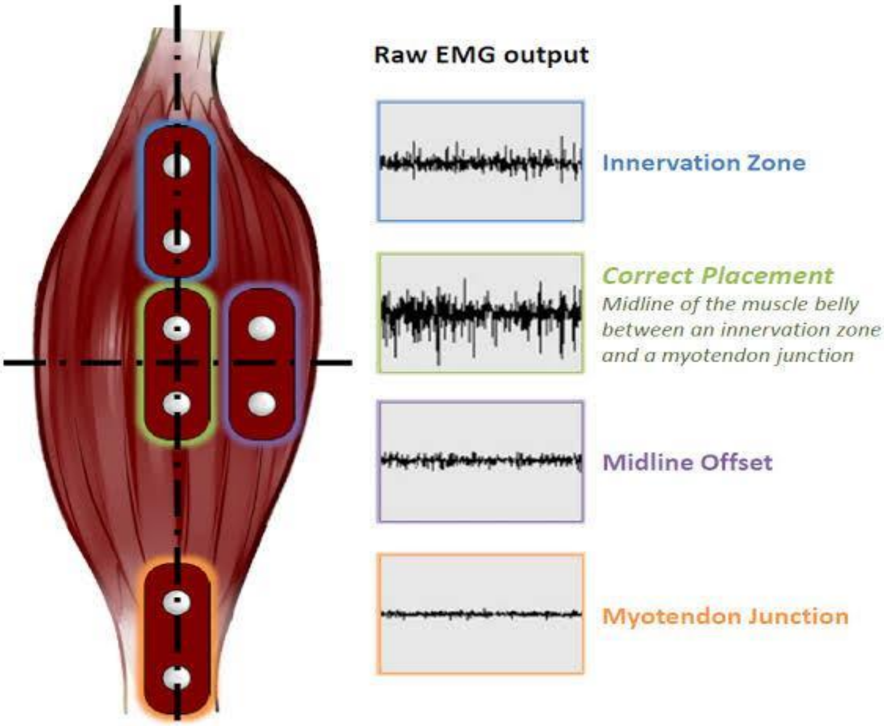

Figure 3.2.2: Sensor Placement

When the muscle is flexed in a certain way, the sensor acquires and converts the EMG signals from physical parameters to electric analog signal through the surface electrodes. This analog signal can be read by the Arduino board to view the results on the Arduino IDE.

The Arduino board is connected to the sensor with 3 pins. The main pin is the signal pin from the Myoware board to the analog pin. The other 2 pins are the +5V and ground pin as seen in Figure 3.2.3. Using the Arduino board the analog signals from the sensor are connected to the analog pin of the Arduino board so it can read the values. The script is written to read the analog value at the pin assigned which converts the analog signal to digital signal. This digital signal can be viewed in the serial plotter of the Arduino IDE software and also as values in the serial monitor. The analog values from the ADC are converted to millivolts or volts which are displayed on the serial monitor of the IDE software for the data to be viewed. This data from the serial monitor can be pasted in a text file for later.

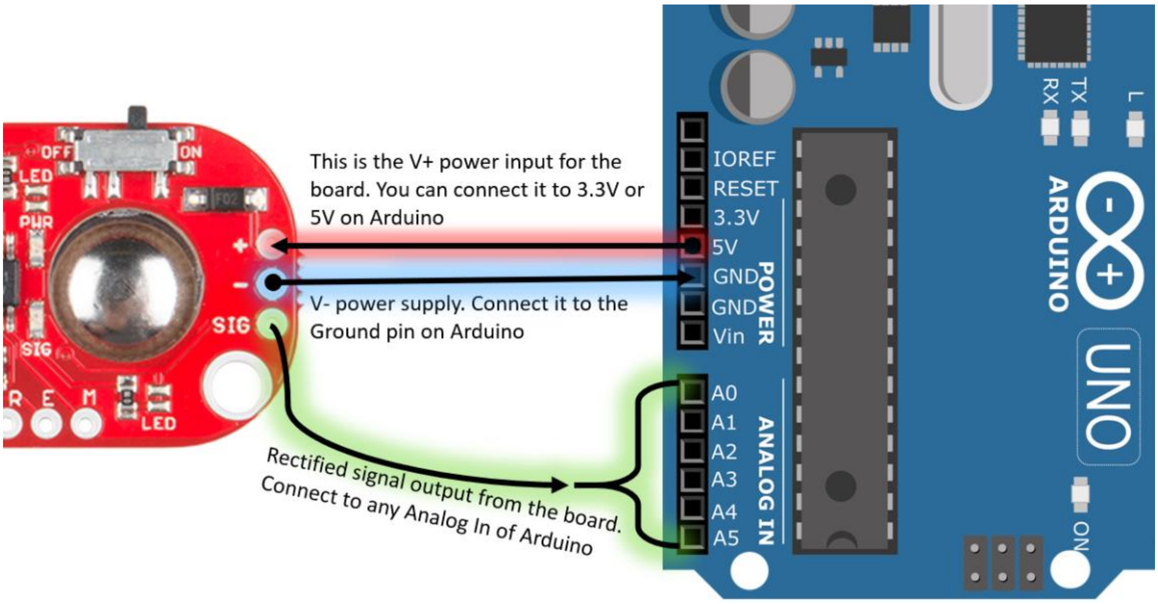

Figure 3.2.3: Sensor to Arduino Connection

For the database classification section of this system, we use the raw text files from the database which are separated subject wise as well as each individual action performed. In each text file there are approx. 10000 rows taken over a period of 15 seconds and has 8 columns which are the 8 channels from the database where 8 sensors were placed to acquire the data from the subjects. The 8 sensors are placed on the upper arms (biceps and triceps), and upper legs (thighs and hamstrings) namely at Right bicep (Channel 1), Right tricep (Channel 2), Left bicep (Channel 3), Left tricep (Channel 4), Right thigh (Channel 5), Right hamstring (Channel 6), Left thigh (Channel 7) and Left hamstring (Channel 8). Through these sensors the data was recorded for 20 actions. Out of those 20 actions 10 were normal and 10 were aggressive actions.

All the data from the text files were raw so they were filtered using the Savitzky-Golay filter in MATLAB. The filter is applied to a set of digital points for smoothing the data to get better signals. This processed data is saved in text file like the original data. Now from the text file the feature extraction is done in python using the code of sliding window and after extraction of feature it is saved in as csv file. This csv file is than used for the classification of the data. The data from these files are divided into normal and aggressive. There are 3 types of models that were used for classification. They are Logistic Regression, random Forest and Naïve Bayes. Before giving this data to the classification models it has to be standardized to get better data for the models. Due to the poor dimension ratio, four cross validations in which there is training models on three subjects and testing on the one left out in the subject in each loop. Using these methods, we obtain the accuracies for the different classification models.

The ROS-Gazebo part in this system is used to design the simulation of the robotic movement of the upper limb exoskeleton. Here the Robot Operating System is used to get the relevant packages to be used to make the model. There is a URDF code written which has all the relevant links and connectors like the revolute joints and fixed links to make a simulation to make the model move and depict a real system. The rviz software is used to show the inside controls of the robotic model and the gazebo actually shows the simulation. Inverse kinematics are used for the calculations of joint parameters to handle the orientation and positions. The model can be made to show many degrees of freedom. This data can be used to move the motor and control the exoskeleton arm with all the data.

For the 3D design of the arm exoskeleton, we used solidworks. In the software we decide a drawing layout for the entire arm. It is a tap down approach to assemble all the back part to the curve which is done by a layout sketch or the geometry of other part. We created a layout in the assembly slide and we draw the parts of the arm, the back, curve, and the side parts. This is then converted into sketch entities. We also made holes for the motors which can be used for the movement. From the sketch the entire arm is assembled together. So after that we applied the fillet and give a proper appearance to it. The fillet creates internal or external face on the part and the same slide is taken from the sketch part and dropped onto the layout. After that we built a wrist support stand. We went to shapes and took a small rod for the support of the wrist and hand. The joints are made by drawing slot to join the joints. The curve was made like an arc in the part file so then we construct the arc. Finally, all these parts are assembled together and the whole arm is ready. So, with this all components of arm designed in various modules to obtain the final designed model.

3.3 EMG SENSOR CIRCUIT

The Myoware Muscle Sensor measures, filters, rectifies, and amplifies the electrical activity of a muscle and produces an analog output signal that can easily be read by a microcontroller, enabling novel, muscle-controlled interfaces. This muscle sensor measures a muscle's activity by monitoring the electric potential generated by muscle cells. This is referred to as electromyography (EMG). The sensor amplifies and processes the complex electrical activity of a muscle and converts it into a simple analog signal that can easily be read by any microcontroller with an analog-to-digital converter (ADC), such as an Arduino or even a Maestro servo controller.

The internal circuit diagram is shown below in Figure 3.3.1

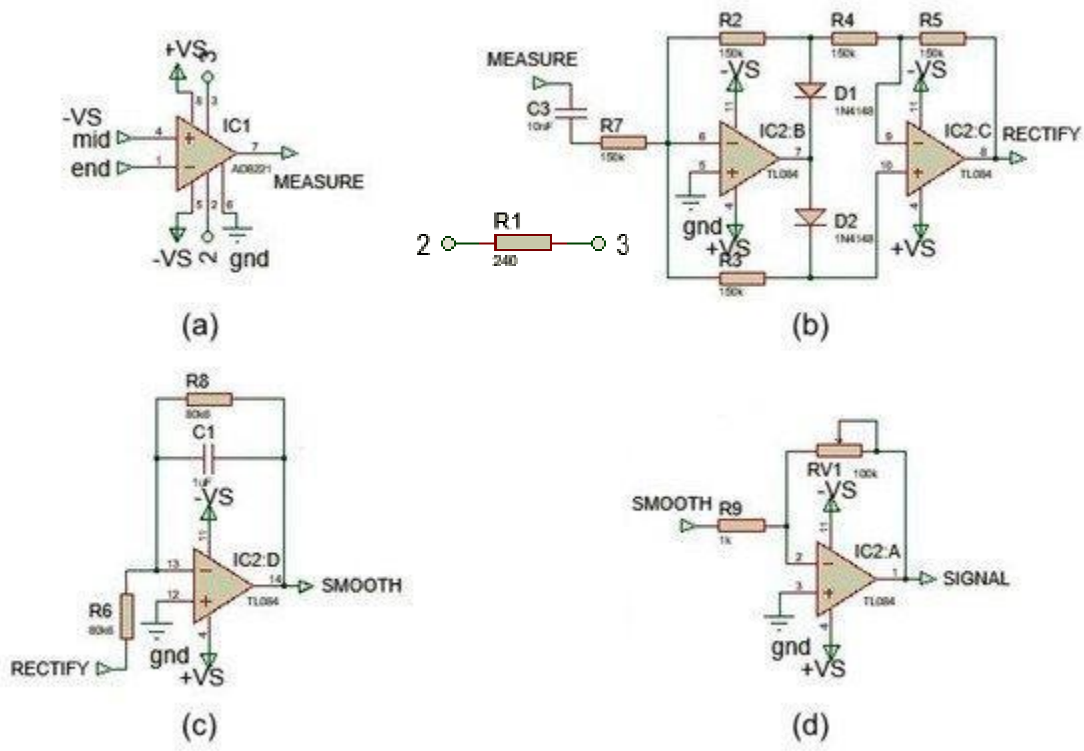

Figure 3.3.1: Signal conditioning steps. (a) Difference between first and second electromyographic signals, (b) signal rectification, (c) signal smoothing, (d) variable signal amplification.

The Figure 3.3.1 shows the internal circuit of the Myoware Muscle sensor. In order to acquire the EMG signal, a three-electrode configuration (two differential input and a ground reference) is used. Since the EMG voltage range detected by electrodes is very low and the signal is very noisy due to external sources such skin thickness and small vibrations so it is necessary to amplify and filter the EMG signal appropriately using an analog-to-digital converter (ADC).

In order to carry out the signal conditioning operations, the board includes several active and passive electronic components that allow the EMG signal conditioning so it can be acquired by the ADC of the microcontroller. The circuit is mainly composed of operational amplifiers and passive components such as resistors, capacitors, diodes and all the operational amplifiers are powered with a dual power supply. The signal conditioning includes the following operations: (i) The calculation of the difference between first and second electromyographic signals (Figure 3.3.1 (a)), (ii) Signal rectification (Figure 3.3.1 (b)), Signal smoothing (Figure 3.3.1 (c)), and Variable signal amplification (Figure 3.3.1 (d)).

The first step as seen in Figure 3.3.1 (a) is using a wide supply range instrumentation amplifier, with rail-to-rail output - the AD8226. This operational amplifier calculates the difference between the signals V+ and V- and amplifies the difference of a factor K which depends on the resistance present between pins 2 and 3 which is a resistor of 240 Ω guarantees a signal amplification.

The second step Figure 3.3.1 (b) consists of rectifying the output signal from the OP-AMP. Before the rectification circuit, a capacitor was inserted in order to couple the AC signal and remove the DC components. Specifically, by using a capacity of 0.01 μF, spectral components below 106 Hz were suppressed. Then, the obtained signal was rectified by a diode network and two Junction gate Field-Effect Transistor (JFET) - input operational amplifiers (TL084). In this step, the negative signal was reversed and transformed into a positive signal (full-wave rectification), thus allowing the calculation of the EMG signal power.

The third step Figure 3.3.1 (c) is useful to calculate the amplitude envelope shape of the signal in order to give an effective indication of the EMG signal power. This is implemented with an active first-order low-pass filter, using the same TL084 OP-AMP. The low pass filter has a cut-off frequency at about 2 Hz, and therefore, the signal is smoothed by removing the high-frequency spectral components.

Finally Figure 3.3.1 (d) is necessary to further amplify the smoothed signal to adapt it to the full-scale value input range of the ADC. This operation is performed by another TL084 OP-AMP configured as an inverting amplifier. The amplification level is set by the potentiometer located on the OP-AMP feedback network. The signal resulting from this last stage is read by the ADC.

Table 3.3.1: Electrical Specification of Myoware Muscle Sensor

Parameter	Min	TYP	Max
Supply Voltage	+2.9V	+3.3V or +5V	+5.7V
Adjustable Gain Potentiometer	0.01 Ω	50 kΩ	100 kΩ
Output Signal Voltage EMG Envelope Raw EMG (centered about +Vs/2)	 0V 0V	 -- --	 +Vs +Vs
Input Impedance	--	110 GΩ	--
Supply Current	--	9 mA	14 mA
Common Mode Rejection Ratio (CMRR)	--	110	--
Input Bias	--	1 pA	--

Table 3.3.1

3.4: DATABASE DETAILS

The database is called 'EMG Physical Action Dataset' acquired from UCI Machine Learning repository [58]. The dataset was provided by 'Theo Theodoridis from the School of Computer Science and Electronic Engineering at the University of Essex'. The protocols that were followed while acquiring the EMG data are that there were three male subjects and one female subject (age 25 to 30). Throughout 20 individual experiments, each subject had to perform ten normal and ten aggressive activities. The subject's performance has been recorded by the Delsys EMG apparatus, interfacing human activity with myoelectrical contractions.

The data acquisition process involved eight skin-surface electrodes placed on the upper arms (biceps and triceps), and upper legs (thighs and hamstrings). The overall number of electrodes is 8, which corresponds to 8 input time series one for a muscle channel (ch1-8). Each time series contains approx. 10000 samples (approx. 15 actions per experimental session for each subject). Each file in the dataset contains in overall 8 columns

A segment defines a body segment or limb. Right arm (R-Arm), Left arm (L-Arm), Right leg (R-Leg), Left leg (L-Leg). A channel corresponds to an electrode attached on a muscle.

A pair of muscles that corresponds to a segment: R-Bic: right bicep (C1), R-Tri: right tricep (C2), L-Bic: left bicep (C3), L-Tri: left tricep (C4), R-Thi: right thigh (C5), R-Ham: right hamstring (C6), L-Thi: left thigh (C7) and L-Ham: left hamstring (C8)

There are 20 classes of which 10 are normal and 10 aggressive physical actions.

- Normal: Bowing, Clapping, Handshaking, Hugging, Jumping, Running, Seating, Standing, Walking, Waving
- Aggressive: Elbowing, Frontkicking, Hammering, Headering, Kneeing, Pulling, Punching, Pushing, Sidekicking, Slapping

Database Details:

Subjects Gender	No. Of Subjects	Sensor Place On	No. Of Channels	No Of Readings	No Of Times Action Performed	Availability Of Data
Male	3	Hand & Leg	8	10000	15	Public
Female	1					

Data Set Characteristics:	Time-Series	Number of readings:	Approx. 10000	Area:	Physical
Attributes Characteristics:	Real	Number of Channels:	8	Associated Tasks:	Classification

CHAPTER 4: SYSTEM OVERVIEW AND HARDWARE SETUP

4.1: EMG SIGNAL ACQUISITION AND PROCESSING

Electromyography (EMG) is a technique for evaluating and recording the electrical activity produced by skeletal muscles. EMG is performed using an instrument called an electromyograph to produce a record called an electromyogram. An electromyograph detects the electric potential generated by muscle cells when these cells are electrically or neurologically activated. The signals can be analysed to detect abnormalities, activation level, or recruitment order, or to analyse the biomechanics of human or animal movement. Needle EMG is an electrodiagnostic medicine technique commonly used by neurologists. Surface EMG is a non-medical procedure used to assess muscle activation by several professionals, including physiotherapists, kinesiologists and biomedical engineers. In Computer Science, EMG is also used as middleware in gesture recognition towards allowing the input of physical action to a computer as a form of human-computer interaction.

EMG testing has a variety of clinical and biomedical applications. Needle EMG is used as a diagnostics tool for identifying neuromuscular diseases, or as a research tool for studying kinesiology, and disorders of motor control. EMG signals are sometimes used to guide botulinum toxin or phenol injections into muscles. Surface EMG is used for functional diagnosis and during instrumental motion analysis. EMG signals are also used as a control signal for prosthetic devices such as prosthetic hands, arms and lower limbs. Paraspinal sEMG, also referred to as paraspinal EMG scanning, has been explored as a technique to evaluate abnormal patterns of electrical activity in the paraspinal muscles in individuals with back pain symptoms such as spasm, tenderness, limited ROM, or postural disorders. The technique is performed using electrodes placed on the skin surface, with recordings made at rest, in various positions, or after a series of exercises.

4.1.1: Electrodes, Placement and Preparation

Skin Preparation:

- Thoroughly clean the skin of any oils, creams, dirt, dead skin etc.
- Use water to clean the area and ensure skin is fully dry before placing the electrodes on the skin.
- If hairy, use beard trimmers or scissors to clip the hair. Do not shave the area as this cause tiny micro abrasions which will make the stimulation uncomfortable.
- Ensure there are no wrinkles on the electrodes when placed on the skin

Electrode Size:

Any muscle lying under an electrode will be stimulated. Therefore, select the correct size to ensure only the muscles you want to target are stimulated.
Standard sizes are:

- 1.25 inch/3.2cm round: Consider these smaller electrodes for smaller muscles e.g., around the thumb.
- inch/5cm round: Most commonly used size.
- by 3.5 inch/5cm by 9cm rectangular: Consider these large rectangle electrodes for larger muscles such as hamstrings and quadriceps

Looking after your electrodes:

- The key to longevity of electrodes is slowing down the drying out of them when not in use.
- When removed from the skin, slightly moisten the sticky side of the electrode (a damp fingertip works well).
- Place the clear backing back on the sticky side after moistening.
- Place the electrodes back in their bag for storing.
- Typically, standard electrodes will last about 30 applications.

Electrode Placement – Most commonly used:

- Wrist and Finger extension: 1 lead with 2 electrodes. Place 1 electrode just up from the wrist on the finger extensor motor point and place the 2nd electrode further up the forearm on the tendinous part.
- Grasp - Finger flexion with thumb flexion and adduction: 1 lead with 2 electrodes. Place 1 electrode near the wrist on the underside of the forearm and the 2nd electrode over the fleshy part at the base of the thumb.
- Alternating between Wrist/Finger extension and Wrist/Finger flexion: 2 leads. First lead is the same electrode placement for wrist and finger extension. The second lead has one electrode placed near the wrist on the underside of the forearm and the 2nd electrode about midway up the underside of the forearm.
- Elbow flexion: 1 lead, 2 electrodes. Both electrodes placed mid upper arm on the biceps muscle. Ensure they have a minimum of 2 fingers space between them.
- Elbow extension: 1 lead, 2 electrodes. Both electrodes placed on the back of the upper arm on the triceps muscle. Ensure they have a minimum of 2 fingers space between them.
- Shoulder Subluxation: 2 options available. Option 1 is with 1 lead and 2 electrodes where 1 electrode is placed on supraspinatus (the fleshy part just up from the shoulder blade) and 1 electrode on posterior deltoid (the back of the upper arm, just beneath the subluxation gap). Option 2 is with 2 leads. Set up lead 1 as per option 1 above. On lead 2 place 1 electrode on the middle of the upper arm and the 2nd electrode on the front of the upper arm; both positioned just beneath the subluxation gap.

4.1.2: EMG SIGNAL ACQUISITION

Electromyography (EMG) is a diagnostic procedure that evaluates the health condition of muscles and the nerve cells that control them. These nerve cells are known as motor neurons. They transmit electrical signals that cause muscles to contract and relax. An EMG translates these signals into graphs or numbers, helping doctors to make a diagnosis.

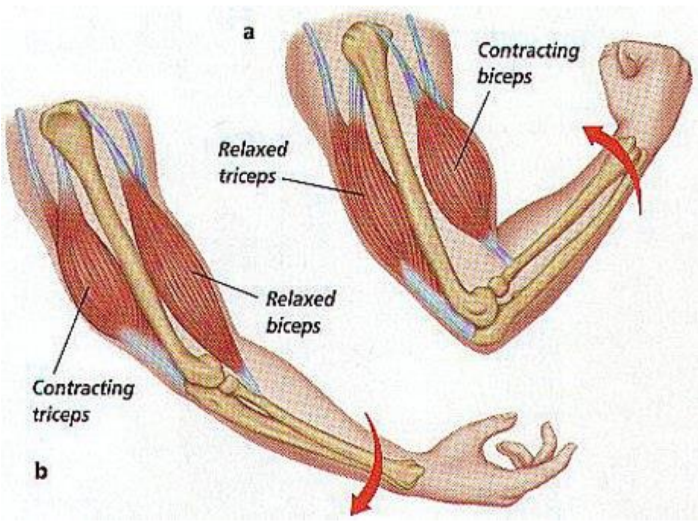

Figure 4.1.2.1: Muscle contraction

The electrical activity picked up by the electrodes is displayed on an oscilloscope. An audio-amplifier is used so the activity can be heard. EMG measures the electrical activity of muscle during rest, slight contraction, and forceful contraction. Muscle tissue does not normally produce electrical signals during rest. When an electrode is placed, a brief period of activity can be seen on the oscilloscope.

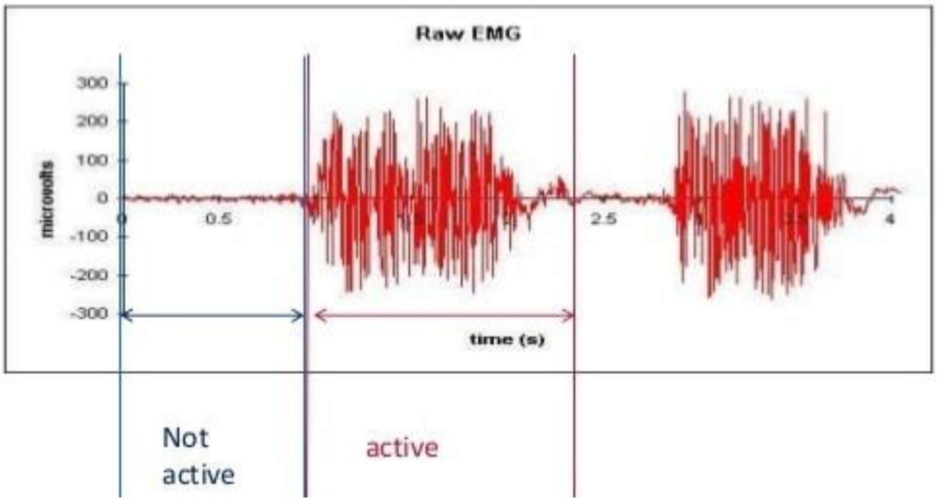

Figure 4.1.2.2: Muscle signal

How EMG is measured?

Surface EMG assesses muscle function by recording muscle activity from the surface above the muscle on the skin. Surface electrodes are able to provide only a limited assessment of muscle activity. Surface EMG can be recorded by a pair of electrodes or by a more complex array of multiple electrodes. More than one electrode is needed because EMG recordings display the potential difference between two separate electrodes.

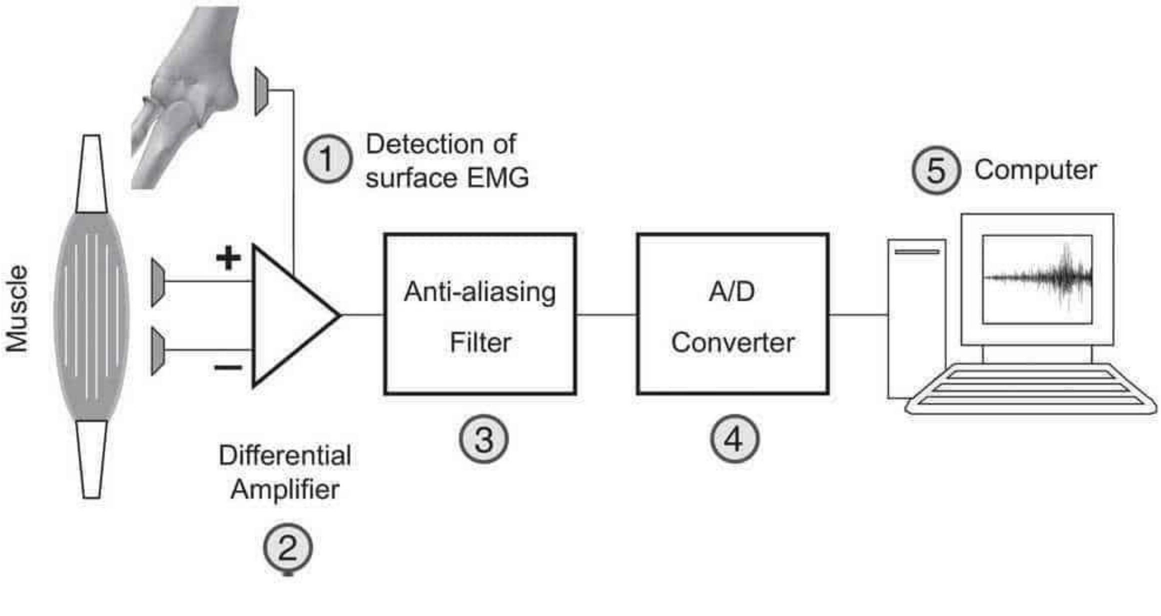

Figure 4.1.2.3: Basic EMG acquisition method

4.1.3 : RAW DATA PROCESSING IN MATLAB

Data collection and source

The source of our dataset is 'EMG Physical Action Dataset' found on UCI Machine Learning repository. The dataset was provided by 'Theo Theodoridis from the School of Computer Science and Electronic Engineering at the University of Essex'. The data was obtained from an experimental study done at Essex involving three male and one female subject (Age 25 – 30) who have experienced aggression in scenarios such as physical fighting. The subjects were asked to perform the following ten normal and ten aggressive activities:

Normal: Bowing, Clapping, Handshaking, Hugging, Jumping, Running, Seating, Standing, Walking, Waving.
Aggressive: Elbowing, Front Kicking, Hammering, Headering, Kneeing, Pulling, Punching, Pushing, Side kicking, Slapping

The performance of each subject was recorded using an EMG apparatus which involved placing eight skin-surface electrodes on different muscles of the subjects: R-Bic: right bicep, R-Tri: right tricep, L-Bic: left bicep, L-Tri: left tricep, R-Thi: right thigh, R-Ham: right hamstring, L-Thi: left thigh, L-Ham: left hamstring.

The eight electrodes take continuous records of muscles for each activity. There are about 10,000 samples per activity, with a sampling frequency of 200Hz and about 15 actions in each experimental session for each subject. One data frame records activity for one action. Since there are 20 actions per subject, and there are four subjects, we have a total of 80 data frames. A single data frame represents an action which contains approximately 10,000 rows and eight columns representing each channel. The aggressive actions vary from normal actions in terms of frequency, amplitude and signal pattern.

Raw Data Visualization and Processing

To see how the data looks like we use a python script to visualize the raw data in jupyter notebook using a Python script.

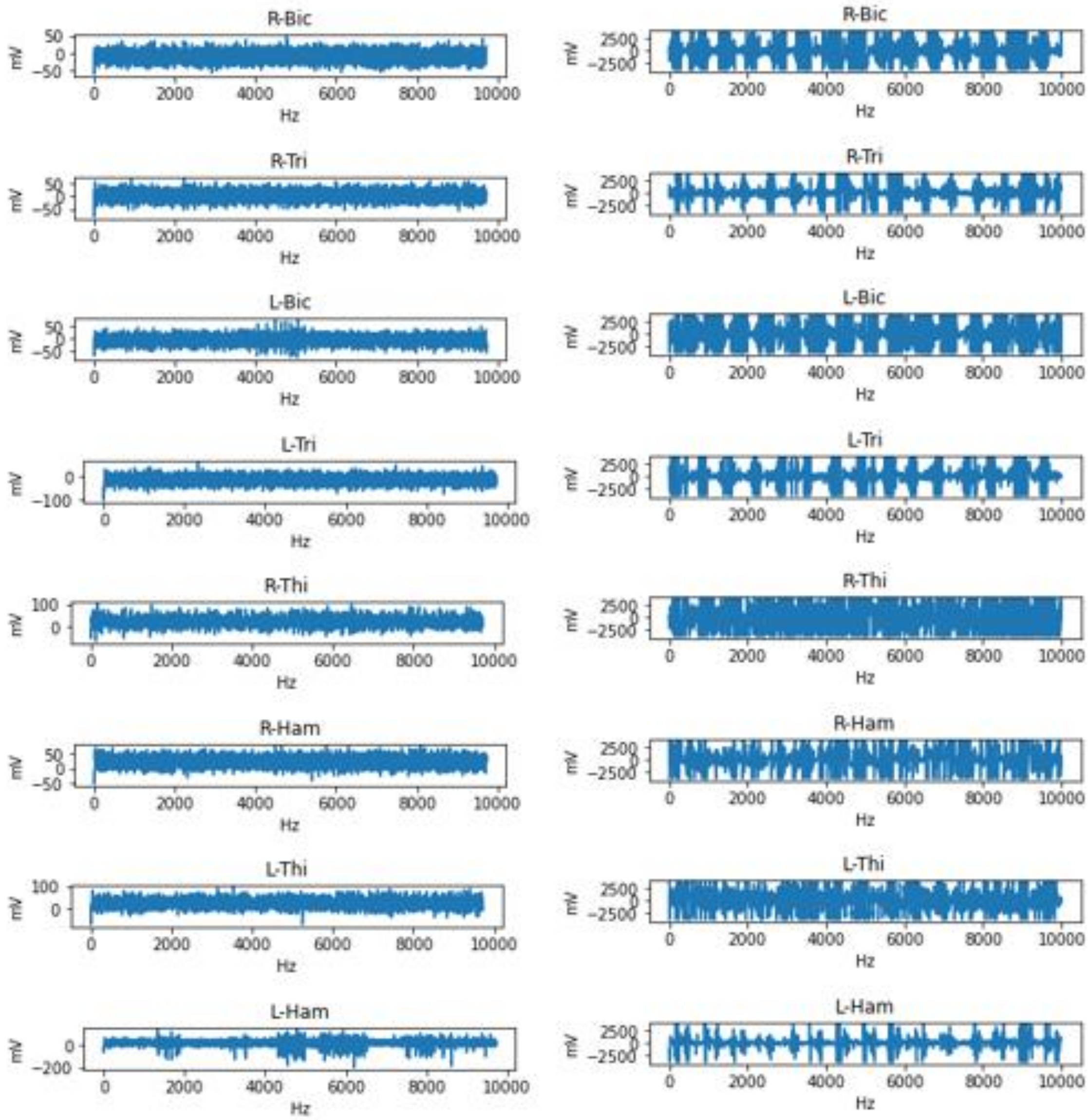

(a) (b)

Figure 4.1.3: (a) Sub1 Standing and (b) Sub1 Hammering

The difference between the muscle signals of normal and aggressive activities regarding both pattern and amplitude scale can be seen in the Figure 4.1.3 (a & b). The data is noisy and unclean because the electrical signal interacts with blood vessels and tissues between the skin and muscle.

Using MATLAB, we rectified the data by converting the signal to a single polarity, to ensure that signals don't get disrupted during analysis. The Savitzky-Golay filter was applied to smoothen the data and eliminate noise. A Savitzky-Golay filter is a digital filter that can be applied to a set of digital data points for the purpose of smoothing the data and to increase the precision of the data without distorting the signal. This is a process known as convolution where by fitting successive sub-sets of adjacent data points with a low-degree polynomial by the method of linear least squares. When the data points are equally spaced, an analytical solution to the least-squares equations can be found, in the form of a single set of "convolution coefficients" that can be applied to all data sub-sets, to give estimates of the smoothed signal, (or derivatives of the smoothed signal) at the central point of each subset. The method, based on established mathematical procedures, was popularized by Abraham Savitzky and Marcel J. E. Golay, who published tables of convolution coefficients for various polynomials and subset sizes in 1964. The method has been extended for the treatment of 2D and 3D data.

Applications:

The data consists of a set of points $\{x_j, y_j\}$, $j = 1, ..., n$, where x_j is an independent variable and y_j is an observed value. They are treated with a set of m convolution coefficients, C_i, according to the expression

$$Y_j = \sum_{i=\frac{1-m}{2}}^{\frac{m-1}{2}} C_i\, y_{j+i}, \qquad \frac{m+1}{2} \le j \le n - \frac{m-1}{2}$$

For example, for smoothing by a 5-point quadratic polynomial, $m = 5$, $i = -2, -1, 0, 1, 2$ and the jth smoothed data point, Y_j, is given by

$$Y_j = \frac{1}{35}(-3y_{j-2} + 12y_{j-1} + 17y_j + 12y_{j+1} - 3y_{j+2})$$

where, $C_{-2} = -3/35$, $C_{-1} = 12 / 35$, etc. There are numerous applications of smoothing, which is performed primarily to make the data appear to be less noisy than it really is. The following are applications of numerical differentiation of data.

When calculating the nth derivative, an additional scaling factor of $\frac{n!}{h^n}$ may be applied to all calculated data points to obtain absolute values. The data which we get after Savitzky-Golay filter is clean and processed.

Moving average:

A moving average filter is commonly used with time series data to smooth out short-term fluctuations and highlight longer-term trends or cycles. It is often used in technical analysis of financial data, like stock prices, returns or trading volumes. It is also used in economics to examine gross domestic product, employment or other macroeconomic time series. An unweighted moving average filter is the simplest convolution filter. Each subset of the data set is fitted by a straight horizontal line.

Feature engineering in time series:

In supervised learning, feature engineering aims to scale strong relationships between the new input and output features. The time series modelling or sequential modelling there is no input variable to the model or any output variable. Since the features of data and methods about the time series modelling work in a different nature, this data consists of time features in the data with some values that are changing with the time feature.

By looking at such data the features of any time series data are the time or the main feature used in modelling is time and that is also responsible for predicting good results. In time series it is required to perform feature engineering with the time variable.

Tsfresh library:

Feature engineering plays a crucial role in many of the data modelling tasks. This is simply a process that defines important features of the data using which a model can enhance its performance. In time series modelling, feature engineering works in a different way because it is sequential data and it gets formed using the changes in any values according to the time.

Tsfresh package:

tsfresh is an open-source python package that helps in feature engineering of time series data. The time series is sequential data so this package can also be used with any kind of sequential data. One thing that is mandatory about the data it should have generated using an independent variable. For example, in time-series data the time variable is an independent variable.

Utilizing this tool, we can extract features and perform analysis based on the new insights. Feature extraction is also helpful in making clusters from the time series or we can also perform classification and regression tasks using feature extraction. The package is compatible with pandas library for data manipulation and also it is compatible with the sklearn library that helps us in providing various machine learning models.

IMPLEMENTATION:

After the installation of the tsfresh, we can use the package. We have to extract time-series features from each of action data frames to feed it to classification models. Each action data frame contains the particular action performed about 15 times so there are 15 crest and troughs of the wave in the data. The individual time- series actions is divided into many smaller windows and extracted features for each window using sliding/moving window approach. After every fixed interval of record, the features are extracted using sliding - window approach.

The features extracted from the windows will represent the original data. There have approximately 10,000 records in each action data frame, so we considered the following three combinations of extracting features:

- Action window of size 500 records sliding after every 50 records.
- Action window of size 800 records sliding after every 80 records.
- Action window of size 1000 records sliding after every 100 records.

For all three combinations, we extracted all possible time-series features tsfresh could calculate. So each action data frame was converted into a new factorized data frame with 6305 columns and different rows.

Modelling Methods:

We did classify actions into normal and aggressive. Since there are 10 normal and 10 aggressive actions for each subject, we assigned the label ‘0’ to normal and ‘1’ to aggressive actions and stacked them together to get a single data frame representing each subject. The classification was done using the following models: All the features in our data are numeric, and we have binary output so Logistic Regression was used. Random Forest classifier was used since we could easily interpret the importance it gives to different features.

The amount-to-dimensionality ratio is very low. To avoid overfitting, we used Linear Logistic regression and Naive Bayes are used. Random Forest classifier was unaffected by the difference in scales between the features in a high dimension dataset. Thus, Logistic Regression, Random Forest, and Naive Bayes are the classification models. We also used a default random choice model to compare the performance of our models.

Standardization:

Normalizing the dataset is required before machine learning models can be used. The muscle activation varies between the subjects when performing the same action as each subject vary in terms of age, gender and strength. If normalization was not executed, the performance of the models would have been affected as the difference in scales of the features prevent the models from learning data better. Standardization of all subject is done using mean and variance of subject. Scikit-learn standard scalar used to convert data into standard normal distribution.

Scikit Learn:

Scikit-learn (formerly scikits.learn and also known as sklearn) is a free software machine learning library for the Python programming language. It features various classification, regression and clustering algorithms including support-vector machines, random forests, gradient boosting, *k*-means and DBSCAN, and is designed to interoperate with the Python numerical and scientific libraries NumPy and SciPy. Scikit-learn is a NumFOCUS fiscally sponsored project.

The scikit-learn project started as scikits.learn, a Google Summer of Code project by French data scientist David Cournapeau. Its name stems from the notion that it is a "SciKit" (SciPy Toolkit), a separately-developed and distributed third-party extension to SciPy] The original codebase was later rewritten by other developers. In 2010 Fabian Pedregosa, Gael Varoquaux, Alexandre Gramfort and Vincent Michel, all from the French Institute for Research in Computer Science and Automation in Rocquencourt, France, took leadership of the project and made the first public release on February the 1st 2010. Of the various scikits, scikit-learn as well as scikit-image were described as "well-maintained and popular" in November 2012. Scikit-learn is one of the most popular machine learning libraries on GitHub. Scikit-learn is largely written in Python, and uses NumPy extensively for high-performance linear algebra and array operations. Furthermore, some core algorithms are written in Cython to improve performance. Support vector machines are implemented by a Cython wrapper around LIBSVM; logistic regression and linear support vector machines by a similar wrapper around LIBLINEAR. In such cases, extending these methods with Python may not be possible. Scikit-learn integrates well with many other Python libraries, such as Matplotlib and plotly for plotting, NumPy for array vectorization, Pandas dataframes, SciPy, and many more.

Four-fold cross-validation:

Database has poor amount to dimensionality ratio. Thus, we require four-fold cross validation in which there is training models on three subjects and testing on one left out the subject in each loop. For each cross-validation loop:

Calculated the confusion matrix, accuracy, recall, false-positive rate, true-positive rate and precision at 50% cut-off. There is also ROC curve and corresponding AUC value at each time to assess the models at different cut-off values. There is an overall ROC curve generalizing the performance of models.

Accuracy and ROC curve are two important metrics for choosing a particular model. Accuracy is the metric that will tell us how correctly the models can classify the unseen labels and informs us of the model’s generalization capability. ROC curves tell us the overall performance of the model irrespective of the cut-off threshold selected and hence tell us about the utility of the model.

Cross-validation (statistics):

Cross-validation, sometimes called rotation estimation or out-of-sample testing, is similar model validation techniques for assessing how the results of a statistical analysis will generalize to an independent data set. Cross-validation is a resampling method that uses different portions of the data to test and train a model on different iterations. It is mainly used in settings where the goal is prediction, and one wants to estimate how accurately a predictive model will perform in practice. In a prediction problem, a model is usually given a dataset of known data on which training is run (training dataset), and a dataset of unknown data (or first seen data) against which the model is tested (called the validation dataset or testing set). The goal of cross-validation is to test the model's ability to predict new data that was not used in estimating it, in order to flag problems like overfitting or selection bias [and] to give an insight on how the model will generalize to an independent dataset.

One round of cross-validation involves partitioning a sample of data into complementary subsets, performing the analysis on one subset (called the training set), and validating the analysis on the other subset (called the validation set or testing set). To reduce variability, in most methods multiple rounds of cross-validation are performed using different partitions, and the validation results are combined (e.g. averaged) over the rounds to give an estimate of the model's predictive performance.

Exhaustive cross-validation:

Exhaustive cross-validation methods are cross-validation methods which learn and test on all possible ways to divide the original sample into a training and a validation set.

LOGISTIC REGRESSION:

In statistics, the (binary) logistic model (or logit model) is a statistical model that models the probability of one event (out of two alternatives) taking place by having the log-odds (the logarithm of the odds) for the event be a linear combination of one or more independent variables ("predictors"). In regression analysis, logistic regression (or logit regression) is estimating the parameters of a logistic model (the coefficients in the linear combination). Formally, in binary logistic regression there is a single binary dependent variable, coded by an indicator variable, where the two values are labelled "0" and "1", while the independent variables can each be a binary variable (two classes, coded by an indicator variable) or a continuous variable (any real value). The corresponding probability of the value labelled "1" can vary between 0 (certainly the value "0") and 1 (certainly the value "1"), hence the labelling] the function that converts log-odds to probability is the logistic function, hence the name. The unit of measurement for the log-odds scale is called a logit, from logistic unit, hence the alternative names.

Binary variables are widely used in statistics to model the probability of a certain class or event taking place, such as the probability of a team winning, of a patient being healthy, etc., and the logistic model has been the most commonly used model for binary regression since about 1970. Binary variables can be generalized to categorical variables when there are more than two possible values (e.g., whether an image is of a cat, dog, lion, etc.), and the binary logistic regression generalized to multinomial logistic regression. If the multiple categories are ordered, one can use the ordinal logistic regression (for example the proportional odds ordinal logistic model). The logistic regression model itself simply models probability of output in terms of input and does not perform statistical classification (it is not a classifier), though it can be used to make a classifier, for instance by choosing a cut-off value and classifying inputs with probability greater than the cut-off as one class, below the cut-off as the other; this is a common way to make a binary classifier.

Logistic regression is used in various fields, including machine learning, most medical fields, and social sciences. For example, the Trauma and Injury Severity Score (TRISS), which is widely used to predict mortality in injured patients, was originally developed by Boyd et al. using logistic regression. Many other medical scales used to assess severity of a patient have been developed using logistic regression. Logistic regression may be used to predict the risk of developing a given disease (e.g. diabetes; coronary heart disease), based on observed characteristics of the patient (age, body mass index, results of various blood tests, etc.). The technique can also be used in engineering, especially for predicting the probability of failure of a given process, system or product. It is also used in marketing applications such as prediction of a customer's propensity to purchase a product or halt a subscription, etc. In economics it can be used to predict the likelihood of a person ending up in the labour force, and a business application would be to predict the likelihood of a homeowner defaulting on a mortgage. Conditional random fields, an extension of logistic regression to sequential data, are used in natural language processing.

RANDOM FOREST:

Random forests or random decision forests is an ensemble learning method for classification, regression and other tasks that operates by constructing a multitude of decision trees at training time. For classification tasks, the output of the random forest is the class selected by most trees. For regression tasks, the mean or average prediction of the individual trees is returned. Random decision forests correct for decision trees' habit of overfitting to their training set. Random forests generally outperform decision trees, but their accuracy is lower than gradient boosted trees. However, data characteristics can affect their performance.

The first algorithm for random decision forests was created in 1995 by Tin Kam Ho using the random subspace method, which, in Ho's formulation, is a way to implement the "stochastic discrimination" approach to classification proposed by Eugene Kleinberg. An extension of the algorithm was developed by Leo Breiman and Adele Cutler, who registered "Random Forests" as a trademark in 2006 (as of 2019, owned by Minitab, Inc.).The extension combines Breiman's "bagging" idea and random selection of features, introduced first by Ho and later independently by Amit and Geman in order to construct a collection of decision trees with controlled variance.

Random forests are frequently used as "blackbox" models in businesses, as they generate reasonable predictions across a wide range of data while requiring little configuration. The general method of random decision forests was first proposed by Ho in 1995. He established that forests of trees splitting with oblique hyperplanes can gain accuracy as they grow without suffering from overtraining, as long as the forests are randomly restricted to be sensitive to only selected feature dimensions. A subsequent work along the same lines concluded that other splitting methods behave similarly, as long as they are randomly forced to be insensitive to some feature dimensions. Note that this observation of a more complex classifier (a larger forest) getting more accurate nearly monotonically is in sharp contrast to the common belief that the complexity of a classifier can only grow to a certain level of accuracy before being hurt by overfitting. The explanation of the forest method's resistance to overtraining can be found in Kleinberg's theory of stochastic discrimination.

The early development of Breiman's notion of random forests was influenced by the work of Amit and Geman who introduced the idea of searching over a random subset of the available decisions when splitting a node, in the context of growing a single tree. The idea of random subspace selection from Ho was also influential in the design of random forests. In this method a forest of trees is grown, and variation among the trees is introduced by projecting the training data into a randomly chosen subspace before fitting each tree or each node. Finally, the idea of randomized node optimization, where the decision at each node is selected by a randomized procedure, rather than a deterministic optimization was first introduced by Thomas G. Dietterich.

The proper introduction of random forests was made in a paper by Leo Breiman. A method of building a forest of uncorrelated trees using a CART like procedure, combined with randomized node optimization and bagging. This paper combines several ingredients, some previously known and some novel, which form the basis of the modern practice of random forests, in particular:

- Using out-of-bag error as an estimate of the generalization error.
- Measuring variable importance through permutation.

The report also offers the first theoretical result for random forests in the form of a bound on the generalization error which depends on the strength of the trees in the forest and their correlation.

NAIVE BAYES:

In statistics, Naive Bayes classifiers are a family of simple "probabilistic classifiers" based on applying Bayes' theorem with strong (naive) independence assumptions between the features (see Bayes classifier). They are among the simplest Bayesian network models, but coupled with kernel density estimation, they can achieve high accuracy levels.

Naive Bayes classifiers are highly scalable, requiring a number of parameters linear in the number of variables (features/predictors) in a learning problem. Maximum-likelihood training can be done by evaluating a closed-form expression, which takes linear time, rather than by expensive iterative approximation as used for many other types of classifiers.

In the statistics literature, naive Bayes models are known under a variety of names, including simple Bayes and independence Bayes. All these names reference the use of Bayes' theorem in the classifier's decision rule, but naive Bayes is not a Bayesian method.

Naive Bayes is a simple technique for constructing classifiers: models that assign class labels to problem instances, represented as vectors of feature values, where the class labels are drawn from some finite set. There is not a single algorithm for training such classifiers, but a family of algorithms based on a common principle: all naive Bayes classifiers assume that the value of a particular feature is independent of the value of any other feature, given the class variable. For example, a fruit may be considered to be an apple if it is red, round, and about 10 cm in diameter. A naive Bayes classifier considers each of these features to contribute independently to the probability that this fruit is an apple, regardless of any possible correlations between the colour, roundness, and diameter features.

In many practical applications, parameter estimation for naive Bayes models uses the method of maximum likelihood; in other words, one can work with the naive Bayes model without accepting Bayesian probability or using any Bayesian methods. Despite their naive design and apparently oversimplified assumptions, naive Bayes classifiers have worked quite well in many complex real-world situations. In 2004, an analysis of the Bayesian classification problem showed that there are sound theoretical reasons for the apparently implausible efficacy of naive Bayes classifiers. Still, a comprehensive comparison with other classification algorithms in 2006 showed that Bayes classification is outperformed by other approaches, such as boosted trees or random forests. An advantage of naive Bayes is that it only requires a small number of training data to estimate the parameters necessary for classification.

4.2: ROS and Gazebo

Gazebo Model:

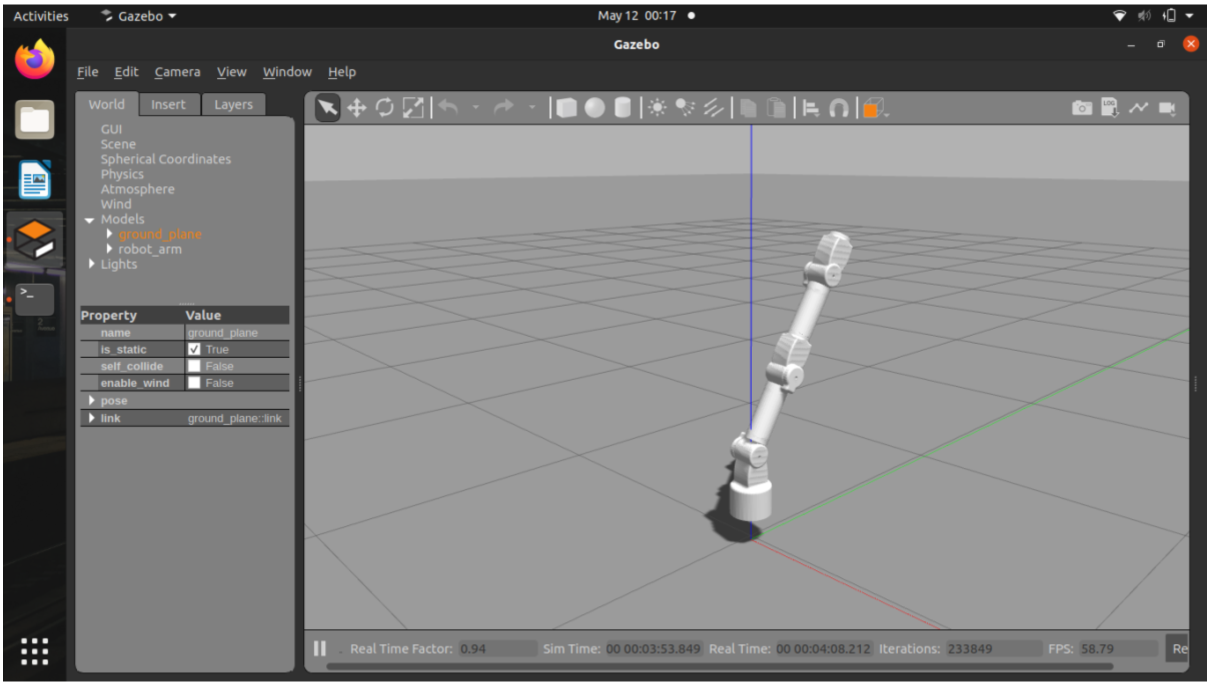

Fig 4.2.1: A arm model simulated in Gazebo

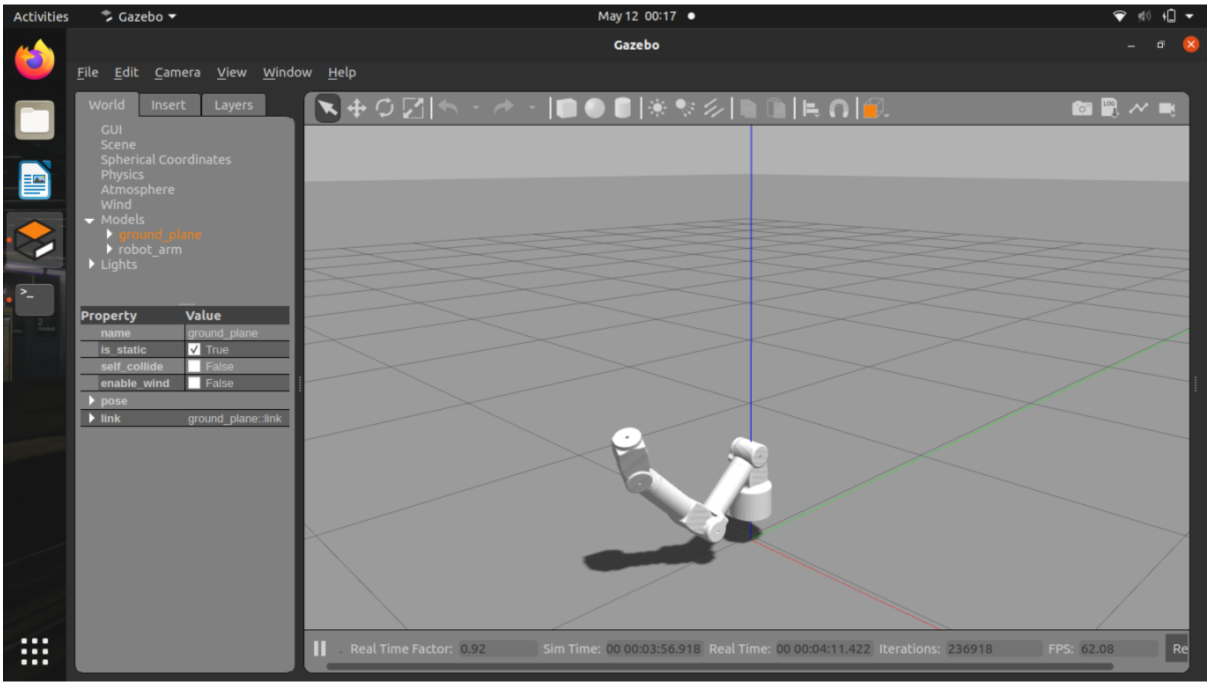

Fig 4.2.2: A arm in Gazebo after manual control

The Gazebo model is an application in the robot operating system where in the user can build their own structure using predefined blocks such as square, triangle, rectangle, circle and so on.

The Figure 4.2.1 and 4.2.2 show the model in gazebo. These blocks can be arranged in x,y,z plane. The blocks can be moved in any space by giving proper joints angle. The blocks may be moving or may be at static place. The blocks can also be moved by giving proper rotation, revolute, prism etc. We took blocks such as cylinder and square joints which represents 5 DOF arm and can be joint using proper links. By giving proper parameters to joints we could move the arm.

Rviz Execution:

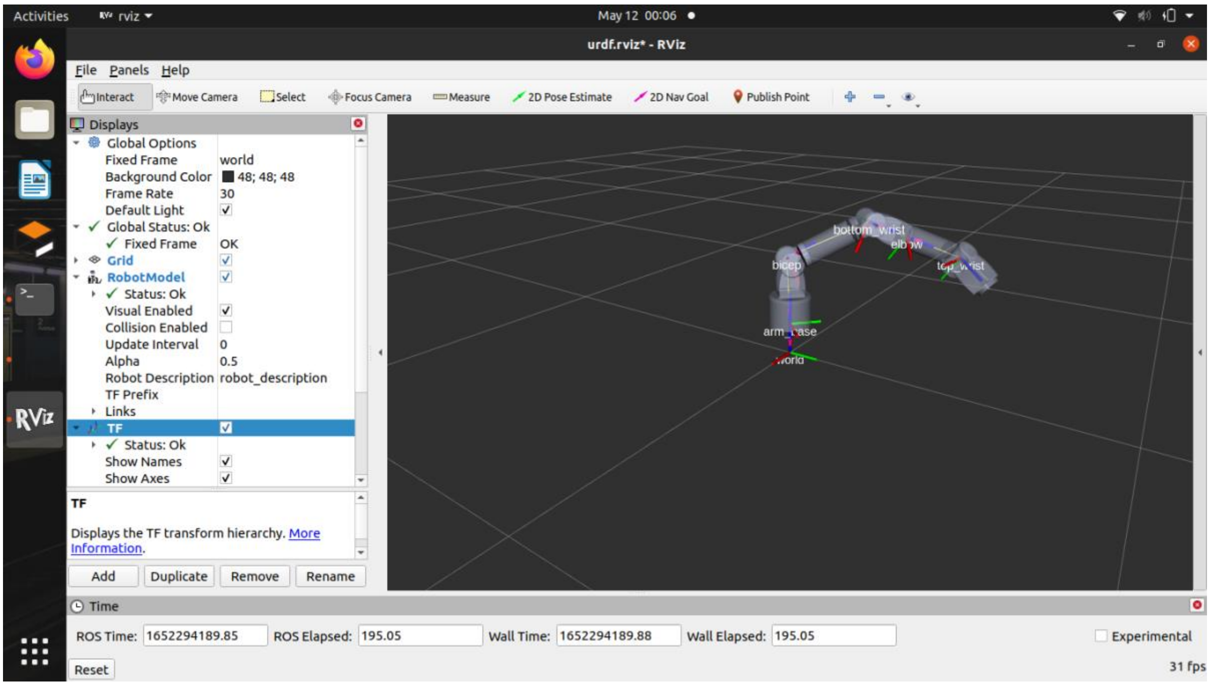

Fig 4.2.3: 5 DoF model movement

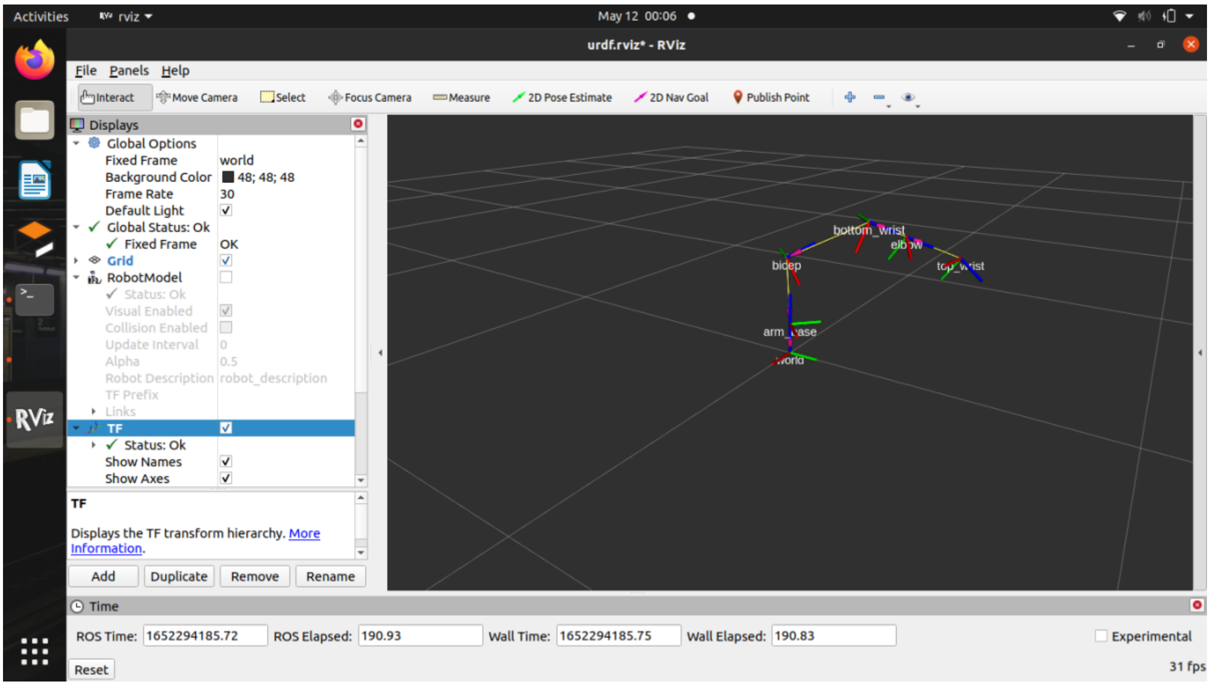

Fig 4.2.4: Different model axis

Assume that we know the starting point of the robot, a desired final point of the robot, the geometrical description of the robot and geometrical description with the motion panning is the technique to find an optimum path that moves the robot gradually from the start. Figure 4.2.3 and 4.2.4 show the model in Rviz and the DoF movement by manual control.

In case of a robotic arm, the motion planner finds the trajectory consisting of joint spaces of each joint in which the links of the robot should never collide with the environment, avoid self-collision between two links and also not violate the joints limits.

Degree of Freedom (DoF):

A 'Degree of Freedom' (DoF) as it relates to robotic arms, is an independent joint that can provide freedom of movement of the manipulator, either in a rotational or translational (linear) sense. For every geometric axis that a joint can rotate around or extend along, this is counted as a Single Degree of Freedom. In theory, there are quite a few types of joints that provide varying numbers of degrees of freedom in terms of rotation and translation (see the chart below). In practice, however, most robotic arms will be made up of a series of joints that provide one degree of freedom. The two most common joints are:

- **Revolute Joint:** Providing one degree of rotational freedom
- **Prismatic Joint:** Providing one degree of linear freedom

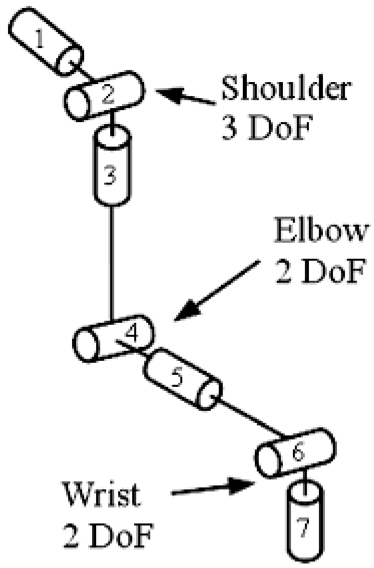

Figure 4.2.5: Human arm DoFs

As seen in Figure 4.2.5, the shoulder joint has 3 degrees of freedom: front and back flexion, internal and external expansion, internal and external rotation, the elbow joint with 1 degrees of freedom: flexion, the forearm with 1 degrees of freedom: pronation, supination, and the wrist with 2 degrees of freedom: back bends, surround.

Types of Different Joints Used in Robots:

1. Revolute (Rotary) Joints Provide One degree-of-freedom (DOF) for the Robot Links: A revolute joint is like a door hinge. It provides one DOF of motion between two bodies that it connects. The rotation is around the joint axis, and the positive rotation can be determined using the right-hand rule.
2. Linear (sliding) Joints Provide One degree-of-freedom (DOF) for the Robot Links: A linear, sliding, or prismatic joint provides a linear motion between two links. It will again provide only one DOF between two links: Linear (sliding) Joints Provide One degree-of-freedom for the Robot Links.
3. Universal Joints Provide Two Degrees of Freedom for the Links they Connect: It is the universal joint, which is two revolute joints with joint axes orthogonal to each other thus, it can provide two rotational DOFs around roll and pitch axes that are x and y axes.
4. Spherical Joints Provide Three Degrees of Freedom Between the Connecting Links: The spherical, ball-and-socket, or shoulder joint can provide three DOFs, which are two degrees of freedom of the joint plus spinning about the joint axis.
5. Cylindrical Joints Provide Two Degrees of Freedom Between the Connecting Links: It is a cylindrical joint that can provide an independent translation and rotation about a single fixed joint axis; thus, it has two DOFs.
6. Helical Joints Provide One Degree of Freedom Between the Rigid Bodies they Connect: The joint is the helical, or screw joint that provides a simultaneous rotation and translation about a screw axis and can provide one degree of freedom. The difference between this joint and the cylindrical joint is that in the cylindrical joint, the rotation and translation are independent, thus providing us with 2 DOFs, but in the helical joint, this motion is simultaneous, so it only has 1 DOF.

KINEMATICS

Kinematics is a branch of classical mechanics that describes the motion of points, bodies (objects),and systems of bodies(groups of objects) without considering the forces that caused the motion. Kinematics, as a field of study, is often referred to as the "geometry of motion" and is occasionally seen as a branch of mathematics. A kinematics problem begins by describing the geometry of the system and declaring the initial conditions of any known values of position, velocity and/or acceleration of points within the system.

Kinematics studies the motion of bodies without consideration of the forces or moments that cause the motion. Robot kinematics refers the analytical study of the motion of a robot manipulator. Formulating the suitable kinematics models for a robot mechanism is very crucial for analysing the behaviour of industrial manipulators.

Kinematics is used in astrophysics to describe the motion of celestial bodies and collections of such bodies. In mechanical engineering, robotics, and biomechanics kinematics is used to describe the motion of systems composed of joined parts (multi-link systems)such as an engine, a robotic arm or the human skeleton. Kinematic analysis is the process of measuring the kinematic quantities used to describe motion. In engineering, for instance, kinematic analysis may be used to find the range of movement for a given mechanism and working in reverse, using kinematic synthesis to design a mechanism for a desired range of motion.

Forward of kinematics:

Forward Kinematics refers to the use of the kinematic equations of a robot to compute the position of the end-effector from specified values for the joint parameters. The forward kinematic equations can be used as a method in 3D computer graphics for animating models.

The essential concept of forward kinematic animation is that the positions of particular parts of the model at a specified time are calculated from the position and orientation of the object, together with any information on the joints of an articulated model. So for example if the object to be animated is an arm with the shoulder remaining at a fixed location, the location of the tip of the thumb would be calculated from the angles of the shoulder, elbow, wrist, thumb and knuckle joints. Three of these joints (the shoulder, wrist and the base of the thumb) have more than one degree of freedom, all of which must be taken into account. If the model were an entire human figure, then the location of the shoulder would also have to be calculated from other properties of the model.

Forward kinematic animation can be distinguished from inverse kinematic animation by this means of calculation - in inverse kinematics the orientation of articulated parts is calculated from the desired position of certain points on the model. It is also distinguished from other animation systems by the fact that the motion of the model is defined directly by the animator - no account is taken of any physical laws that might be in effect on the model, such as gravity or collision with other models.

Inverse Kinematics:

In computer animation and robotics, inverse kinematics is the mathematical process of calculating the variable joint parameters needed to place the end of a kinematic chain, such as a robot manipulator or animation character's skeleton, in a given position and orientation relative to the start of the chain. The reverse process that computes the joint parameters that achieve a specified position of end-effector is known as inverse kinematics.

Inverse kinematics is also used to recover the movements of an object in the world from some other data, such as a film of those movements, or a film of the world as seen by a camera which is itself making those movements. This occurs, for example, where a human actor's filmed movements are to be duplicated by an animated character.

In robotics, inverse Kinematics makes use of the kinematics equations to determine the joint parameters that provides desired position for each of the robot's end-effectors. Specification of the movement of a robot so that its end-effectors achieve the desired tasks is known as motion planning. Inverse kinematics transforms the motion plan into joint actuator trajectories for the robot.

The movement of a kinematic chain, whether it is a robot or an animated character, is modelled by the kinematics equations of the chain. These equations define the configuration of the chain in terms of its joint parameters. Forward kinematics uses the joint parameters to compute the configuration of the chain, and inverse kinematics reverses this calculation to determine the joint parameters that achieve a desired configuration.

While analytical solutions to the inverse kinematics problem exist for a wide range of kinematic chains, computer modelling and animation tools often use Newton's method to solve the non-linear kinematics equations. Other applications of inverse kinematic algorithms include interactive manipulation, animation control and collision avoidance.

4.3: 3D Design and Development

3D design is the process of using computer-modelling software to create an object within a three-dimensional space. This means that the object itself has three key values assigned to it in order to understand where it exists within the space. The object can be created from simple shapes all the way up to complex high-polygon models. A polygon is one triangle, and it takes many triangles to make a circle or complex object.

We designed a models to give wide flexibility and also fit perfectly for the average person and be comfortable to wear and use. The model was designed in Solidworks.

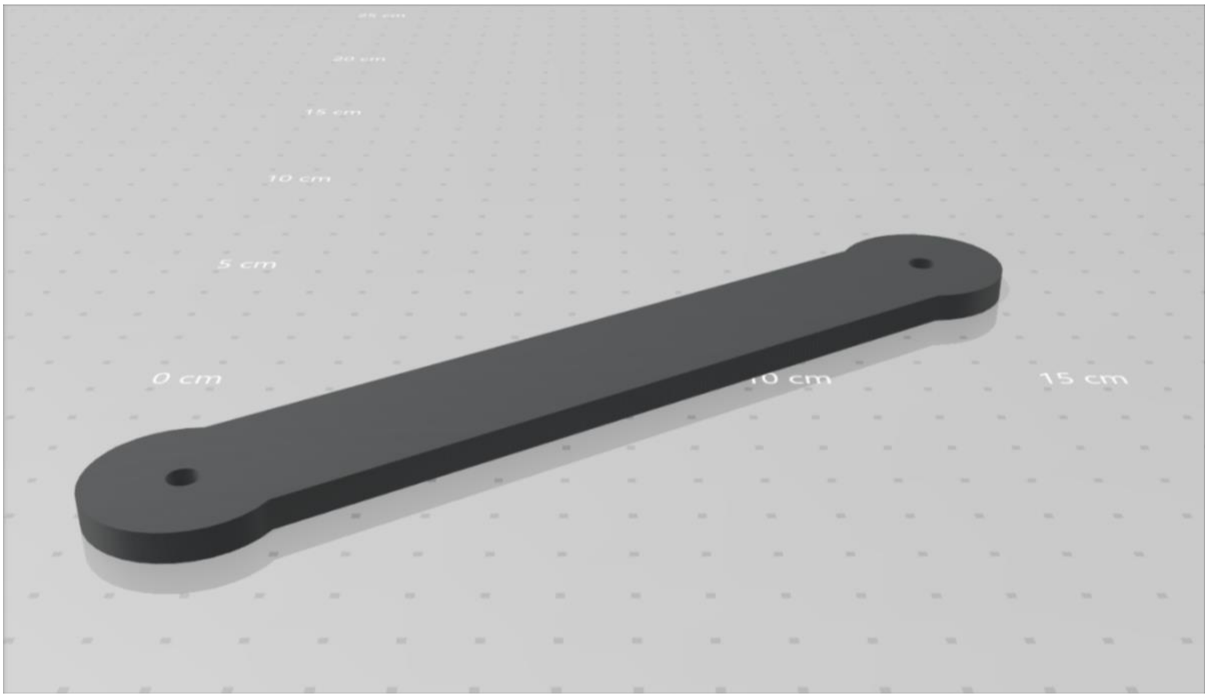

Figure 4.3.1: Back part of the model

Figure 4.3.1 is the back plate of the model which is used to support the weight of the whole exoskeleton system. This plate will be attached to the body with some belts around the chest area. There will be a motor connected to the at one end of the plate where it will also be connected to the shoulder curve part of the model for more flexibility.

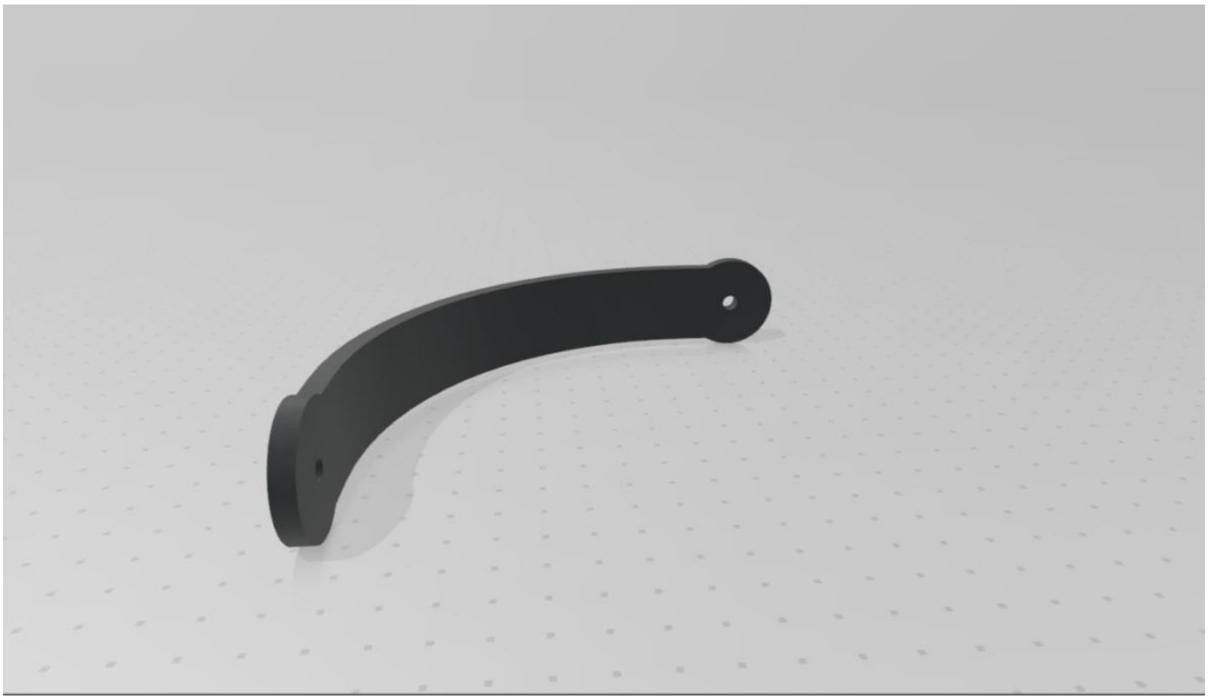

Figure 4.3.2: Shoulder curve of the model

Figure 4.3.2 is the shoulder curve part of the exoskeleton which gives support and more freedom for the movement of the shoulder joint. It is connected to the bicep part of the model.

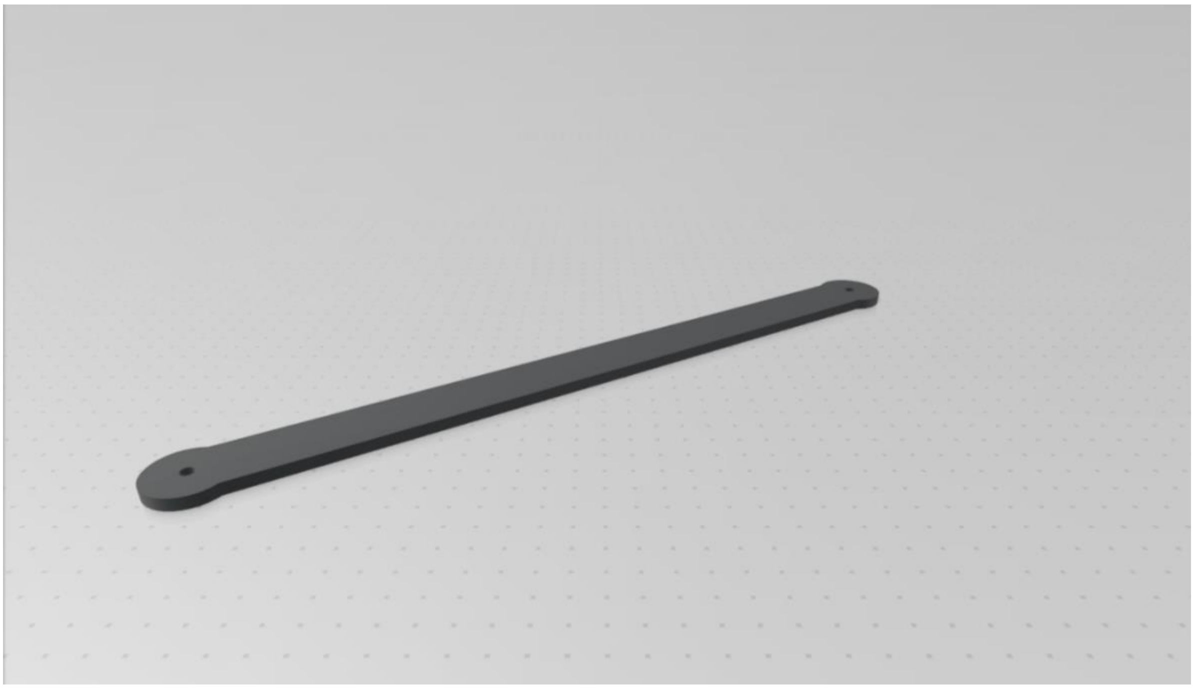

Figure 4.3.3: Bicep Part of the model

Figure 4.3.3 is the bicep part of the model which will also be connected to the shoulder curve part along with motors and the other end is connected to the arm part of the model along with another motor. This will act like the main load bearing support.

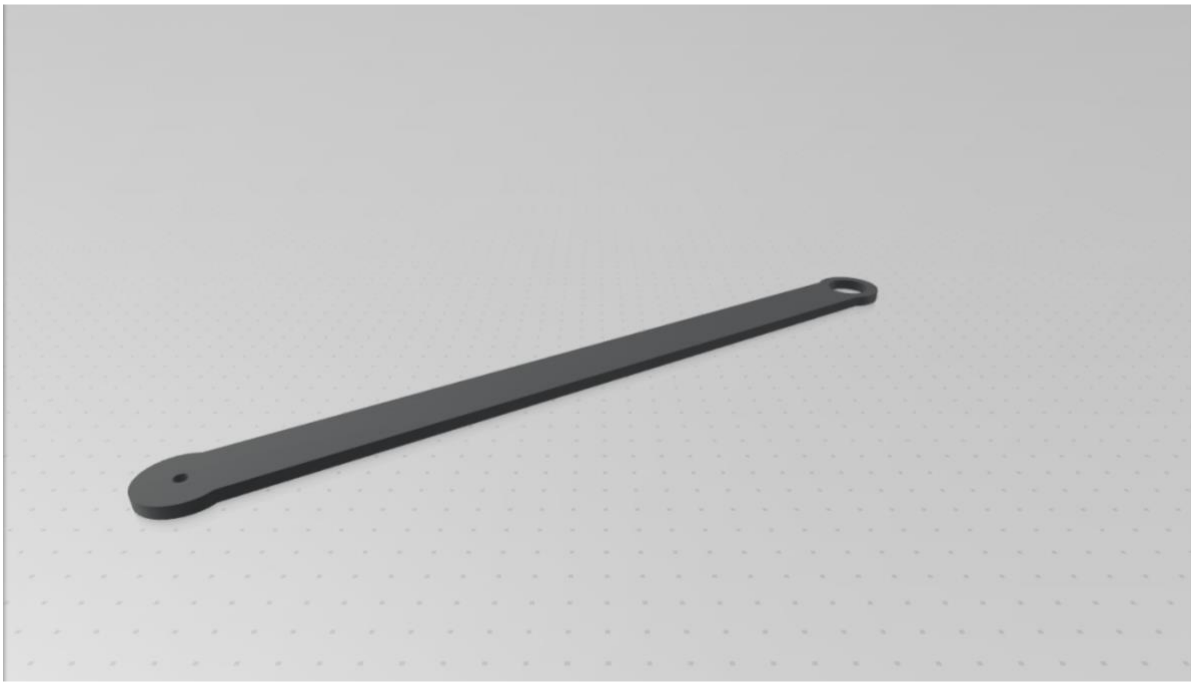

Figure 4.3.4: Hand part of the model

Figure 4.3.4 is the fore arm part of the model which has a handle bar where the wrist will be positioned for support. This will help with elbow movement for activities like eating and waving.

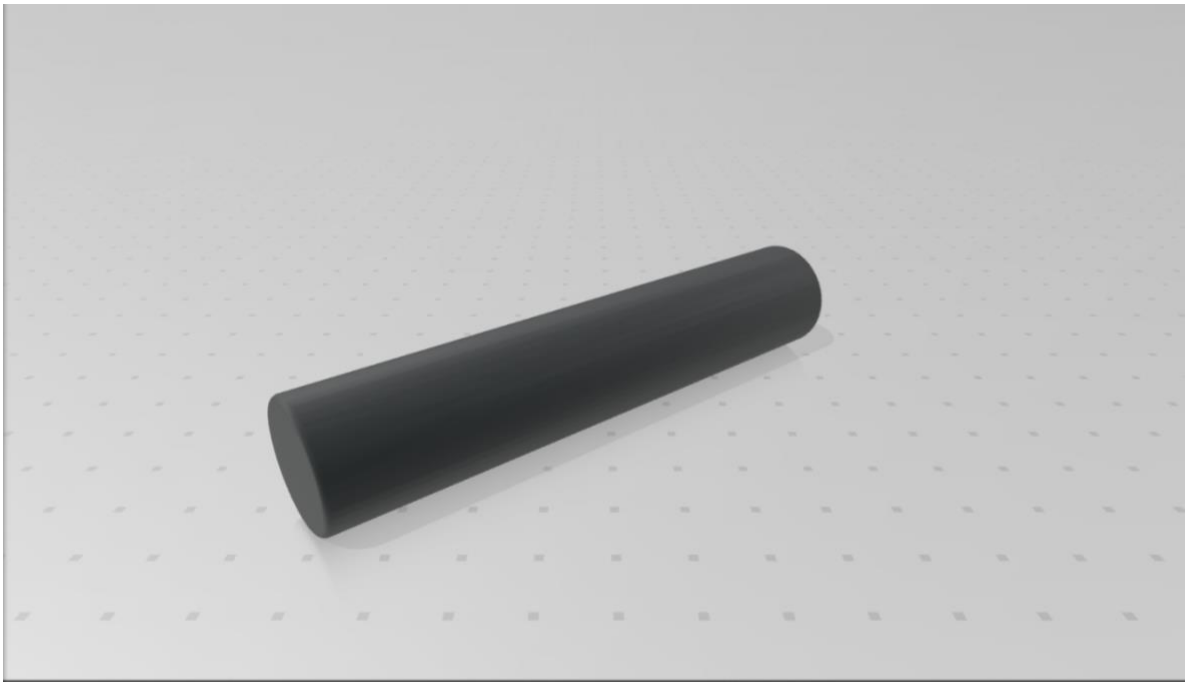

Figure 4.3.5: Handle part of the model

Figure 4.3.5 is the handle bar for the support of the wrist. It is small and light weight and it is helpful for resting of the wrist.

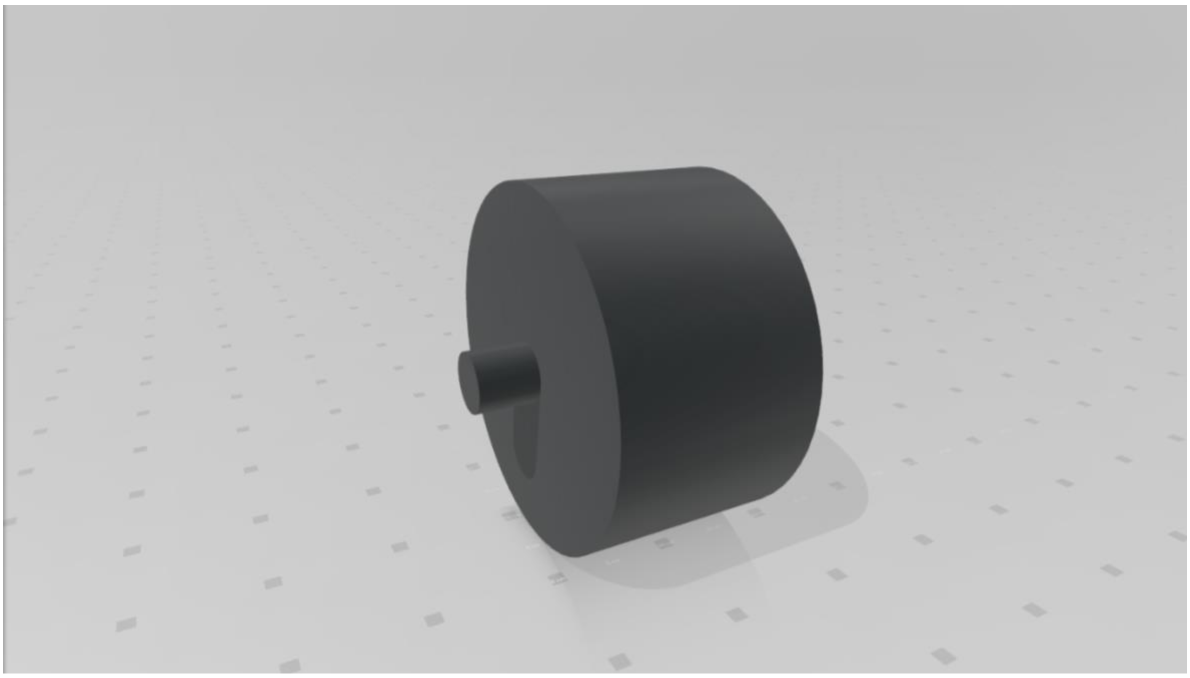

Figure 4.3.6: Demo motor of the model

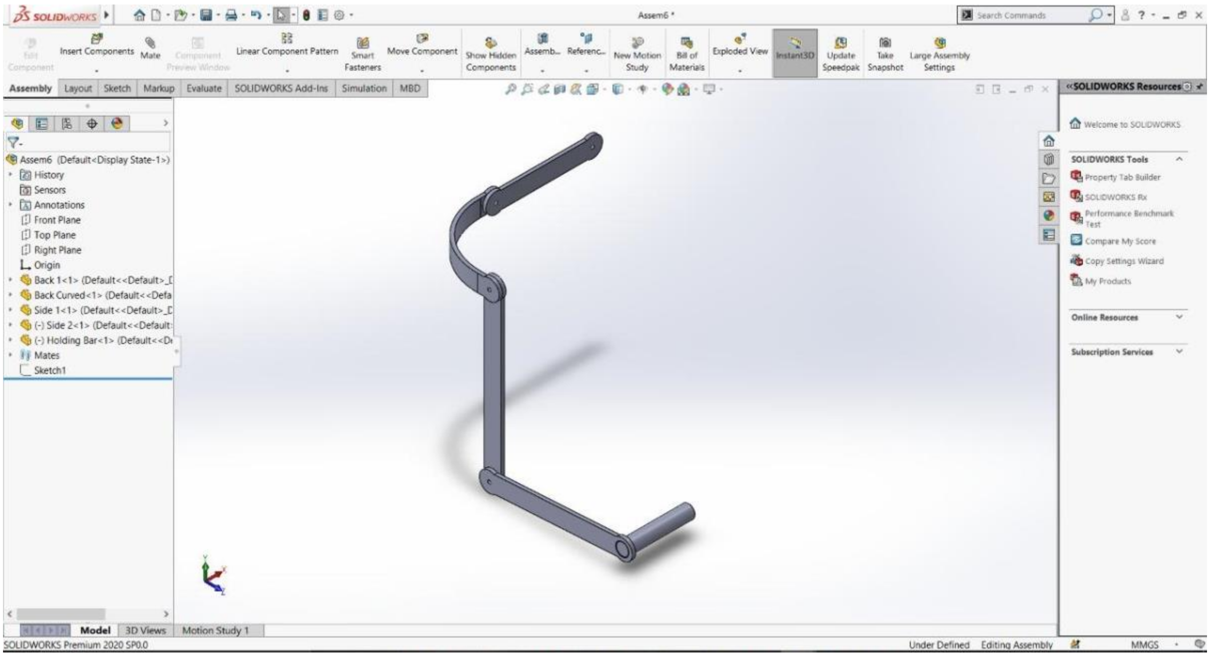

Figure 4.3.7: Final Model

Figure 4.3.6 is just a sample demo which represents the motor and the Figure 4.3.7 is the entire 3D model of the exoskeleton designed and developed in Solidworks using various individual parts and connecting them together to form the final model.

4.4: Hardware Setup

Myoware Muscle Sensor

The Myoware Muscle Sensor from Advancer Technologies measures, filters, rectifies, and amplifies the electrical activity of a muscle and produces an analog output signal that can easily be read by a microcontroller, enabling novel, muscle-controlled interfaces. This muscle sensor from Advancer Technologies measures a muscle's activity by monitoring the electric potential generated by muscle cells. This is referred to as electromyography (EMG). The sensor amplifies and processes the complex electrical activity of a muscle and converts it into a simple analog signal that can easily be read by any microcontroller with an analog-to-digital converter (ADC), such as an Arduino or even a Maestro servo controller. As the target muscle group flexes, the sensor's output voltage increases. The exact relationship between the output voltage and the muscle activity can be fine-tuned using an on-board gain potentiometer.

The Myoware Muscle Sensor is an updated version of Advancer Technologies' older Muscle Sensor v3 with a number of improvements, notably single-supply operation (no need for a negative voltage supply) and built-in snap connectors for electrodes. Other new features include a raw EMG output, reverse power protection, a power switch, and LED indicators. In order to attach to skin, the sensor requires three electrodes (not included) that snap into the sensor's snap-style connectors, which make it easy to attach and detach electrodes. Two connectors are located directly on the PCB, and the third is located at the end of the attached reference electrode cable.

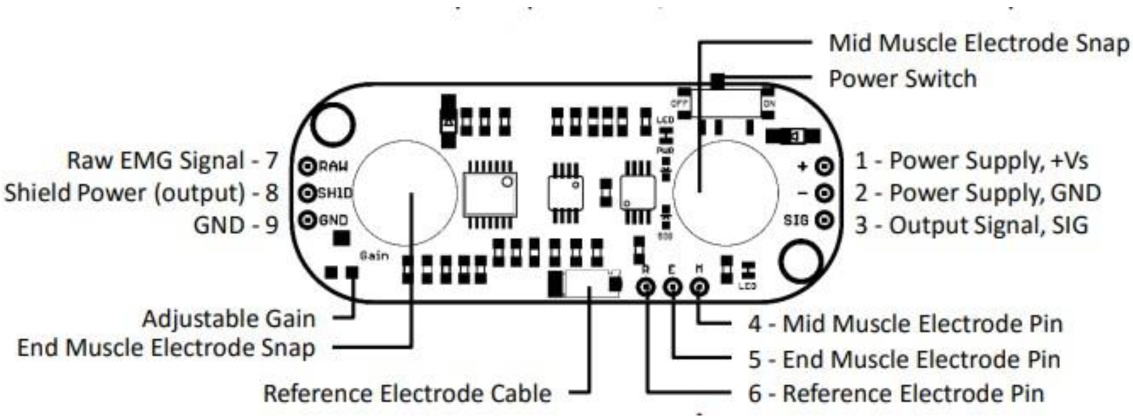

Figure 4.4.1: Sensor Layout

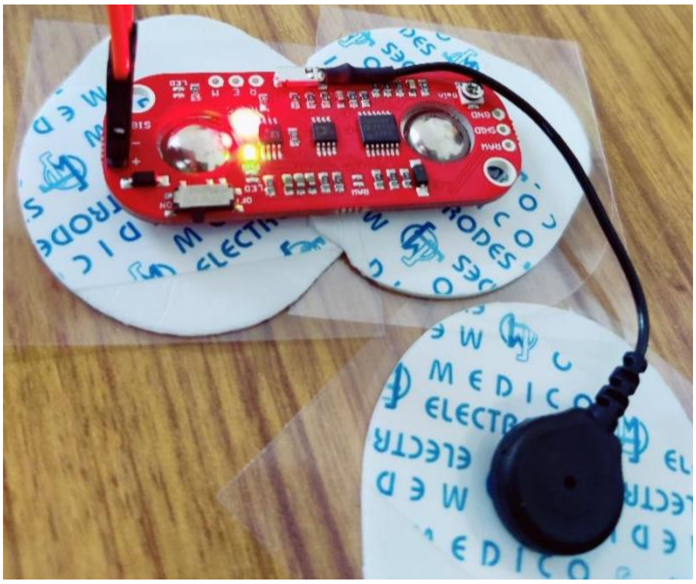

Figure 4.4.2: Sensor with Surface Electrodes

Analog to digital conversion:

The digitization process of the analog signal is carried out with an Analog to Digital Converter (ADC). Nowadays, the ADC has become a common component of modern electronic devices. Their use has become highly varied and widespread. Before using the ADC, its specifications, advantages and limitations have to be analysed in order to select the most appropriate one for the application. Control of the motor will be developed after the EMG signal is converted into digital format. A particular ADC has a specific range of conversion i.e. there are maximum and minimum levels defined for an ADC over which it can operate. An ADC can convert the analog signal over a certain number of bits. The number of bits which an ADC can convert is known as its “quantization scheme”. If an ADC has a defined range and a quantization scheme of *‘n-bits’.* After the EMG signal has been amplified up to a suitable level, the range of an ADC should be selected so that it can comprehend a particular voltage level. The number of quantization bits is important, as they determine the resolution of the ADC. The more the number of quantization bits, the less will be resolution of the ADC; the more it will help in control purposes. The ADC sampling rate is also a key consideration. It should be kept as large as possible so that the data loss of EMG is kept at a minimum.

The ADC on the Myoware Sensor is AD8648

The AD8648 is a quad, rail to-rail, input and output, single supply amplifier featuring low offset voltage, wide signal bandwidth, and low input voltage and current noise. The combination of 24 MHz bandwidth, low offset, low noise, and very low input bias current makes these amplifiers useful in a wide variety of applications. Filters, integrators, photodiode amplifiers, and high impedance sensors all benefit from the combination of performance features. AC applications benefit from the wide bandwidth and low distortion. The AD8648 family offers high output drive capability, which is excellent for audio line drivers and other low impedance applications. Applications for the part include portable and low powered instrumentation, audio amplification for portable devices, portable phone headsets, bar code scanners, and multipole filters. The ability to swing rail to rail at both the input and output enables designers to buffer CMOS ADCs, DACs, ASICs, and other wide output swing devices in single-supply systems.

Surface Electrodes:

Figure 4.4.3

Surface EMG electrodes provide a non-invasive technique for measurement and detection of EMG signal. The theory behind these electrodes is that they form a chemical equilibrium between the detecting surface and the skin of the body through electrolytic conduction, so that current can flow into the electrode. These electrodes are simple and very easy to implement. Application of needle and fine wire electrodes require strict medical supervision and certification. Surface EMG electrodes require no such formalities. Surface EMG electrodes have found their use in motor behaviour studies, neuromuscular recordings, sports medical evaluations and for subjects who object to needle insertions such as children. Apart from all this, surface EMG is being increasingly used to detect muscle activity in order to control device extensions to achieve prosthesis for physically disabled and amputated population. Surface EMG has some limitations Since these electrodes are applied on the skin, hence, they are generally used for superficial muscles. Crosstalk from other muscles is a major problem. Their position must be kept stable with the skin otherwise, the signal is distorted.

EMG signal acquisition circuit diagram:

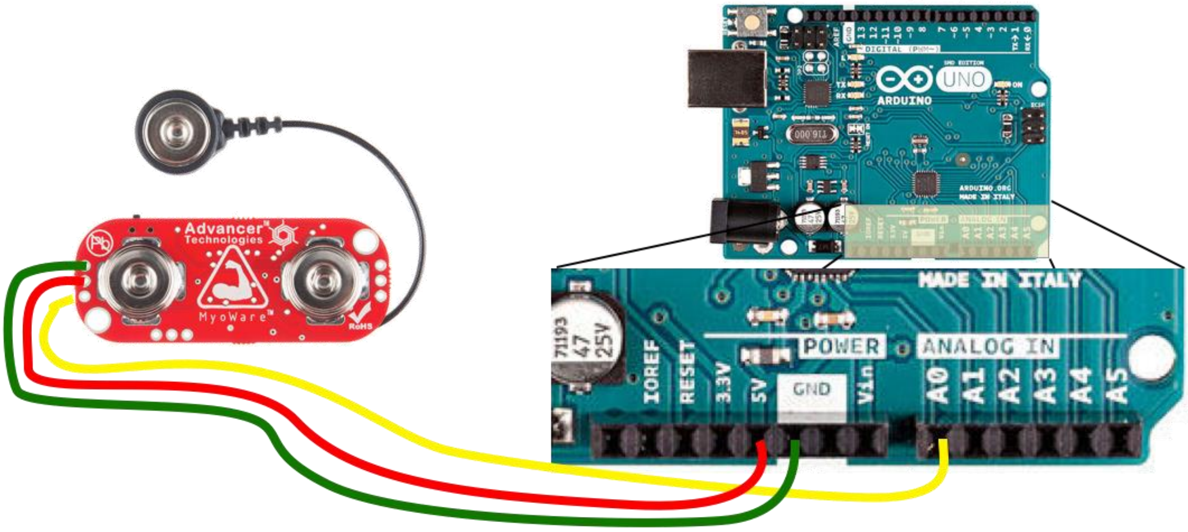

Figure 4.4.4: Sensor to Arduino Connection

The connection from the Myoware sensor to the Arduino is shown in Figure 4.4.4 which was used to display data and waveforms on the Serial Plotter and Monitor.

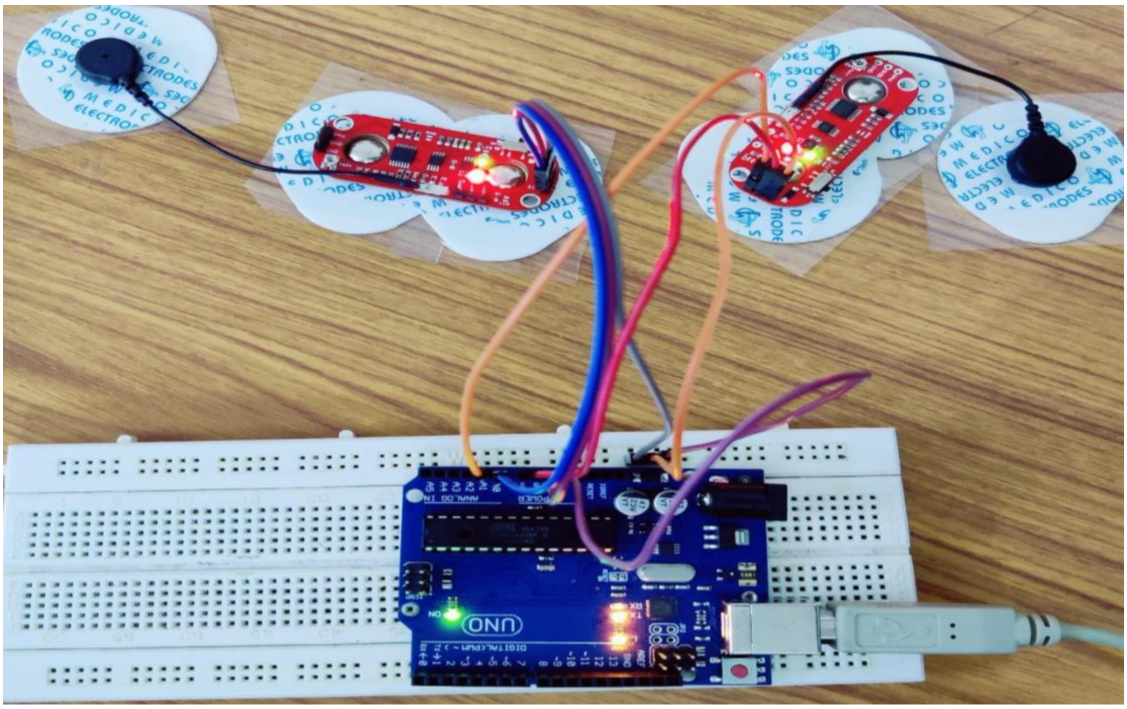

Figure 4.4.5: Dual sensor to Arduino Connection

The Figure 4.4.5 shows the connection made to obtain dual channel sensor data. This is where two Myoware sensors are connected to the Arduino board and the signals are given to the two analog pin which can display both the outputs on the Serial Monitor and the Serial Plotter.

Servo motor control using Myoware sensor:

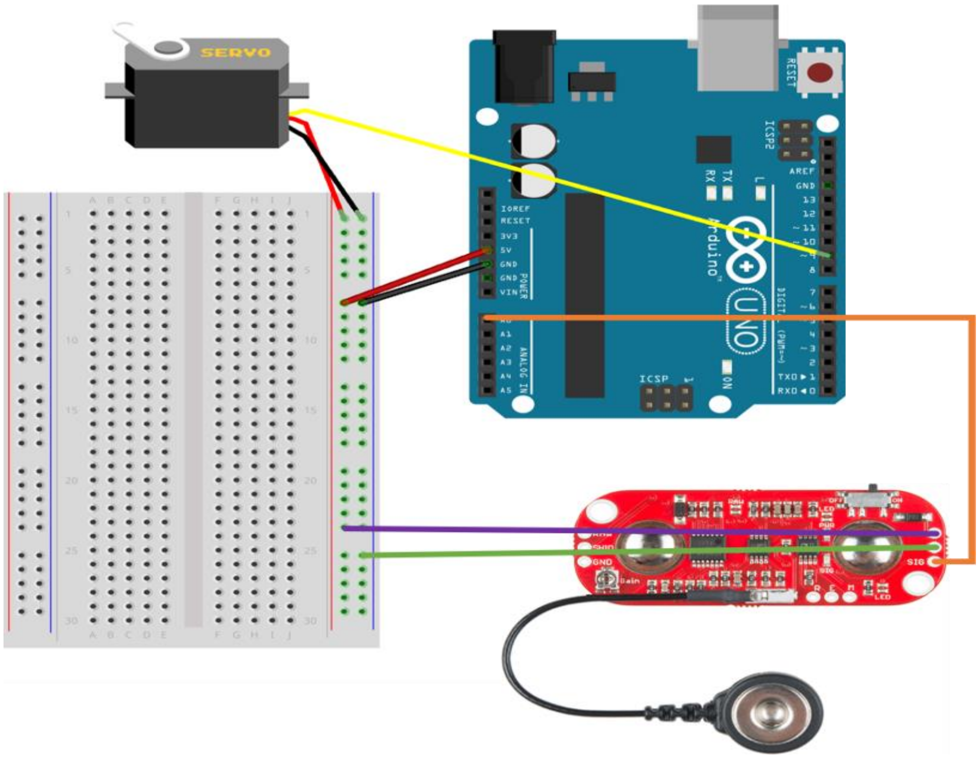

Figure 4.4.6: Servo Motor control using Sensor

The Figure 4.4.6 and 4.4.7 shows the connections to the motor. Using the Myoware sensor we obtain the values and use the data to make the motor move on flexing of the muscles.

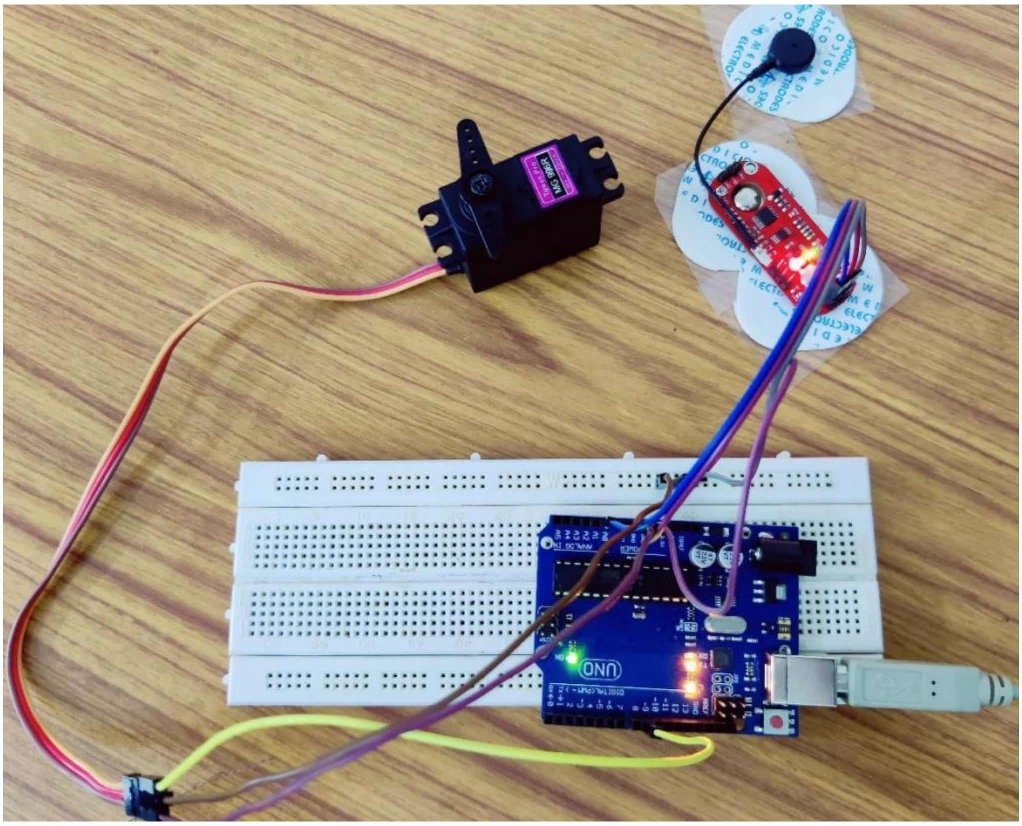

Figure 4.4.7

The Figure 4.4.8 is showing the connection of connecting motors using the motor driver control board.

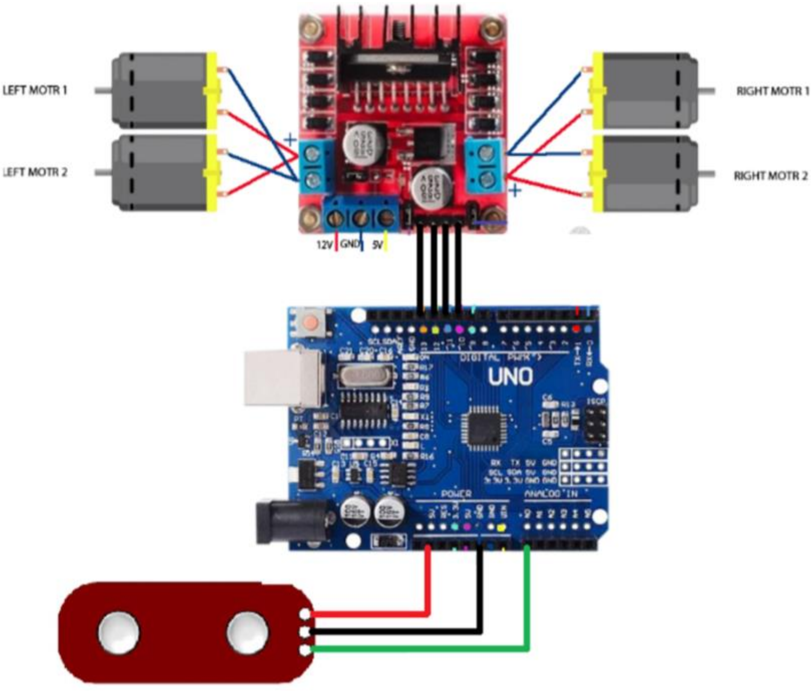

Figure 4.4.8: Multiple Motor control using Sensor

Servo Motor:

Figure 4.4.9

This High-Torque MG996R Digital Servo features metal gearing resulting in extra high 10kg stalling torque in a tiny package. The MG996R is essentially an upgraded version of the famous MG995 servo, and features upgraded shock-proofing and a redesigned PCB and IC control system that is make much accurate than its predecessor. The gearing and motor have also been upgraded to improve dead bandwidth and centring. The unit comes complete with 30cm wire and 3 pin 'S' type female header connector that fits most receivers. This high-torque standard servo can rotate approximately 120 degrees (60 in each direction). The MG996R Metal Gear Servo also comes with a selection of arms and hardware.

DC Worm Gear Motors:

These simple motors have some great characteristics which make them suitable for a wide range of applications. They are generally low speed but capable of extremely high torque. Worm drives offer a break feature which means when there is no power applied to the worm drive, the load cannot turn the motor. They offer a right-angle gearbox for practical mounting in tight spaces.

A worm gear drive consists of two elements:

1. Driving element: Screw
2. Driven element: Helical gear

Driving element is called Worm and Driven element is called Worm gear or Worm Wheel. Worm gear drives are typically used for transmission of power between two non-parallel and non-intersecting shafts.

Figure 4.4.10

Working: The worm continuously rotates and drives the worm wheel. Worm and worm gear from a lower pair as they have sliding contact with each other. In a worm gear drive, power is always transmitted from worm-to-worm wheel. Power cannot be transmitted from worm wheel to worm. This phenomenon is called self-locking. It is highly useful in many applications. Velocity ratio is determined by the number of teeth on worm gear and the number starts on Worm. Power transmission decreases with increase in velocity ratio.

Motor Driver Module:

L298N: The L298N is an integrated monolithic circuit in a 15- lead Multi watt and PowerSO20 packages. It is a high voltage, high current dual full-bridge driver de-signed to accept standard TTL logic level sand drive inductive loads such as relays, solenoids, DC and stepping motors. Two enable inputs are provided to enable or disable the device independently of the in-put signals. The emitters of the lower transistors of each bridge are connected together rand the corresponding external terminal can be used for the connection of an external sensing resistor. An additional Supply input is provided so that the logic works at a lower voltage.

CHAPTER 5: RESULTS AND CONCLUSION

5.1: RESULTS

MYOWARE SENSOR OUTPUT WAVEFORMS

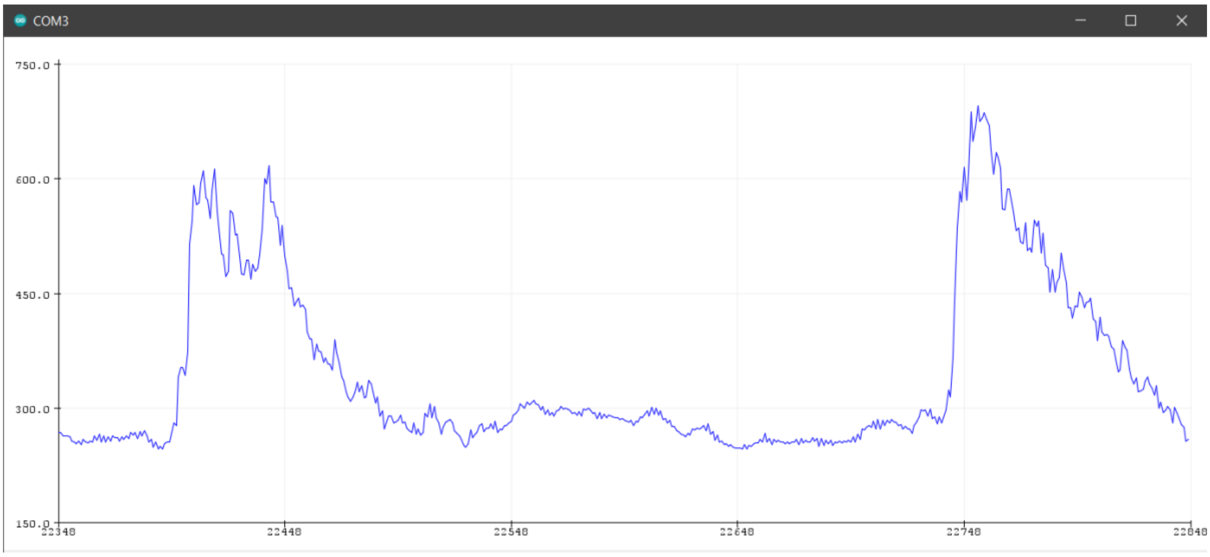

Graph 5.1.1: Single Channel

The above graph shows the output in single channel mode when sensor is placed at the biceps where it was flexed twice.

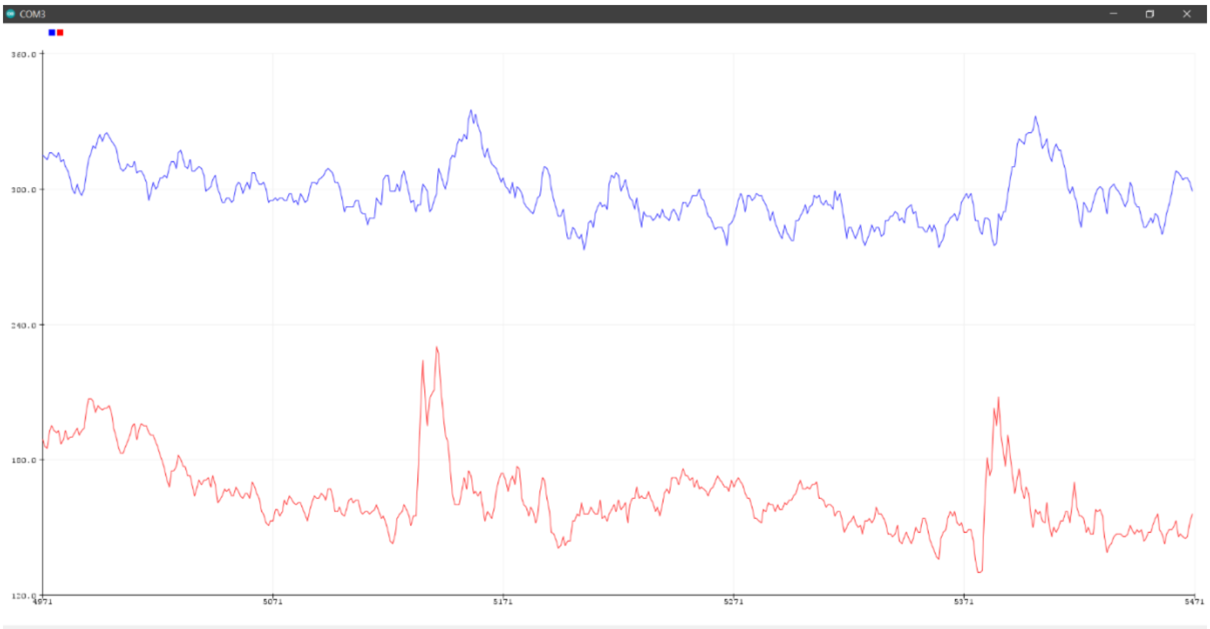

Graph 5.1.2: Dual Channel (Normal)

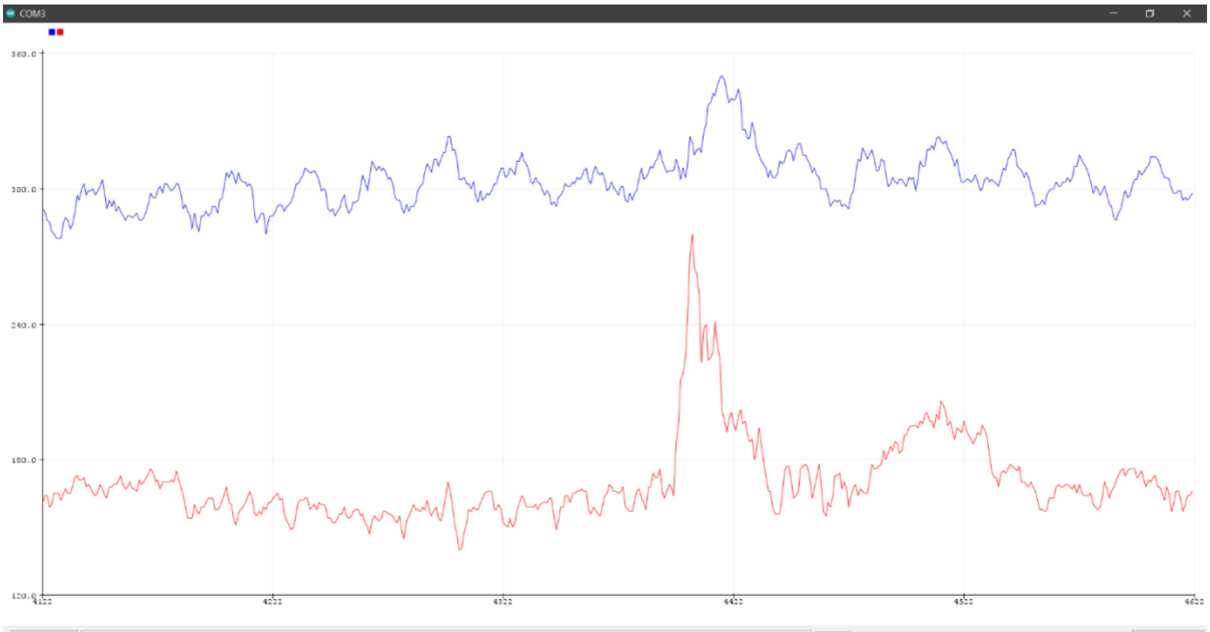

Graph 5.1.3: Dual Channel (Flex)

Graph 5.1.2 and 5.1.3 shows the output obtained in Dual Channel mode where one sensor was connected to bicep (Blue) and the other sensor was connected to tricep (Red). Graph 5.1.2 shows the action was performed twice to get the two peaks in the signal and Graph 5.1.3 shows the muscle being flexed more than normal to get the signal.

DATABASE ANALYSIS

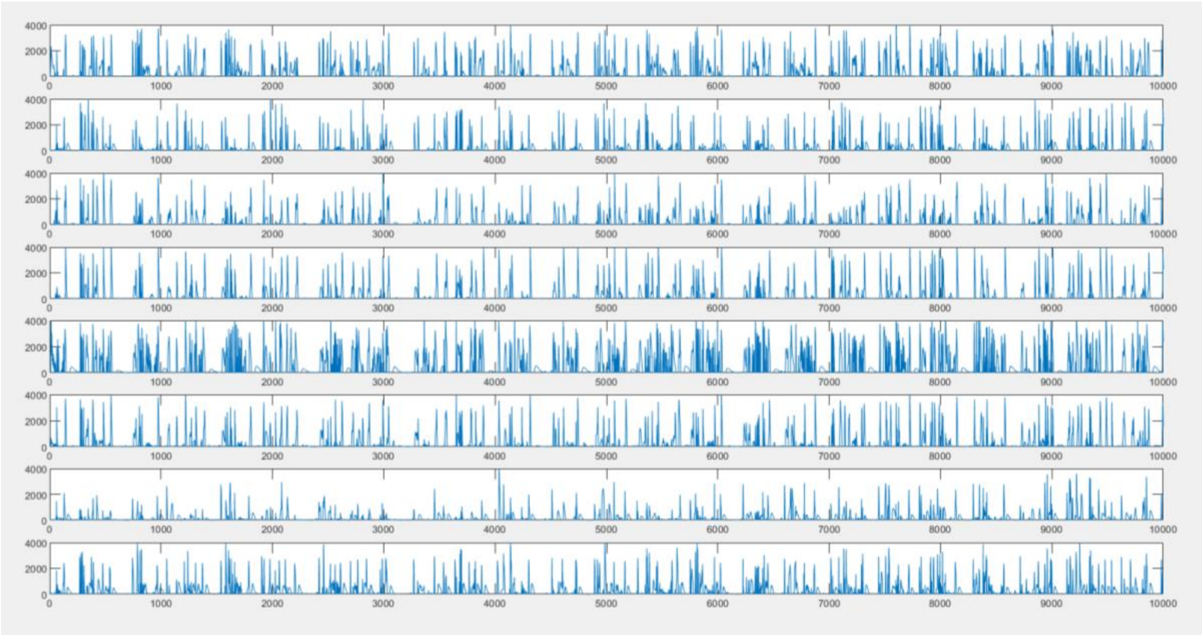

Figure 5.1.1: Raw Data

The Figure 5.1.1 shows the Raw data of the 8 channels of one of the action from the subject that was randomly selected and viewed in MATLAB.

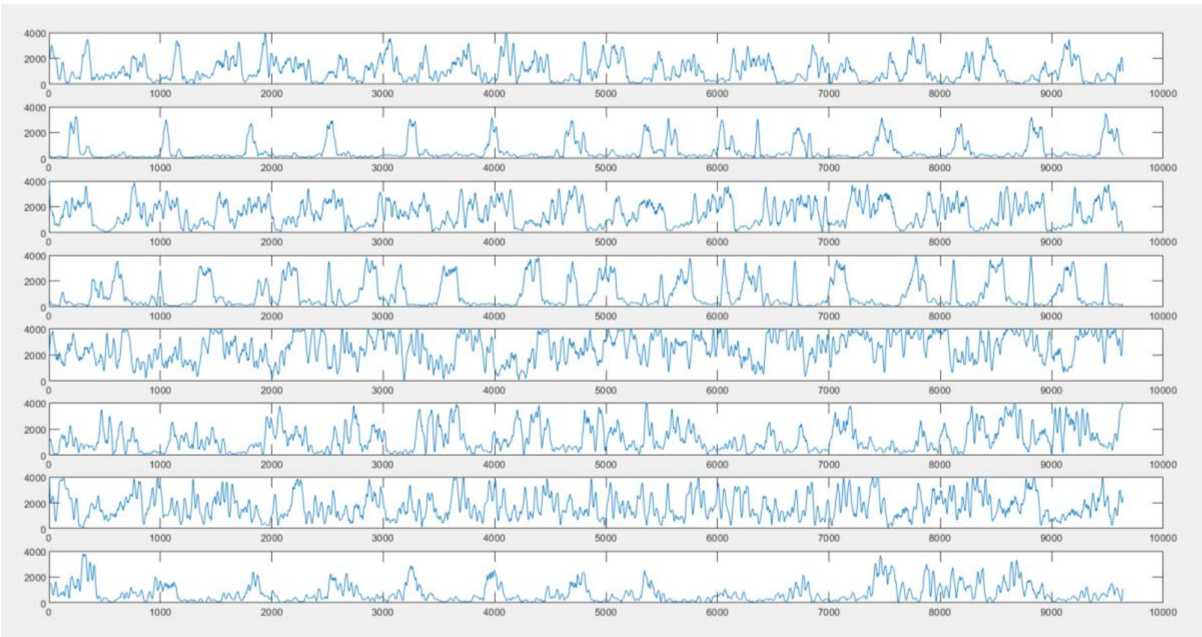

Figure 5.1.2: Processed Data

The Figure 5.1.2 shows the Processed data of 8 channels viewed in MATLAB.

Accuracies obtained from database processing with different techniques:

1. For 500 window size and 50 step size:

MODEL	AVERAGE ACCURACY
Default	49.43%
Naives Bayes	84.52%
Logistic Regression	86.23%
Random Forest	89.77%

Table 5.1.1: Average Accuracy

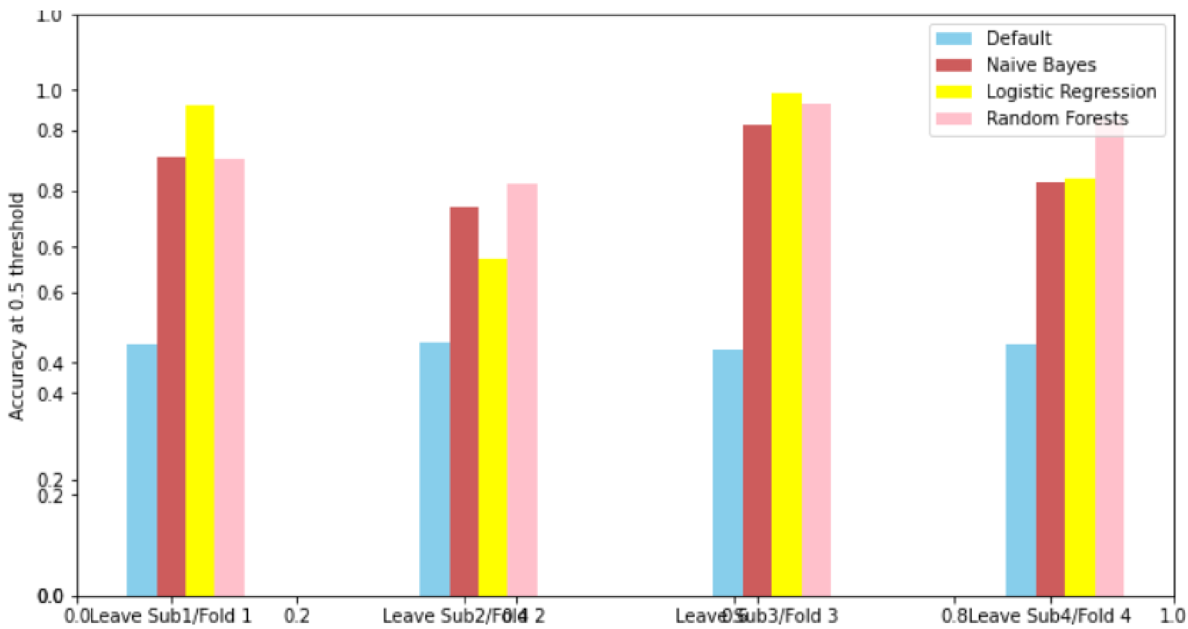

Graph 5.1.4: Average Accuracy Graph

Table 5.1.1 and Graph 5.1.4 show the average accuracies obtained using Four Cross Validation method. This accuracy is the average of 4 different combinations.

2. For 800 window size and 80 step size:

MODEL	AVERAGE ACCURACY
Default	49.52%
Naives Bayes	81.89%
Logistic Regression	80.06%
Random Forest	84.03%

Table 5.1.2: Average Accuracy

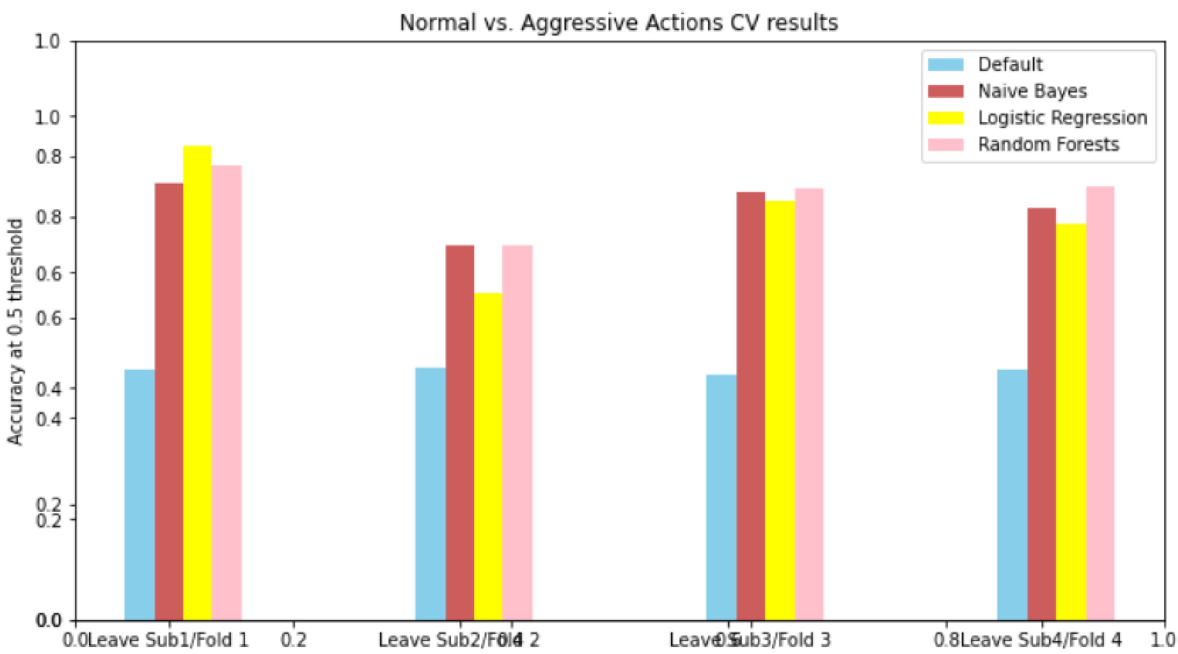

Graph 5.1.5: Average Accuracy Graph

Table 5.1.2 and Graph 5.1.5 show the average accuracies obtained using Four Cross Validation method. This accuracy is the average of 4 different combinations.

3. For 1000 window size and 100 step size:

MODEL	AVERAGE ACCURACY
Default	49.50%
Naives Bayes	81.79%
Logistic Regression	79.60%
Random Forest	80.70%

Table 5.1.3: Average Accuracy

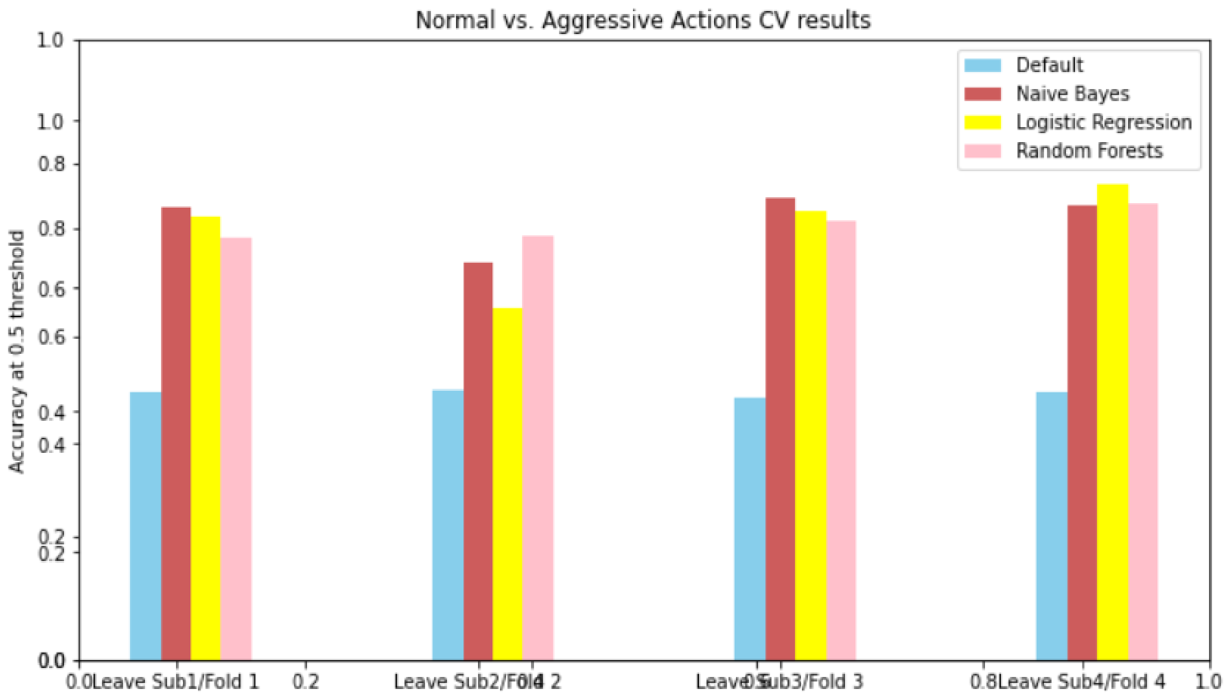

Graph 5.1.6: Average Accuracy Graph

Table 5.1.3 and Graph 5.1.6 show the average accuracies obtained using Four Cross Validation method. This accuracy is the average of 4 different combinations.

Rviz Output:

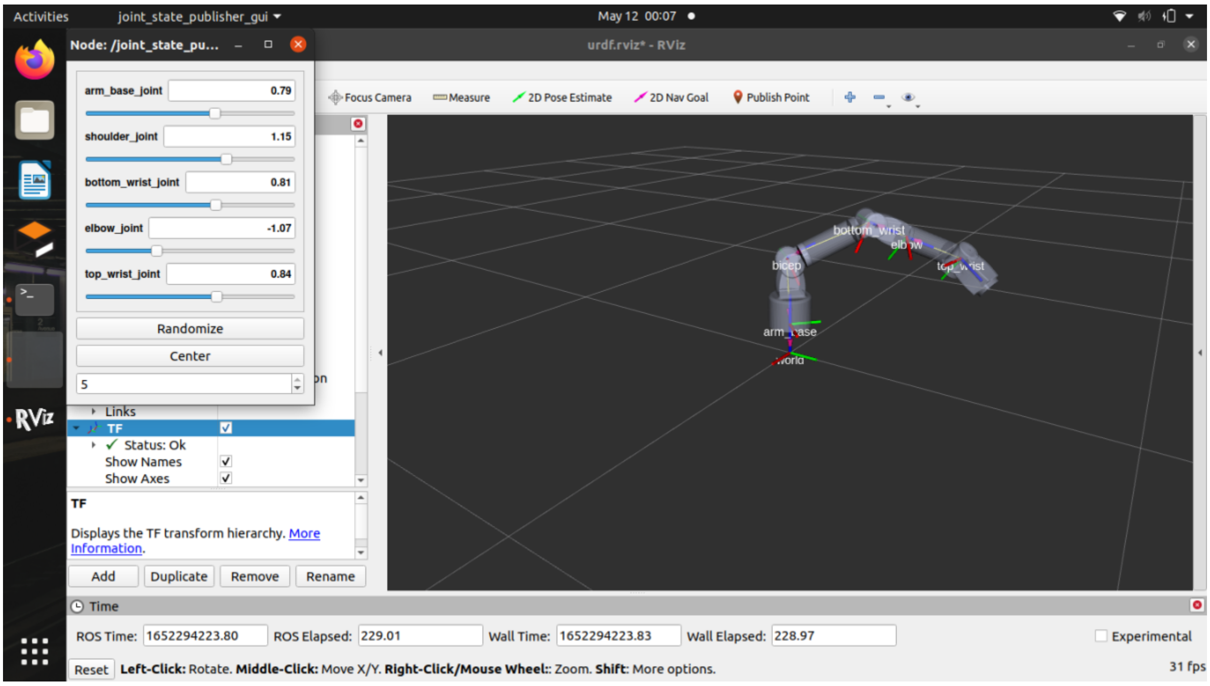

Figure 5.1.3: Rviz Simulation

The above figure shows the output of the model in Rviz. It is a 5 DoF model. The node controller is used to adjust and move the arm to different locations. Since it’s a 5 DoF model it can be moved and changed position to fit different purpose it can be used for. To move the arm a code can be written or the controller can be used in this case.

3D model output in Solidworks:

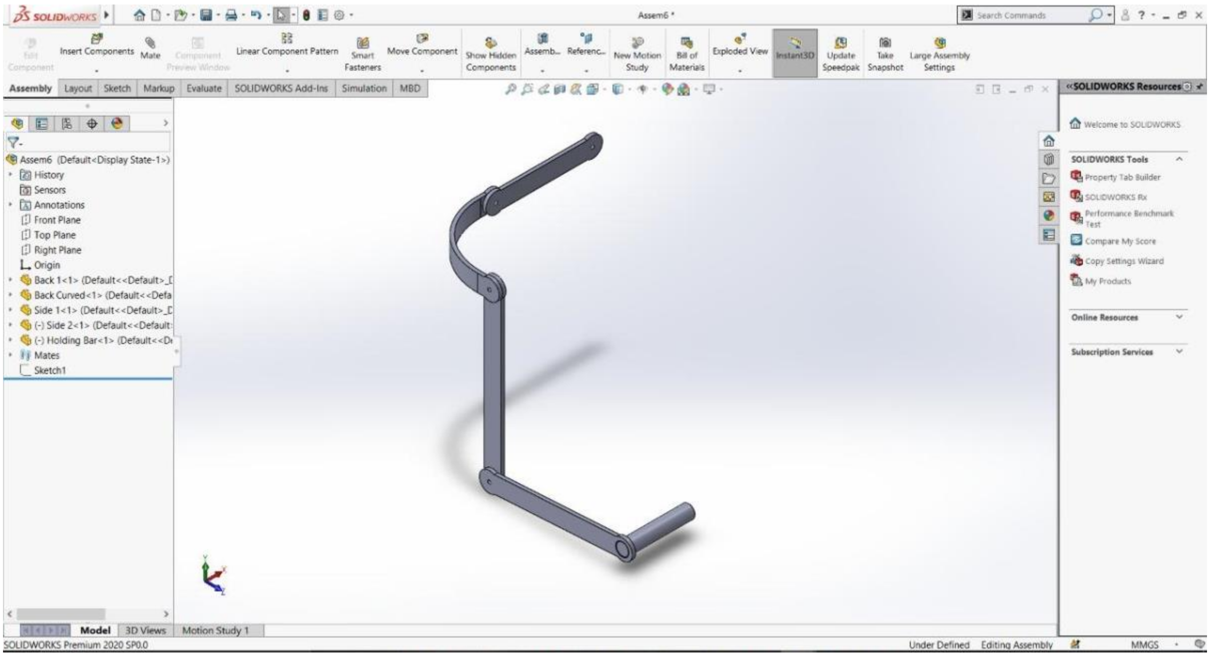

Figure 5.1.4: 3D model in Solidworks

The Figure 5.1.4 was the model made in solidworks which was then given to the Don Bosco College of Engineering for 3D printing the model and getting it in the physical form for further assessment.

Figure 5.1.5 is the shoulder part of the printed model. This is the connection between the back plate and side plate.

Figure 5.1.5: Shoulder part

Figure 5.1.6: Back plate

The back plate the main support to the body at the back which can be seen in Figure 5.1.6 and will help with the overall strength of the model. This back plate is joint to the side plate as seen in Figure 5.1.7 which is near the biceps and will have a motor attachment at the joints for movement.

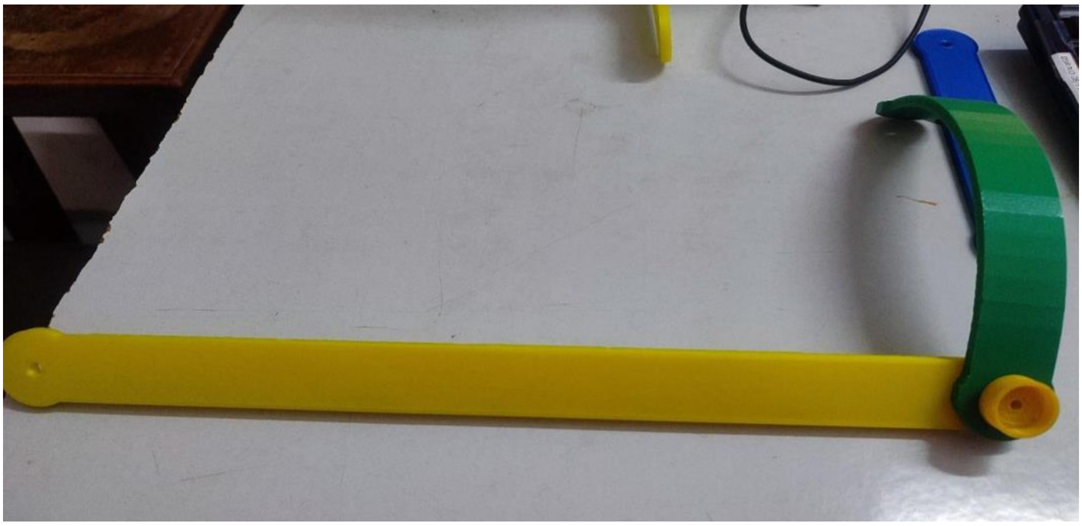

Figure 5.1.7: Side plate

Figure 5.1.8: Lower arm plate

This lower arm plate supports the area which is connected to the wrist handle to get the support and movements.

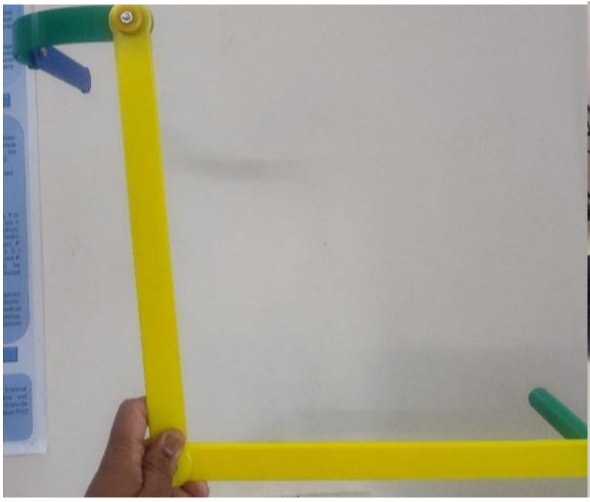

Figure 5.1.9

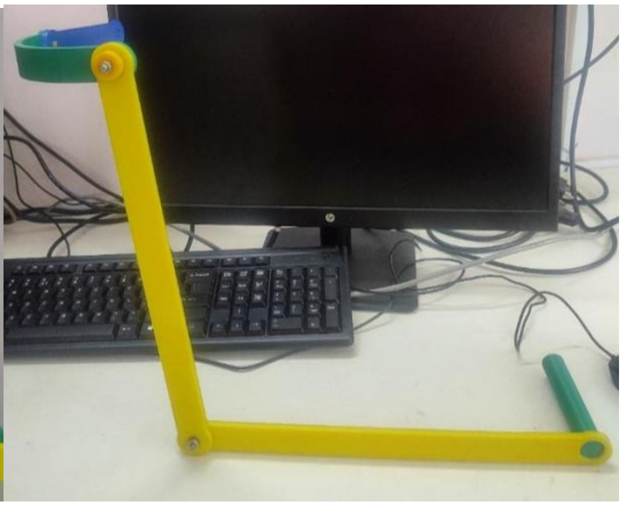

Figure 5.1.10

The Figure 5.1.9 and Figure 5.1.10 shows the different parts of the 3d printed model joint together to form the whole piece which can have the various movements.

Figure 5.1.11: Complete model

The complete model was printed and assembled to show how the connection look and how the model feels and weights to check for comfort and strength. Figure 5.1.11 shows the front view of the model.

5.2: CONCLUSION

The purpose of this project was to design and develop an upper limb exoskeleton using EMG signals which is capable of giving support to the arm and help with rehabilitation of the arm. The classification model was made for normal and aggressive actions and the data was reviewed further. The simulation was carried out in gazebo and rviz software which is used for the path finding and the movement of the arm and the 3D model was designed in solidworks software to support the whole project. Although the overall system of exoskeleton was not led to completion, the success in implementing various sub systems proves that there is a possibility of the practical implementation of the project after many trials.

APPLICATIONS

Rehabilitation robots have become important tools in stroke rehabilitation. Compared to manual arm training, robot-supported training can be more intensive, of longer duration and more repetitive. Therefore, robots have the potential to improve the rehabilitation process in stroke patients. Whereas a majority of previous work in upper limb rehabilitation robotics has focused on end-effectors-based robots, a shift towards exoskeleton robots is taking place because they offer a better guidance of the human arm, especially for movements with a large range of motion.

The exoskeleton arm is found to be useful in diverse situations as mentioned below:

- Disabled people can regain the use of their limbs using the exoskeleton.
- The exoskeleton can be used as a means of rehabilitation.
- Industrial workers, dock workers and loaders who are engaged in jobs which entail lifting of heavy loads on a daily basis are empowered by the exoskeleton.
- Nurses who have to carry heavy patients can effectively do so with the exoskeleton.
- Exoskeletons have become widely popular in the military field as well, helping soldiers to carry armaments over challenging terrain.

LIMITATIONS

- Due to limited power supply, we cannot put motors with more torque and weight capacity.
- There can be issues with the surface electrodes since they are one time use.
- They cannot stretch or expand and are fixed in size.
- The measurement of the arm needs to be perfect since there shouldn't be any mistake done while 3-D printing the arm because it's expensive to make the model again and again and is time consuming.
- Due to the limitation of the EMG sensor, we would not get the same reading frequently as there would be a lot of noise because of the surface of the skin and electrode texture.
- Limited Motion Range where unlike in a human being who has a large range of motions that they can perform, certain flexibility. If they have an exoskeleton attached to their frame some movement will be restricted.

FUTURE WORKS

Exoskeletons have remarkable potential. But there is still a lot of work to be done to reduce the cost and increase the movements it can make along with the increase in power supply. Exoskeleton power supplies must be light, reliable and long-lasting. That combination of qualities is difficult to achieve and very expensive.

In the future we can change the control of the design of the model to make it better. A pressure sensor can also be used to get feedback. Furthermore, we can try our best to interface it to the brain and make it work with the brain waves. We can also design our own EMG sensor to make it cheaper along with an appropriate control system to do the entire exoskeleton. We are thinking of designing lower limb exoskeleton for the people who are having lower limb issues.

BIBLIOGRAPHY

[1] Yagin, Nicholas. "Apparatus for Facilitating Walking". U.S. Patent 440,684 filed February 11, 1890 and issued November 18, 1890.

[2] L. Aksman, “Force Estimation Based Compliance Control of a Two Link Harmonically Driven Robotic Manipulator,” Master’s Thesis, University of Maryland, Dec. 2006.

[3] M. Bergamasco, B. Allotta, L. Bosio, L. Ferretti, G. Parrini, G. Prisco, F. Salsedo, and G. Sartini, “An arm exoskeleton system for teleoperation and virtual environments applications,” in Proc. of the IEEE Intl. Conf. on Robotics and Automation, San Diego, 1994, pp. 1449–1454.

[4] M. Bergamasco, G.M. Prisco, “Virtual Surfaces Contour Following: An Experimental Approach Exploiting an Arm Exoskeleton as Haptic Interface,” in Proc. of the ASMEDymanic Systems and Control Division, vol.57-2, 1995, pp.681-687.

[5] M.A. Buckley, G.R. Johnson, “Computer simulation of the dynamics of human arm and orthosis linkage mechanism,” in Proc. Inst. Mech. Engrs. Part H, vol. 211, 1997, pp.349-357.

[6] D.G. Caldwell, N. Tsagarakis, D. Badihi, G.A. Medrano-Cerda, “Pneumatic Muscle Actuator Technology: a light weight power system for a Humanoid Robot,” in Proc. of the IEEE Int. Conf. on Robotics & Automation, Leuven, Belgium, May 1998, pp.3053-3058.

[7] de la Tejera, Javier A.; Bustamante-Bello, Rogelio; Ramirez-Mendoza, Ricardo A.; Izquierdo-Reyes, Javier (24 December 2020). "Systematic Review of Exoskeletons towards a General Categorization Model Proposal". Applied Sciences. **11** (1): 76. doi:10.3390/app11010076

[8] Xu, H.; Xiong, A. Advances and Disturbances in sEMG-Based Intentions and Movements Recognition: A Review. IEEE Sens. J. **2021**, 21, 13019–13028.

[9] Pawl Herbin, M. P., 2021. Human-robot cooperative control system based on serial elastic actuator bowden cable drive in ExoArm 7-DOF upper extremity exoskeleton. Elsevier Ltd, doi.org/10.1016/j.mechmachtheory.2021.104372.

[10] Ren, B.; Zhang, Z.; Zhang, C.;Chen, S. Motion Trajectories Prediction of Lower Limb Exoskeleton Based on Long Short-Term Memory (LSTM) Networks. Actuators 2022, 11, 73. https://doi.org/10.3390/act11030073.

[11] Lad PR, Patil DS, Patil SC, et al. EMG analysis of dominant and non-dominant arm of latissimus dorsi muscles in bowlers of Karad, Maharashtra, India. J Evolution Med Dent Sci 2021;10(36):3088-3093, DOI:10.14260/jemds/2021/630

[12] Anubhav Gupta, Ritika Inamke, Akash Darak. 2014. "EMG Signal Analysis and Application for Arm" International Journal of Engineering Research & Technology (IJERT) 3 (8).

[13] Ruonala V, Pekkonen E, Airaksinen O, Kankaanpaa M, Karjalainen PA, Rissanen SM (2022) Changes in elbow flexion EMG morphology during adjustment of deep brain stimulator in advanced Parkinson’s disease. PLoS ONE 17(4):e0266936. https://doi.org/10.1371/journal.

[14] Chen et al. "Comparative effects of EMG-driven robot-assisted therapy versus task-oriented training on motor and daily function in patients with stroke: a randomized cross-over trial” Journal of NeuroEngineering and Rehabilitation (2022) 19:6 https://doi.org/10.1186/s12984-021-00961-w

[15] Gull, Muhammad & Bai, Shaoping & Bak, Thomas. (2020). A Review on Design of Upper Limb Exoskeletons. Robotics. 9. 16. 10.3390/robotics9010016.

[16] Ashley M. Stewart, Christopher G. Pretty, Mark Adams, XiaoQi Chen, Review of Upper Limb Hybrid Exoskeletons, IFAC-PapersOnLine, Volume 50, Issue 1, 2017, Pages 15169-15178,ISSN 2405-8963, 10.1016/j.ifacol.2017.08.2266.

[17] Paweł Herbin, Mirosław Pajor, Human-robot cooperative control system based on serial elastic actuator bowden cable drive in ExoArm 7-DOF upper extremity exoskeleton, Mechanism and Machine Theory, Volume 163, 2021, 104372, ISSN 0094-114X, doi.org/10.1016/j.mechmachtheory.2021.104372.

[18] Ruben Fuentes-Alvarez, Joel Hernandez, Ivan Matehuala-Moran, Mariel Alfaro-Ponce, Ricardo Lopez-Gutierrez, Sergio Salazar, Rogelio Lozano, Assistive robotic exoskeleton using recurrent neural networks for decision taking for the robust trajectory tracking, Expert Systems with Applications, Volume 193, 2022, 116482, ISSN 0957-4174, https://doi.org/10.1016/j.eswa.2021.116482.

[19] Christine Linnenberg, Robert Weidner, Industrial exoskeletons for overhead work: Circumferential pressures on the upper arm caused by the physical human-machine-interface, Applied Ergonomics, Volume 101, 2022, 103706, ISSN 0003-6870, https://doi.org/10.1016/j.apergo.2022.103706.

[20] Triwiyanto, Triwiyanto, Triana Rahmawati, I Putu Alit Pawana, and Evrinka Hikaristiana Maulidia. “Investigation of Electrode Location to Improve the Accuracy of Wearable Hand Exoskeleton Trainer Based on Electromyography.” Journal of Biomimetics, Biomaterials and Biomedical Engineering. Trans Tech Publications, Ltd., March 28, 2022. https://doi.org/10.4028/p-y7g473.

[21] Triwiyanto, Triwiyanto, Endro Yulianto, Sari Luthfiyah, Syevana Dita Musvika, Anita Miftahul Maghfiroh, M. Ridha Mak’ruf, Dyah Titisari, and S.B. Ichwan. “Hand Exoskeleton Development Based on Voice Recognition Using Embedded Machine Learning on Raspberry Pi.” Journal of Biomimetics, Biomaterials and Biomedical Engineering. Trans Tech Publications, Ltd., March 28, 2022. https://doi.o10.4028/p-ghjg94.

[22] Eric B. Weston, Mina Alizadeh, Hamed Hani, Gregory G. Knapik, Reid A. Souchereau & William S. Marras (2022) A physiological and biomechanical

investigation of three passive upper-extremity exoskeletons during simulated overhead work, Ergonomics, 65:1, 105-117, DOI: 10.1080/00140139.2021.1963490

[23] Chuang Liu and Jingzhou Song 2019 IOP Conf. Ser.: Earth Environ. Sci. 252 022079

[24] Feilong Jiang, Hao Liu, Qingwei Li, Jian Cao, Xiaoliang Yin, Rui Dong, "Man-Machine Synergy Control for Pneumatically Powered Exoskeleton Based on Surface Electromyogram Signal", Mathematical Problems in Engineering, vol. 2022, Article ID 6897221, 14 pages, 2022. https://doi.org/10.1155/2022/6897221.

[25] Samui, Suman. (2020). An experimental study on upper limb position invariant EMG signal classification based on deep neural network. Biomedical Signal Processing and Control. 55. 10.1016/j.bspc.2019.101669.

[26] Fahreddin Sadikoglu, Cemal Kavalcioglu, Berk Dagman, Electromyogram (EMG) signal detection, classification of EMG signals and diagnosis of neuropathy muscle disease, Procedia Computer Science, Volume 120, 2017, Pages 422-429, ISSN 1877-0509, doi.org/10.1016/j.procs.2017.11.259.

[27] Toledo-Pérez, Diana C., Juvenal Rodríguez-Reséndiz, Roberto A. Gómez-Loenzo, and J. C. Jauregui-Correa. 2019. "Support Vector Machine-Based EMG Signal Classification Techniques: A Review" Applied Sciences 9, no. 20: 4402. https://doi.org/10.3390/app9204402

[28] Glowinski, Sebastian & Blazejewski, Andrzej. (2019). An exoskeleton arm optimal configuration determination using inverse kinematics and genetic algorithm. Acta of bioengineering and biomechanics / Wroclaw University of Technology. 21. 10.5277/ABB-01268-2018-02.

[29] Akira Furui, Takuya Igaue, Toshio Tsuji, EMG pattern recognition via Bayesian inference with scale mixture-based stochastic generative models, Expert Systems with Applications, Volume 185, 2021, 115644, ISSN 0957-4174, 10.1016/j.eswa.2021.115644.

[30] Fu Zinvi, A. Y. Bani Hashim, Z. Jamaludin, and I. S. Mohamad. 2021. "Review on EMG Acquisition and Classification Techniques: Towards Zero Retraining in the Influenece of User and Arm Position Independence". International Journal of Integrated Engineering 13 (4):1-15, https://doi.org/10.30880/ijie.2021.13.04.001

[31] Al-Rashid Agha, Rawan & Mahdi, Zhwan & Sefer, Muhammed & Hamarash, Ibrahim. (2021). A ROS-Gazebo Interface for the Katana Robotic Arm Manipulation. UKH Journal of Science and Engineering. 5. 26-37. 10.25079/ukhjse.v5n1y2021.pp26-37.

[32] Cornejo-Lupa, M.A.;Cardinale, Y.; Ticona-Herrera, R.;Barrios-Aranibar, D.; Andrade, M.; Diaz-Amado, J. OntoSLAM: AnOntology for Representing Location and Simultaneous Mapping Information for Autonomous Robots. Robotics 2021, 10, 125. https://doi.org/10.3390/robotics10040125.

[33] Rivera, Zandra B., Marco C. De Simone, and Domenico Guida. 2019. "Unmanned Ground Vehicle Modeling in Gazebo/ROS-Based Environments" Machines 7, no. 2: 42. https://doi.org/10.3390/machines7020042.

[34] Guowei Cui et al 2021. "The simulation of a service robot for task planning" J. Phys.: Conf. Ser. 1887 012012.

[35] Molina-Leal, A. Gómez-Espinosa, A.; Escobedo Cabello, J.A.; Cuan-Urquizo, E.; Cruz-Ramírez, S.R. Trajectory Planning for a Mobile Robot in a Dynamic Environment Using anLSTM Neural Network. Appl. Sci.2021, 11, 10689. https://doi.org/10.3390/app112210689.

[36] Maaroof, Omar W., Mehmet İ.C. Dede, and Levent Aydin. 2022. "A Robot Arm Design Optimization Method by Using a Kinematic Redundancy Resolution Technique" Robotics 11, no. 1: 1. https://doi.org/10.3390/robotics11010001.

[37] Marchesi, Giorgia, Giulia Ballardini, Laura Barone, Psiche Giannoni, Carmelo Lentino, Alice De Luca, and Maura Casadio. 2022. "Modified Functional Reach Test: Upper-Body Kinematics and Muscular Activity in

Chronic Stroke Survivors" Sensors 22, no. 1: 230. https://doi.org/10.3390/s22010230.

[38] Deng, Y., and Chang, J. (. (September 20, 2021). "Human-Like Posture Correction for Seven-Degree-of-Freedom Robotic Arm." ASME. J. Mechanisms Robotics. April 2022; 14(2): 024501. https://doi.org/10.1115/1.4051842.

[39] Uyulan, Çağlar. 2022. "Design and Stability Analysis of a Robust-Adaptive Sliding Mode Control Applied on a Robot Arm with Flexible Links" Vibration 5, no. 1: 1-19. https://doi.org/10.3390/vibration5010001.

[40] Wang, Jiwu & Xu, Junxiang. (2021). Kinematic Modeling and Simulation of Dual-Arm Robot. Journal of Robotics, Networking and Artificial Life. 8. 10.2991/jrnal.k.210521.013.

[41] Esposito,D.; Centracchio,J.; Andreozzi,E.; Savino,S.; Gargiulo,G.D.; Naik,G.R.; Bifulco,P. Design of a 3D-Printed Hand Exoskeleton Based on Force - Myography Control for Assistance and Rehabilitation. Machines 2022, 10, 57. https://doi.org/10.3390/machines10010057.

[42] Cheng Chi, Xianyi Zeng, Pascal Bruniaux & Guillaume Tartare (2022) A study on segmentation and refinement of key human body parts by integrating manual measurements, Ergonomics, 65:1, 60-77, DOI: 10.1080/00140139.2021.1963489.

[43] Chen Y, Wang Y, Luo SC, Zheng X, Kankala RK, Wang SB, Chen AZ. Advances in Engineered Three-Dimensional (3D) Body Articulation Unit Models. Drug Des Devel Ther. 2022;16:213-235. doi.org/10.2147/DDDT.S344036.

[44] Lee, CY., Lan, S.C., Lin, JJ. et al. Realization of Natural Human Motion on a 3D Biped Robot for Studying the Exoskeleton Effective. J. Med. Biol. Eng. 41**,** 856–869 (2021). https://doi.org/10.1007/s40846-021-00634-y.

[45] Li, Xiaodi & Li, Xu & liu, Ting & Lu, Yong & Shang, Chengshuo & Ding, Xiaokang & Zhang, Jicai & Feng, Yongjun & Xu, Fu-Jian. (2021). Wearable,

Washable, and Highly Sensitive Piezoresistive Pressure Sensor Based on a 3D Sponge Network for Real-Time Monitoring Human Body Activities. ACS Applied Materials & Interfaces. 13. 10.1021/acsami.1c09975.

[46] Hsieh, H.C.; Chen, D.F.; Chien, L.; Lan, C.C. Design of a Parallel Actuated Exoskeleton for Adaptive and Safe Robotic Shoulder Rehabilitation. IEEE/ASME Trans. Mechatron. **2017**, 22, 2034–2045.

[47] Lessard, S.; Pansodtee, P.; Robbins, A.; Trombadore, J.M.; Kurniawan, S.; Teodorescu, M. A soft exosuit for flexible upper-extremity rehabilitation. IEEE Trans. Neural Syst. Rehabil. Eng. **2018**, 26, 1604–1617.

[48] Vlachos, E.; Jochum, E.; Demers, L.P. HEAT: The harmony exoskeleton self-assessment test. In Proceedings of the 2018 27th IEEE International Symposium on Robot and Human Interactive Communication (RO-MAN), Nanjing, China, 27–31 August 2018; pp. 577–582.

[49] Bai, S.; Christensen, S.; Islam, M.R.U. An upper-body exoskeleton with a novel shoulder mechanism for assistive applications. In Proceedings of the 2017 IEEE International Conference on Advanced Intelligent Mechatronics (AIM), Munich, Germany, 3–7 July 2017; pp. 1041–1046.

[50] Castro, M.N.; Rasmussen, J.; Andersen, M.S.; Bai, S. A compact 3-DOF shoulder mechanism constructed with scissors linkages for exoskeleton applications. Mech. Mach. Theory **2019**, 132, 264–278.

[51] Crea, S.; Cempini, M.; Moisè, M.; Baldoni, A.; Trigili, E.; Marconi, D.; Cortese, M.; Giovacchini, F.; Posteraro, F.; Vitiello, N. A novel shoulder-elbow exoskeleton with series elastic actuators. In Proceedings of the 2016 6th IEEE International Conference on Biomedical Robotics and Biomechatronics (BioRob), Singapore, 26–29 June 2016; pp. 1248–1253.

[52] Ebrahimi, A.; Gröninger, D.; Singer, R.; Schneider, U. Control parameter optimization of the actively powered upper body exoskeleton using subjective feedbacks. In Proceedings of the 3rd International Conference on Control,

Automation and Robotics (ICCAR), Nagoya, Japan, 24–26 April 2017; pp. 432–437.

[53] Mao, Y.; Agrawal, S.K. Transition from mechanical arm to human arm with CAREX: A cable driven ARm EXoskeleton (CAREX) for neural rehabilitation. In Proceedings of the 2012 IEEE International Conference on Robotics and Automation, Saint Paul, MN, USA, 14–18 May 2012; pp. 2457–2462.

[54] C. Turlapaty and B. Gokaraju, "Feature Analysis for Classification of Physical Actions Using Surface EMG Data," in IEEE Sensors Journal, vol. 19, no. 24, pp. 12196-12204, 15 Dec.15, 2019, 10.1109/JSEN.2019.2937979.

[55] Necmettin Sezgin, "Analysis of EMG Signals in Aggressive and Normal Activities by Using Higher-Order Spectra", The Scientific World Journal, vol. 2012, Article ID 478952, 5 pages, 2012. doi.org/10.1100/2012/478952.

[56] Alcin, Omer & Budak, Ümit & Aslan, Muzaffer & Akbulut, Yaman & Cömert, Zafer & Akpınar, Muhammed & Sengur, Abdulkadir. (2020). Classification of physical actions from surface EMG signals using the wavelet packet transform and local binary patterns. 10.1088/978-0-7503-3279-8ch8.

[57] N. Sukumar, S. Taran and V. Bajaj, "Physical Actions Classification of Surface EMG Signals Using VMD," 2018 International Conference on Communication and Signal Processing (ICCSP), 2018, pp. 0705-0709, doi: 10.1109/ICCSP.2018.8524547.

[58] https://archive.ics.uci.edu/ml/datasets/EMG+Physical+Action+Data+Set

APPENDIX

ARDUINO UNO Board:

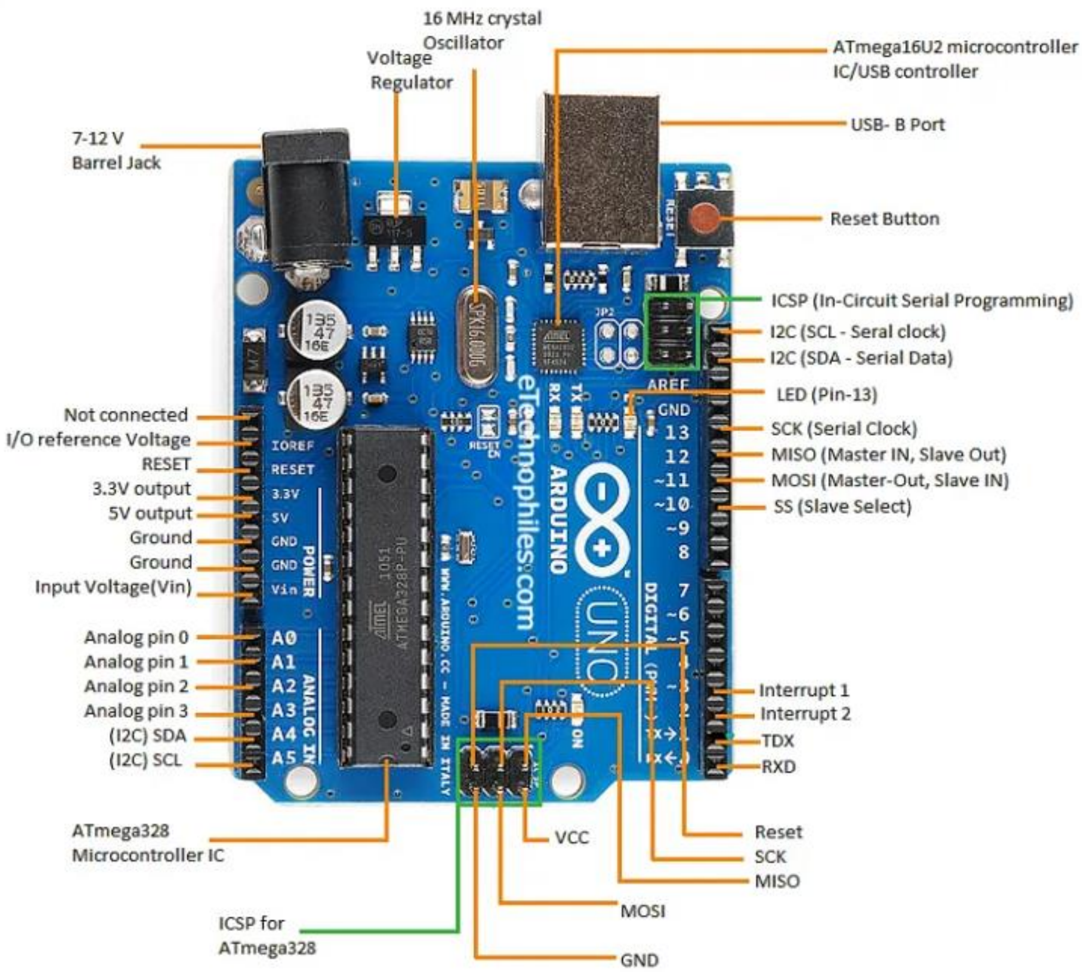

The **Arduino Uno** is an open-source microcontroller board based on the Microchip ATmega328P microcontroller and developed by Arduino.cc. The board is equipped with sets of digital and analog input/output (I/O) pins that may be interfaced to various expansion boards (shields) and other circuits. The board has 14 digital I/O pins (six capable of PWM output), 6 analog I/O pins, and is programmable with the Arduino IDE (Integrated Development Environment), via a type B USB cable. It can be powered by the USB cable or by an external 9-volt battery, though it accepts voltages between 7 and 20 volts. It is similar to the Arduino Nano and Leonardo.

SPECIFICATIONS:

Supply current:	9 mA
Microcontroller	ATmega328P
Operating Voltage	5V
Input Voltage (recommended)	7-12V
Input Voltage (limit)	6-20V
Digital I/O Pins	14 (of which 6 provide PWM output)
PWM Pins	6(Pin 3, 5, 6, 9, 10, and 11)
Analog Input Pins	6
Communication protocol	UART x 1, SPI x 1, I2C x 1
DC Current per I/O Pin	20 mA
DC Current for 3.3V Pin	50 mA
ICSP Header	2
Flash Memory	32 KB (ATmega328P) of which 0.5 KB used by the bootloader
SRAM	2 KB (ATmega328P)
EEPROM	1 KB (ATmega328P)
Clock Speed	16 MHz
LED_BUILTIN	13
Power Sources	Power Jack, USB port, Vin pin
Length	68.6 mm
Width	53.4 mm
Weight	25 g

MYOWARE MUSCLE SENSOR

Dimensions

Size:	2.1″ × 0.8″
Weight:	7.5 g

General Specifications

Minimum operating voltage:	2.9 V
Maximum operating voltage:	5.7 V
Reverse voltage protection?:	Y

- Adjustable gain
- Both EMG envelope and raw EMG outputs available
- Embedded electrode connectors – electrodes snap directly into MyoWare (alternatively, external electrode cables can be connected)
- LED Indicators – one power LED, and one LED that brightens when the muscle is flexed
- Power switch
- Reverse voltage protection
- Two mounting holes

HIGH TORQUE DC GEARED MOTOR 10RPM

Stall Torque<kgcm>	120
Shaft Diameter <mm>	6
Gear Box Diameter <mm>	37
Shaft Length <mm>	30
Motor Length <mm>	63
Weight In Grams	180
Gear Box Ratio	1:1620

DC Worm Gear Motors

The worm continuously rotates and drives the worm wheel. Worm and worm gear from a lower pair as they have sliding contact with each other. In a worm gear drive, power is always transmitted from worm-to-worm wheel. Power cannot be transmitted from worm wheel to worm. This phenomenon is called self-locking. It is highly useful in many applications. Velocity ratio is determined by the number of teeth on worm gear and the number starts on Worm. Power transmission decreases with increase in velocity ratio.

Specifications

- DC 12V Worm Gear Motor.
- Metal Net Weight 360gms.
- Rated Current 0.06A.
- Rated Torque 35kg.cm.
- Reduction Ratio 1:634.
- No Load Speed-Geared Box 5r/min.
- Motor 3500rpm
- Gear Box Shaft Size 8x14mm/0.3”x0.55”(DXL).
- Female Thread Diameter 3mm/0.12”
- Motor Body Size 55x30mm/2.2”x1.2”.
- Gear Box Size 58x40x30mm/2.3”x1.6”x1.2”(LxWxH).

Cable length 18cm/7”.

Item weight 399g.

Product dimension 17.8x11.8x4.2cm.

L298N Motor Driver (DUAL FULL-BRIDGE DRIVER)

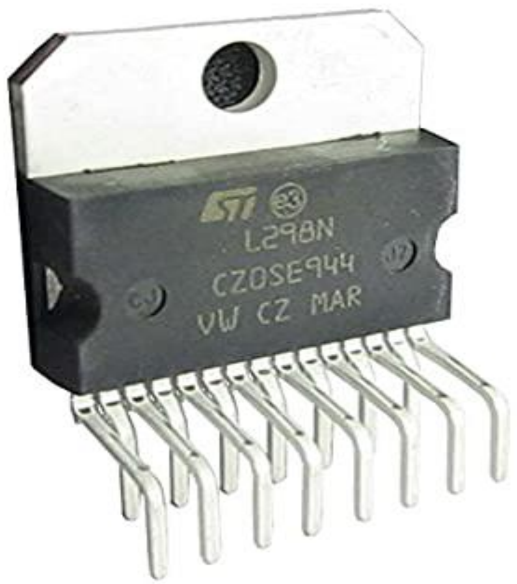

The L298 is an integrated monolithic circuit in a 15-lead multi watt and powerSO20 packages. It is a high voltage, High Current Dual Full Bridge Driver designed to accept standard TTL logic Levels and Drive inductive loads such as relays , solenoids, DC and Stepping Motors. Two enable inputs are provided to enable all disable that device independently of the input signal. The emitter of the lower transistors of each bridge are connected together and the corresponding external terminal can be used for the connection of an external sensing register. An additional supply input is provided so that the logic works at a lower voltage.

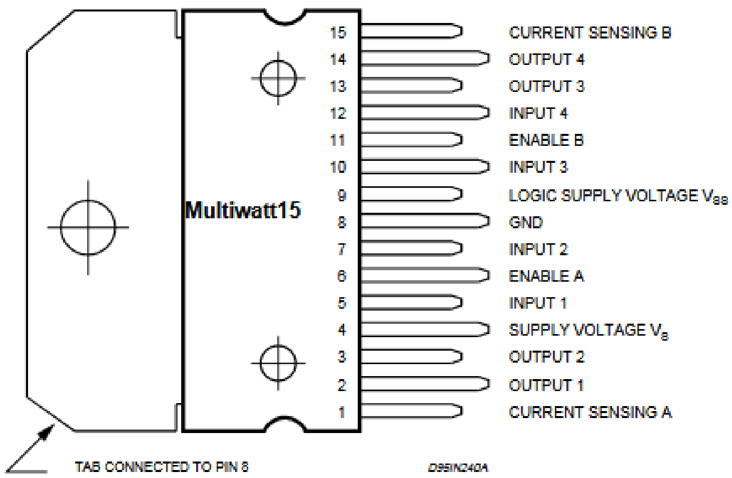

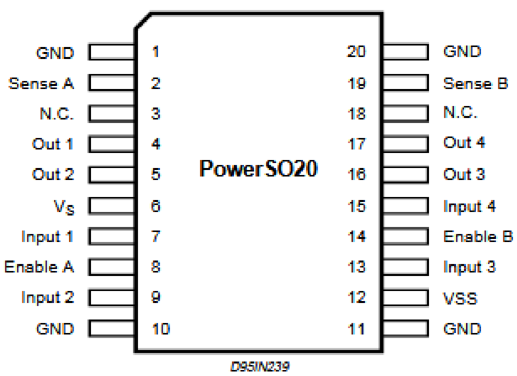

Features

- Operating supply voltage upto 46V.
- Total DC current up to 4A.
- LOW saturation Voltage.
- Over temperature Protection.
- Logical “0” input voltage up to 1.5v (high noise immunity).

INPUT 1	INPUT 2	ACTION
LOW	LOW	Motor Breaks and Stops*
HIGH	LOW	Motor Breaks and Stops*
LOW	HIGH	Motor turns backward
HIGH	HIGH	Motor Breaks and Stops*

To coast a motor to a slower stop, apply a low signal to the enable 1 line. L298N circuit used to drive inductive/magnetic loads.one of the lacking features of the unit is the lack of parasitic(flywheel) diodes to deal with voltage spikes. D1-D8 are used for this purpose. They can be 1N5819 or 1N4007 Diodes.

The four power amplifiers and grouped in pairs of two with individual enable pins (ENA,ENV) and individual current sense pins.(CSA,CSB) for each pair. The current sense pins in general can be tied to ground, but one can insert a low value register, whose voltage reading is proportional to current. ENA,ENB and In1-In4 are all standard 5v TTL logic making connection to most micro controllers easy. ENA will turn on A1 and A2 when with a digital HIGH (5v) and off when LOW (0v) the corresponding outputs will be floating when OFF. Same is true of ENV.

MG996R Servo Motor

This High-Torque MG996R Digital Servo features metal gearing resulting high 10kg stalling torque in a tiny package. The MG996R is essentially an upg raded version of the famous MG995 servo, and features upgraded shock-proofing and a redesigned PCB and IC control system that is make much accurate than its predecessor. The gearing and motor have also been upgraded to improve dead band width and centring. The unit comes complete with 30cm wire and 3 pin 'S' type female header connector that fits most receivers. This high-torque standard servo can rotate approximately 120 degrees (60 in each direction). The MG996R Metal Gear Servo also comes with a selection of arms and hardware to get you set up nice and fast.

Specifications

- Weight: 55 g
- Dimension: 40.7 x 19.7 x 42.9 mm approx.
- Stall torque: 9.4 kgfcm (4.8 V), 11 kg fcm (6 V)
- Operating speed: 0.17 s/60º (4.8 V), 0.14 s/60º (6 V)
- Operating voltage: 4.8 V a 7.2 V
- Running Current 500 mA
- Stall Current 2.5 A (6V)
- Dead band width: 5 µs
- Stable and shock proof double ball bearing design
- Temperature range: 0 ºC –4.8 V a 7.2 V– 900 mA (6V) double ball bearing design55 ºC